

## Air Infiltration through Building Entrances

*Master of Science Thesis in the Master's Programme Structural Engineering and Building Technology*

NICKLAS KARLSSON

Department of Civil and Environmental Engineering  
*Division of Building Technology*

*Building Physics*

CHALMERS UNIVERSITY OF TECHNOLOGY  
Göteborg, Sweden 2013  
Master's Thesis 2013:109



# Air Infiltration through Building Entrances

*Master of Science Thesis in the Master's Programme Structural Engineering and  
Building Technology*

NICKLAS KARLSSON

Department of Civil and Environmental Engineering  
*Division of Building Technology*  
*Building Physics*  
CHALMERS UNIVERSITY OF TECHNOLOGY  
Göteborg, Sweden 2013

Air Infiltration through Building Entrances

*Master of Science Thesis in the Master's Programme Structural Engineering and Building Technology*

NICKLAS KARLSSON

© NICKLAS KARLSSON, 2013

Examensarbete / Institutionen för bygg- och miljöteknik,  
Chalmers tekniska högskola 2013:109

Department of Civil and Environmental Engineering

Division of *Building Technology*

Building Physics

Chalmers University of Technology

SE-412 96 Göteborg

Sweden

Telephone: + 46 (0)31-772 1000

Cover: Illustration of infiltration flow through a sliding door entrance with a vestibule.

Chalmers reproservice / Department of Civil and Environmental Engineering  
Göteborg, Sweden 2013



## Air Infiltration through Building Entrances

*Master of Science Thesis in the Master's Programme Structural Engineering and Building Technology*

NICKLAS KARLSSON

Department of Civil and Environmental Engineering

Division of *Building Technology*

Building Physics

Chalmers University of Technology

### ABSTRACT

There is lack of information concerning the energy performance of different entrance solutions. There is also a lack in guidelines how to model them in building energy simulation software. Building energy simulation software such as IDA-ICE can be used to calculate infiltration through the entrances of buildings. Therefore the focus of this master thesis is to find calculation models for different types of entrances and implement these in IDA-ICE.

Literature studies on infiltration through swing, sliding and revolving doors were conducted. Out of the information acquired in the literature studies three calculation models were selected. For open-type doors such as swing and sliding doors one model was enough. Revolving doors required two models, one for infiltration through the door seals and one for the infiltration due to the motion of the door. These calculation models, mostly design curves were implemented in IDA-ICE by using or manipulating standard components of the software.

A simplified energy model of an office building was created in the sole purpose of analyzing the energy loss of infiltration through the building entrance. An array of six different open-type doors and three revolving doors were simulated under three different door usage schedules. Additionally simulations were conducted on cases with double height of the building, pressurization and depressurization to examine the impact on different entrances from stack effect and mechanically induced pressure difference.

Finally due to cooperation with a fellow student the door models were implemented in an energy model of the Nils Ericson terminal in Gothenburg, Sweden. Thanks to energy consumption data and year and location specific climate data the door models could be validated in some extent.

Key words: Air infiltration, entrances, swing door, sliding door, revolving door, energy simulation, energy modeling, IDA-ICE, bus terminal



## Luftinfiltration genom byggnadsentréer

*Examensarbete inom Structural Engineering and Building Technology*

NICKLAS KARLSSON

Institutionen för Bygg- och Miljöteknik

Avdelningen för Byggnadsteknologi

Byggnadsfysik

Chalmers Tekniska Högskola

### SAMMANFATTNING

Det finns en brist på information kring energieffektiviteten hos olika entrélösningar. Det saknas även riktlinjer för hur de ska modeleras i energisimuleringsmjukvaror. Energisimuleringsmjukvaror som IDA-ICE kan användas för att beräkna infiltration genom byggnadsentréer. Därav ligger fokus i detta masterarbete på att hitta beräkningsmodeller för olika entrétyper och implementera modellerna i IDA-ICE.

Litteraturstudier av infiltration genom slag-, skjut och karuselldörrar har utförts. Från informationen som inhämtades från litteraturstudien valdes tre beräkningsmodeller. För dörrar av öppen typ som slag- och skjutdörrar behövdes enbart en modell. För karuselldörrar krävdes två modeller, en för infiltration genom dörrens tätningsslister och en för infiltrationen som uppstår genom dörrens rörelse. Dessa beräkningsmodeller, mestadels designgrafer implementerades i IDA-ICE genom att använda eller manipulera programmets standardkomponenter.

En förenklad energimodell av en kontorsbyggnad upprättades i syfte att analysera energiförlusterna från infiltration genom byggnadens entré. En uppsättning av 6 olika entrétyper av öppet slag och 3 entréer med karuselldörrar simulerades med olika scheman för personflöden. Ytterligare simuleringar utfördes på fall med dubbel byggnadshöjd samt med över/undertryck för att se vilken effekt skorstenseffekt och mekaniskt framkallat tryck har på entréernas energiprestanda.

Slutligen genom ett samarbete med en kurskamrat så kunde dörrmodellerna implementeras i en energimodell av Nils Ericson terminalen i Göteborg. Genom energianvändningsdata samt med en års- och platsspecifik klimatfil kunde dörrmodellerna valideras i viss utsträckning.

Nyckelord: Luftinfiltration, entréer, slagdörr, skjutdörr, karuselldörr, energisimulering, energimodellering, IDA-ICE, bussterminal



# Contents

ABSTRACT	I
SAMMANFATTNING	III
CONTENTS	IV
PREFACE	VII
NOTATIONS	VIII
1 INTRODUCTION	1
1.1 Background	1
1.2 Purpose and objective	1
1.3 Limitations	1
1.4 Methodology	2
1.5 IDA Climate and Energy	3
2 AIR INFILTRATION THEORY	4
2.1 Introduction	4
2.2 Large vertical opening model CELVO	7
2.3 Power law leak model CELEAK	10
3 OPEN-TYPE DOORS LITERATURE STUDY	11
3.1 Introduction to open-type doors	11
3.1.1 Vestibules	13
3.2 The Khorl Study	14
3.3 The Cho et al study	14
3.4 The Yuill study	16
3.4.1 Vestibules	18
3.4.2 Results	18
3.5 Selected model for open type doors	20
4 REVOLVING DOORS LITERATURE STUDY	22
4.1 Introduction of revolving doors	22
4.2 Studies	24
4.2.1 The Schutrum et al study	24
4.2.2 The Zmeureanu et al study	26
4.2.3 The Lin Du study	27
4.2.4 The Allgayer study	28
4.2.5 Studies made by manufacturers	29
4.3 Selected models for revolving doors	30
4.3.1 Model for calculating leakage through the seals of a revolving door	31

4.3.2	Model for calculating the air exchange induced by the revolving motion of a door	35
4.3.3	Model for door usage	37
5	IMPLEMENTATION OF SELECTED MODELS IN IDA-ICE	38
5.1	Open type doors	38
5.2	Revolving doors	40
5.2.1	Infiltration due to the motion of the door	40
5.2.2	Infiltration through the door seals	46
6	CASE STUDY: SIMPLE OFFICE MODEL	51
6.1	The IDA-ICE model	51
6.2	Evaluation of best and worst wind cases	52
6.3	Door-usage schedules	54
6.4	Simulation cases	56
6.4.1	Reference Case	56
6.4.2	Double height case	57
6.4.3	Case with +5 Pa mechanically induced pressure difference	57
6.4.4	Case with -5 Pa mechanically induced pressure difference	58
7	CASE STUDY: NILS ERICSON TERMINAL, NET	59
7.1	Introduction	59
7.2	Entrances of NET	60
7.2.1	Door usage at NET	61
7.3	Extended model for open type doors	63
7.4	Scale up of revolving door model	64
7.5	Simulation cases	66
7.5.1	Reference case	66
7.5.2	Gate study	67
7.5.3	Main entrance study	67
7.5.4	Optimization studies	67
8	RESULTS FROM THE STUDY CASES	68
8.1	Simple office model	68
8.1.1	Reference case	68
8.1.2	Double height case	72
8.1.3	Mechanically induced pressure difference cases	74
8.2	Nils Ericson Terminal	79
8.2.1	Reference study	79
8.2.2	Gate study	80
8.2.3	Main Entrance Study	82
8.2.4	Optimization cases	84
8.2.5	Revolving door study	86

8.2.6	Impact on the indoor climate	87
9	DISCUSSION AND CONCLUSIONS	88
9.1	General	88
9.2	Revolving doors	88
9.3	Open-type doors	89
9.4	Comparison of results between simple office model and NET	89
9.5	Air curtains	90
10	RECOMMENDATION FOR FURTHER STUDIES	91
11	REFERENCES	92
	APENDIX A: PRESSURE DIFFERENCES	94
	APENDIX B: ENTRANCE TYPES	99
	APENDIX C: DOOR USAGE DATA AND USAGE SCHEDULE INPUT OF NET	100





## **Preface**

In this thesis energy performance for different kinds of entrances has been investigated. The investigations have been done with the building energy simulation software IDA-ICE. From literature studies different calculation models available have been analyzed and implemented into the software.

The report was carried out at the division of Building Technology at the Chalmers University of Technology in Sweden in cooperation with ÅF-infrastructure AB. The project has been supervised by associate professor Angela Sasic who has been a great source of inspiration and support during the entire process.

I specially want to thank fellow student Cajsa Lindström for her cooperation which made it possible to implement my work on a highly detailed building model. I also want to thank my colleagues at ÅF –Infrastructure AB. Finally I want to thank the companies; EQUA, Boon Edam and Besam who helped with software and information.

Göteborg, June 2013

Nicklas Karlsson



# Notations

## Roman upper case letters

$A_{Leak}$	Leakage relative to area
$C_A$	Air flow coefficient $\left[ \frac{m^3}{m^2 \cdot s \cdot Pa^n} \right]$
$C_d$	Discharge coefficient
$C_{d,A}$	Discharge coefficient given by area $\left[ \frac{m^3}{m^2 \cdot s \cdot Pa^n} \right]$
$C_{d,L}$	Discharge coefficient given by length $\left[ \frac{m^3}{m \cdot s \cdot Pa^n} \right]$
$C_m$	Mass flow power law coefficient $\left[ \frac{kg}{s \cdot Pa^n} \right]$
$C_p$	Wind pressure coefficient
$F_p$	Flow of people [ <i>People per hour</i> ]
$N_c$	Number of compartments
$N_{rpm}$	Rotation speed of a revolving door [ <i>rpm</i> ]
$N_{PPC}$	Number of people per compartment
$P_1$	Air pressure in zone 1 [ <i>Pa</i> ]
$P_2$	Air pressure in zone 2 [ <i>Pa</i> ]
$Q_{inf}$	Air infiltration power [ <i>W</i> ]
$R_{usage}$	Usage ratio
$S_{Control}$	Control signal
$S_{final}$	Final control signal
$S_{flow}$	Flow control signal
$T_{in}$	Indoor temperature [ $^{\circ}C$ ]
$T_{out}$	Outdoor temperature [ $^{\circ}C$ ]
$\dot{V}$	Volumetric air flow $\left[ \frac{m^3}{s} \right]$
$\dot{V}_{average}$	Average volumetric air flow $\left[ \frac{m^3}{s} \right]$
$\dot{V}_{inf}$	Volumetric air infiltration flow $\left[ \frac{m^3}{s} \right]$
$\dot{V}_{inf\_prototype}$	Volumetric air infiltration flow of a prototype door $\left[ \frac{m^3}{s} \right]$
$\dot{V}_{max}$	Maximum volumetric air flow $\left[ \frac{m^3}{s} \right]$
$\dot{V}_{modern,worn}$	Air leakage of a modern worn revolving door $\left[ \frac{l}{s} \right]$
$\dot{V}_{modern,maintained}$	Air leakage of a modern maintained revolving door $\left[ \frac{l}{s} \right]$

$\dot{V}_{modern\ door,new}$	Air leakage of a modern new revolving door $\left[\frac{l}{s}\right]$
$\dot{V}_{S,mean}$	Air leakage of a door from the Schutrum study $\left[\frac{l}{s}\right]$
$\dot{V}_{Z,mean}$	Air leakage of a door from the Zmeureanu study $\left[\frac{l}{s}\right]$
$\dot{V}_{\Delta T=x}$	Air flow depending on the temperature difference $\left[\frac{l}{s}\right]$
$W$	Width of a door $[m]$
$W_d$	Wind direction $[^\circ]$
$W_{d,mean}$	Mean wind direction $[^\circ]$
$X$	Flow of people $\left[\frac{People}{5\ minutes}\right]$
$Z_n$	Height of the neutral pressure plane

### Roman lower case letters

$S_{area}$	Scale factor from area differences
$S_{Volume}$	Scale factor from volume differences
$z_{b1}$	Height over floor of the opening bottom in zone 1
$z_{b2}$	Height over floor of the opening bottom in zone 2
$g$	Gravitational constant $\left[\frac{m}{s^2}\right]$
$r$	Average opening ratio
$w$	Width of a fully open door $[m]$
$z_t$	Height of an opening $[m]$
$\dot{m}$	Mass flow $\left[\frac{m^3}{s}\right]$
$\dot{m}_{12}$	Mass flow from zone 1 to zone 2 $\left[\frac{m^3}{s}\right]$
$\dot{m}_{21}$	Mass flow from zone 2 to zone 1 $\left[\frac{m^3}{s}\right]$

### Greek upper case letters

$\Delta P$	Air pressure difference $[Pa]$
$\Delta P_s$	Air pressure difference caused by stack effect $[Pa]$
$\Delta P_{tot}$	Total air pressure difference $[Pa]$
$\Delta P_v$	Air pressure difference caused by ventilation $[Pa]$
$\Delta P_w$	Air pressure difference caused by wind $[Pa]$
$\Delta P_{bottom}$	Air pressure difference at the top of the opening $[Pa]$
$\Delta P_{top}$	Air pressure difference at the bottom of the opening $[Pa]$
$\Delta T$	Temperature difference $[^\circ C]$

### **Greek lower case letters**

$\rho_1$	Air density in zone 1 $\left[\frac{kg}{m^3}\right]$
$\rho_2$	Air density in zone 2 $\left[\frac{kg}{m^3}\right]$
$\rho_a$	Air density $\left[\frac{kg}{m^3}\right]$

### **Abbreviations**

AHU	Air handing unit
CAV	Constant Air Volume, constant air flow
BES	Building energy simulation software
ELA	Equivalent leakage area
IDA-ICE	IDA Climate and Energy a building energy simulation software
NET	Nils Ericsson bus terminal building



# **1 Introduction**

## **1.1 Background**

Today construction and development of more energy efficient buildings is a fact. The development of energy efficient buildings in the current scale is much dependent on the decisions in the EU who set the goal that energy consumption in our buildings has to be reduced by 20% by 2020 compared to 1995.

In order to make our buildings more energy effective, every part of their climate envelope has to be analyzed and improved. Depending on the design, dimensions and use of the building, different building parts play bigger or smaller roles. The entrances of a building have a great effect in buildings where they are frequently used, such as supermarkets, shopping centers, high rise office buildings and terminals.

During several years there have been development and research of energy efficient buildings. This development in combination with the increase in computational capacity has given birth to different tools such as building energy simulation software. This software is used by both scientists and designers to analyze and optimize new and existing buildings in terms of energy performance.

The infiltration of outdoor air is for some buildings the largest energy loss. Today it is common that energy performance of a building is analyzed before the construction of the building. There are many uncertainties when modeling entrances. Such as the effect of a vestibule, the effect of air curtains and the lack of information concerning the energy performance of revolving doors.

Additionally BELOK which is cooperation between the Swedish Agency of Energy and 17 of the largest owners of commercial buildings has in a report concluded that there is a lack of knowledge in the energy performance of different entrance types (BELOK, 2013).

## **1.2 Purpose and objective**

The aim of this thesis is to find calculation models of air infiltration for different entrance types. These models will be implemented in a building energy simulation software in order to study the energy performance of different building entrances.

## **1.3 Limitations**

In order to keep the thesis work within a reasonable time limit some borders has to be made. The base will of the thesis will include the following.

- Review of studies conducted on different entrance types focused to doors with automatic operation
- Input data for different entrances and setups will be extracted from previous studies
- Calculation models for different entrances and setups will be constructed
- Implementation of data and calculation models in the software IDA-ICE.
- Case study on a simple building with different entrance types
- Case study on an existing terminal building

## 1.4 Methodology

The project began with literature studies where knowledge of infiltration theory was acquired. The next step was to search for reports and measurements where the infiltration through different entrances has been studied. Knowledge of the building energy software at an advanced level had to be acquired. When a sufficient level of understanding was obtained the work of implementing the different models in the building energy simulation software began. When these models were implemented, energy simulations on a reference building were conducted. Later on cooperation with Cajsa Lindström started where we conducted energy simulations on the Nils Ericsson Terminal building with focus on different entrance solutions. When all simulations were done the most important results was presented and guidelines for modeling entrances were constructed.



## 1.5 IDA Climate and Energy

The building energy simulation software (BES) used in this study is IDA Indoor Climate and Energy (IDA-ICE). It is a dynamic multi-zone simulation application used for studies on indoor climate and whole year energy consumption. IDA-ICE is chosen for this thesis since it is very transparent. The physical models used can be visualized in code and it is possible to edit or make new models. (EQUA, 2013)

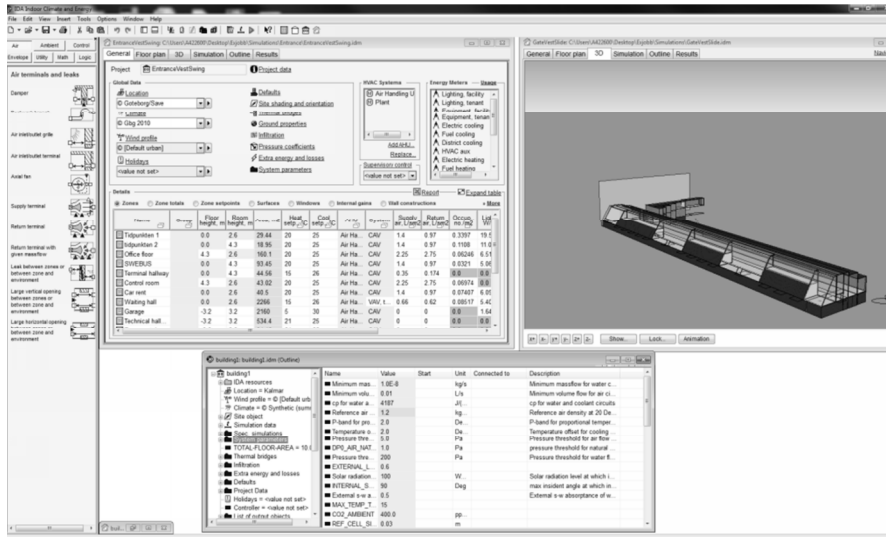


Figure 1.1. A view over the user interface of IDA-ICE.

The models in IDA-ICE are written in the Neutral Model Format (NMF) which is a software independent language for modelling dynamical systems by algebraic equations (Salvalai, 2012). The code is very clear and easy to understand. To be able to implement the code into the IDA-ICE application additional software called IDA-NMF translator is required. The process of creating a new model in IDA-ICE is described in figure 1.2.

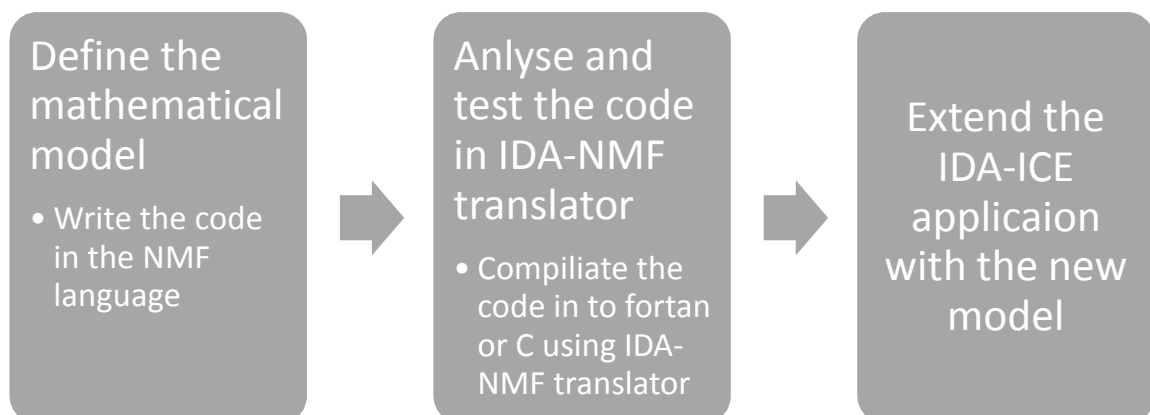


Figure 1.2. The process of creating a new component model.

## 2 Air infiltration theory

This chapter will give an introduction to air infiltration and what consequences this phenomena have on the building. Further on equations and models used in IDA-ICE will be presented.

### 2.1 Introduction

Air infiltration is the unwanted flow of outdoor air into a building through cracks, unintentional openings and the normal use of doors. Air leakage is another name used for air infiltration. For modern air tight houses the infiltration is considered as a small part of the total energy losses. For commercial buildings such as office buildings the door usage is much higher and therefore air infiltration has a larger impact on the total energy consumption. Air infiltration doesn't only affect the energy consumption but also the air quality and thermal comfort of the building (ASHRAE, 2009). Examples of these consequences are found in table 2.1.

Table 2.1. Consequences of air infiltration (Sandberg et al, 2007).

Category:	Consequence:
Energy	Increased heating demand during the heating period
	Increased cooling demand during the cooling period
	Increased energy losses due to disturbances in the ventilation system
Thermal Comfort	Draught
	Cold floors
Air quality	Disturbances in the function of the ventilation system
	Inflow of pollutants, smells, gases and particles

The infiltration flow can be described with the power law model. The power law model as defined with equation 1 is commonly used when calculating infiltration through cracks and narrow corridors. The equations have been extracted from (Hagentoft, 2003).

$$\dot{V} = C_d * \Delta P^n \left[ \frac{m^3}{s} \right] \quad (1)$$

Where

$\dot{V}$  is the volumetric flow rate  $\left[ \frac{m^3}{s} \right]$

$C_d$  is the discharge coefficient  $\left[ \frac{m^3}{s * Pa^n} \right]$

$\Delta P$  is the pressure difference  $[Pa]$

$n$  is the flow exponent

The discharge coefficient can be given per length or per area as defined in equation 2 and 3.

$$C_{d,L} = \left[ \frac{m^3}{m \cdot S \cdot Pa^n} \right] \quad \rightarrow \quad \dot{V} = C_{d,L} * L * \Delta P^n, L [m] \quad (2)$$

$$C_{d,A} = \left[ \frac{m^3}{m^2 \cdot S \cdot Pa^n} \right] \quad \rightarrow \quad \dot{V} = C_{d,A} * A * \Delta P^n, A [m] \quad (3)$$

The energy impact of air infiltration is considered as a product of the mass flow rate of the air infiltration, the heat capacity of air and the temperature difference between inside and outside. This expression is given in equation 4 which has been extracted from (Younes et al, 2012).

$$Q_{inf} = \dot{m} * C_p * (T_{in} - T_{out}) [W] \quad (4)$$

$$\dot{m} = \dot{V} * \rho_a \left[ \frac{kg}{s} \right] \quad (5)$$

Where

$Q_{inf}$  is the air infiltration power [W]

$\dot{m}$  is the air infiltration mass flow rate  $\left[ \frac{kg}{s} \right]$

$T_{in}$  is the indoor air temperature [ $^{\circ}C$ ]

$T_{out}$  is the outdoor air temperature [ $^{\circ}C$ ]

$C_p$  is the specific heat capacity of air  $\left[ \frac{J}{kg \cdot ^{\circ}C} \right]$

$\rho_a$  is the density of air  $\left[ \frac{kg}{m^3} \right]$

The pressure difference over the building envelope is the driving mechanism for air infiltration. There are three mechanisms which contribute to the total pressure difference. These mechanisms are the following:

- Stack pressure
- Wind pressure
- Mechanically induced pressure

In order to calculate the resulting infiltration rate over the building envelope the pressure differences of stack, wind and mechanical systems must be combined. Since the airflow rates are not linear, the pressure differences must be added together before calculating the resulting flow. Separate flows induced by wind, stack and mechanical pressure differences can't be added together (ASHRAE, 2009).

The sum of the pressure differences induced by wind, stack and mechanical ventilation results in the total air pressure difference over the building envelope, see equation 6. In this report the pressure difference is defined positive when the pressure is higher on the outside than on the inside. For more information of the different causes to pressure differences see Appendix A.

$$\Delta P_{\text{tot}} = \Delta P_w + \Delta P_s + \Delta P_v \text{ [Pa]} \quad (6)$$

Where

$\Delta P_{\text{tot}}$  is the total pressure difference [Pa]

$\Delta P_s$  is the pressure difference from the stack effect [Pa]

$\Delta P_w$  is the pressure difference from wind [Pa]

$\Delta P_v$  is the pressure difference from mechanical ventilation [Pa]

(Hagentoft, 2003)

## 2.2 Large vertical opening model CELVO

CELVO is the model used in IDA-ICE to calculate mass flows through large vertical openings such as entrances. The model is bidirectional and it allows flow in two directions simultaneously. The model takes in to count the shape of the pressure profile over the doorway. Depending on the shape of the pressure profile different sets of equations are used. Three different cases of pressure profiles are found in figure 2.1. All equations in this chapter are extracted from (Bring et al, 1999)

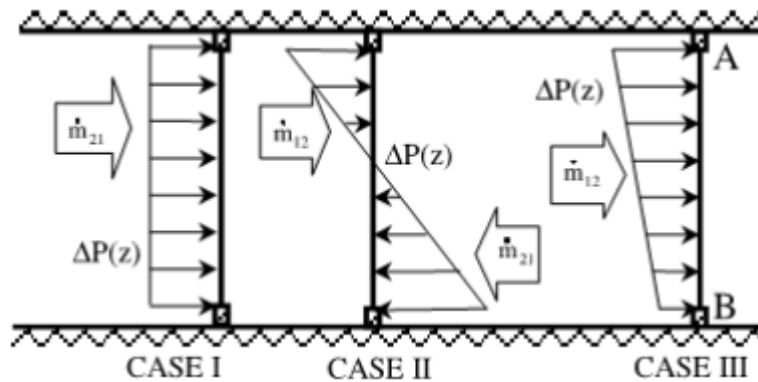


Figure 2.1. Pressure profiles over a large vertical opening (Woloszyn et al, 1999).

The pressure difference at the bottom of the opening is calculated by equation 7.

$$\Delta p_{bottom} = (P_1 - \rho_1 * g * z_{b1}) - (P_2 - \rho_2 * g * z_{b2}) [Pa] \quad (7)$$

Where

$z_{b1}$  and  $z_{b2}$  is the height of the bottom of the door from the floor level in zone 1 and zone 2.

$P_1$  and  $P_2$  are the air pressures in zone 1 and zone 2 [Pa]

$\rho_1$  and  $\rho_2$  are the air densities in zone 1 and zone 2 [Pa]

$g$  is the gravitational constant  $\left[\frac{m}{s^2}\right]$

The pressure difference at the top of the opening is calculated by equation 8.

$$\Delta p_{top} = \Delta p_{bottom} - (\rho_1 * g * z_t + \rho_2 * g * z_t) [Pa] \quad (8)$$

Where

$z_t$  is the height of the opening [m]

In the case 1 as illustrated in figure 2.1 a flat pressure profile, the mass flows are calculated with the equations 9, 10, 11 and 12.

If  $P_1 > P_2$  then

$$\dot{m}_{12} = C_d * w * z_t * \sqrt{2 * \rho_1 (P_1 - P_2)} \left[ \frac{kg}{s} \right] \quad (9)$$

$$\dot{m}_{21} = 0 \left[ \frac{kg}{s} \right] \quad (10)$$

If  $P_1 < P_2$  then

$$\dot{m}_{12} = 0 \left[ \frac{kg}{s} \right] \quad (11)$$

$$\dot{m}_{21} = C_d * w * z_t * \sqrt{2 * \rho_2 (P_1 - P_2)} \left[ \frac{kg}{s} \right] \quad (12)$$

Where

$\dot{m}_{12}$  and  $\dot{m}_{21}$  are the mass flows from zone 1 to zone 2 and from zone 2 to zone 1  $\left[ \frac{kg}{s} \right]$

$C_d$ - is the discharge coefficient set to 0,65 by default.

$w$  - is the width of the opening,  $w * z_t$  represents the area of the opening  $[m]$

In the cases 2 and 3 as illustrated in figure 2.1 where the pressure profile over the opening is inclined the following equations are used.

First the location of neutral pressure level is calculated by equation 13.

$$Z_n = \frac{\Delta p_{bottom}}{g * (\rho_1 - \rho_2)} [m] \quad (13)$$

The help variables Top and Bot is introduced as equation 14 and 15.

$$Top = \frac{C_d * \frac{2}{3} * w * |\Delta p_{top}|^{\frac{3}{2}}}{g * (\rho_1 - \rho_2)} \quad (14)$$

$$Bot = \frac{C_d * \frac{2}{3} * w * |\Delta p_{bottom}|^{\frac{3}{2}}}{g * (\rho_1 - \rho_2)} \quad (15)$$

In the case where the neutral level is below the bottom of the opening, the mass flows are calculated by the equations 16,17,18,19.

If  $\rho_1 > \rho_2$  then

$$\dot{m}_{12} = 0 \left[ \frac{kg}{s} \right] \quad (16)$$

$$\dot{m}_{21} = (Top - Bot) * \sqrt{2 * \rho_2} \left[ \frac{kg}{s} \right] \quad (17)$$

If  $\rho_1 < \rho_2$  then

$$\dot{m}_{12} = (Bot - Top) * \sqrt{2 * \rho_2} \left[ \frac{kg}{s} \right] \quad (18)$$

$$\dot{m}_{21} = 0 \left[ \frac{kg}{s} \right] \quad (19)$$

In the case where the neutral level is above the bottom of the opening, the mass flows are calculated by the equations 20, 21, 22 and 23.

If  $\rho_1 > \rho_2$  then

$$\dot{m}_{12} = (Bot - Top) * \sqrt{2 * \rho_2} \left[ \frac{kg}{s} \right] \quad (20)$$

$$\dot{m}_{21} = 0 \left[ \frac{kg}{s} \right] \quad (21)$$

If  $\rho_1 < \rho_2$  then

$$\dot{m}_{12} = 0 \left[ \frac{kg}{s} \right] \quad (22)$$

$$\dot{m}_{21} = (Top - Bot) * \sqrt{2 * \rho_2} \left[ \frac{kg}{s} \right] \quad (23)$$

In a case where the neutral level is located somewhere in between the bottom and top of the opening, the mass flows are calculated by the equations 24, 25, 26 and 27.

If  $\rho_1 > \rho_2$  then

$$\dot{m}_{12} = Bot * \sqrt{2 * \rho_1} \left[ \frac{kg}{s} \right] \quad (24)$$

$$\dot{m}_{21} = Top * \sqrt{2 * \rho_2} \left[ \frac{kg}{s} \right] \quad (25)$$

If  $\rho_1 < \rho_2$  then

$$\dot{m}_{12} = -Top * \sqrt{2 * \rho_1} \left[ \frac{kg}{s} \right] \quad (26)$$

$$\dot{m}_{21} = -Bot * \sqrt{2 * \rho_2} \left[ \frac{kg}{s} \right] \quad (27)$$

## 2.3 Power law leak model CELEAK

The model used for calculating mass flow through smaller openings such as cracks are called CELEAK in IDA-ICE. This model does not allow simultaneously flow in two directions. There is the option to define the leak as an equivalent leak area ELA, which correspond to the area which in combination with  $C_m=1$  at  $\Delta P=4$  would give the same flow as a leak with the real area and different  $C_m$ . All equations in this chapter are extracted from (Bring et al, 1999)

The mass flow is calculated with equation 28.

$$\dot{m} = C_m * \Delta P^n \left[ \frac{kg}{s} \right] \quad (28)$$

Where

$\dot{m}$  is the mass flow rate  $\left[ \frac{kg}{s} \right]$

$C_m$  is the mass flow power law coefficient  $\left[ \frac{kg}{s * Pa^n} \right]$

If the pressure difference is negative the mass flow is calculated with equation 29.

$$\dot{m} = -C_m * |\Delta P|^n \left[ \frac{kg}{s} \right] \quad (29)$$

The direction of the mass flow is defined with the equations 30, 31, 32 and 33.

If  $\dot{m} > 0$

$$\dot{m}_{12} = \dot{m} \left[ \frac{kg}{s} \right] \quad (30)$$

$$\dot{m}_{21} = 0 \left[ \frac{kg}{s} \right] \quad (31)$$

If  $\dot{m} < 0$

$$\dot{m}_{12} = 0 \left[ \frac{kg}{s} \right] \quad (32)$$

$$\dot{m}_{21} = |\dot{m}| \left[ \frac{kg}{s} \right] \quad (33)$$



### 3 Open-type doors literature study

This chapter will begin with a short introduction to open type doors. Further on different studies concerning air infiltration through open-type doors will be presented. Finally from the information obtained from these studies the selected model for this thesis will be presented.

Some previous studies concerning the energy performance of swing and sliding doors have been conducted. Yuill et al conducted a very useful report in 1996 where discharge coefficients were measured for different entrance types and setups. In combination with various field studies a calculation method for different entrances types depending on the flow of people was constructed (Yuill et al, 1996). A few years later in 2001 Kohri made a probability approach to determine the average opening ratio of a sliding door at different flows of people (Kohri, 2001). Further on as a result of the ASHRAE 90.1 vestibule requirements Cho et al analyzed the energy saving potential of vestibules (Cho et al, 2010). In March 2012 the National Renewable Energy Laboratory published the Retail Building Guide for Entrance Energy Efficiency Measures. This guide presents calculation methods identical to the ones in the Yuill report. Further on the guide describes how and when to use the methods and illustrates the energy savings in an economical way (NREL, 2012).

#### 3.1 Introduction to open-type doors

Swing and sliding doors are the most common doors used as entrances for larger buildings such as shopping malls, office buildings and supermarkets. Swing and sliding doors can be referred as “open-type doors”. Their simple operation makes them a suitable choice as access to buildings. The doors can be designed to obtain good air-tightness in their closed state but while they are open air exchanges are free to occur. (Allgayer, 2007)

Swing doors can be operated manually or with automatic openers while sliding doors are only operated with automatic openers. Both types of doors are commonly installed with a vestibule setup where two door sets are placed so that there is a room or vestibule between them.

Swing doors are the most common type of doors. At buildings with a low flow of people passing through the door way the most common solution is a swing door without automatic operation. Some buildings with low people flow still need to be accessible for disabled people and therefore has the automatic operation. These doors are rather easy to get air tight by applying and maintaining infiltration seals where the door meets the frame (Wulfinghoff 1999). Figure 3.1 illustrates a common swing door. All open-type door solutions in this thesis are found in Appendix B.



*Figure 3.1. To the left a set of swing doors illustrated and to the right a photo of real doors (Archiexpo, 2013).*

The swing door has the following pros and cons.

Pros:

- Excellent air tightness in closed state
- Flexible operation
- Secure solution

Cons:

- Low accessibility
- Dangerous if operated wrongly
- Decreased or no ability to operate at high pressure differences

Sliding doors is the most common entrance solution for buildings with high flows of people. The design and operation gives an excellent accessibility to the building. Compared to swing doors they require more space and they are harder to get air tight. Figure 3.2 illustrates sliding doors.



*Figure 3.2. To the left a sliding door is illustrated and to the right a foto of a real door (Archiexpo,2013).*

The sliding doors have the following pros and cons.

Pros:

- Very good accessibility
- Able to operate under high pressure differences
- High people flow capacity

Cons:

- Require the double width of the opening
- Poor security with standard design
- Harder to get air tight in closed state

### 3.1.1 Vestibules

The idea with a vestibule is that one door have a chance to be closed while the other one is open in that way a direct air exchange between the indoors and outdoors is prevented. By decreasing the direct air exchange with the outside environment results in decreased energy losses and a better indoor climate. When the flow of people through the vestibule increases the chance of having one door closed is decreased. Swing and sliding doors in vestibules setups are illustrated in figure 3.3. Additionally some vestibules have a 90 degree angle between the door sets.

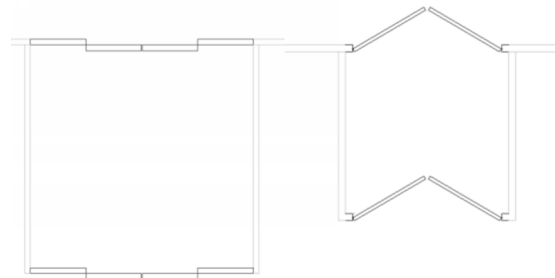


*Figure 3.3. To the left a vestibule with slide doors and to the right a vestibule with swing doors.*

### 3.2 The Khorri Study

The Kohri study brings forward one very important factor in modeling building entrances, the flow of people passing through the door. The flow of people affects the openness of a door which can be expressed in a ratio. It's not only the flow of people itself that affects the openness it is also the shape of the flow. An automatic door is operated by sensors and every operation such as opening or closing takes time. Flow of people is often obtained as people per hour but that doesn't mean that the time between every person that passes through the door is the same. Kohri brings up this issue as a probability problem. A simplified model of how to predict the average openness of a sliding door is presented both for a single door and doors in a vestibule setup (Kohri, 2001).

The opening ratio for a single sliding door is calculated by equation 34.

$$r = 1 - 0,26 * e^{-0,036*X} - 0,74 * e^{-0,0091*X} \quad (34)$$

The opening ratio for sliding door with a vestibule is calculated by equation 35.

$$r = 1 - 0,26 * e^{-0,036*X} - 0,74 * e^{-0,0091*X} \quad (35)$$

Where

$r$  is the average opening ratio of the entrance

$X$  is number of people that pass through the door during 5 minutes

### 3.3 The Cho et al study

As a result of the ASHRAE 90.1 vestibule requirements Cho et al analyzed the energy saving potential of adding a vestibule. It is concluded that building energy software have the potential to calculate the energy impact of door openings in an efficient way but there is a lack of studies on how to model the doors. In this study a mean constant air flow has been calculated with equations from the Yuill study (see chapter 3.4) and is combined by usage data of the door. This study has been very simplified at some parts but it gives an indication of the energy efficiency potential in adding a vestibule.

The following facts can be concluded from the report:

- Obtaining values for the door opening frequency is a vital part in energy modeling. These values can be obtained from either field studies or estimated from given occupancy information
- Small buildings with high door-opening frequency tend to have a larger percentage reduction in total energy use by adding a vestibule compared to larger buildings.
- School buildings which have a very high opening frequency during some hours have a small impact from a vestibule addition. Due to their large area.

The sensitivity analysis showed that the door opening frequency have a large impact on the infiltration rate see table 3.1. And it shows that the infiltration rate have a lower impact on the total energy consumption see table 3.2 (Cho et al, 2010).

Table 3.1. Impact of door-opening frequency on the infiltration rate (Cho et al, 2010).

Percentage Variation of Door-opening Frequency [%]	Door-opening Frequency [peak door openings per hour]	Peak Air Infiltration Rate through Door Openings [cfm]	Percentage Variation [%]
-30 %	63	1417	-26 %
-20 %	72	1585	-17 %
-10 %	81	1751	-8 %
Baseline	90	1913	0 %
10 %	99	2073	8 %
20 %	108	2231	17 %
30 %	117	2386	25 %

Table 3.2. Impact of infiltration on the total energy consumption (Cho et al, 2010).

Variation on Infiltration Rate through Door Openings	Total Energy Consumption Building with Vestibule [MMBtu]	Total Energy Consumption Building without Vestibule [MMBtu]	Percentage Savings	Difference from Baseline
-20%	1,423	1,470	3.20%	0.73%
-10%	1,433	1,486	3.57%	0.36%
Baseline	1,443	1,502	3.93%	Baseline
10%	1,453	1,518	4.28%	0.35%
20%	1,463	1,534	4.63%	0.70%

### 3.4 The Yuill study

In 1996 Yuill et al conducted a research project with the title “Impact of High Use Automatic Doors on Infiltration” (Yuill et al, 1996). The objective of this study was to develop a simple method that design engineers can use to estimate the infiltration through automatic entrance doors.

Two studies were conducted in this research project. One was a laboratory study of the discharge coefficients of doors with various geometries. This study was conducted on a one third scale model at a test facility. A room which was completely air tight was equipped with a fan in one end and a door in the other end. The fan was used to depressurize the room and the airflow of the fan was measured. The airflow through the door is equal to the air flow of the fan. The pressure difference over the door was also measured and with flow and pressure difference known the discharge coefficient could be calculated.

This process was used to determine the discharge coefficient for sliding and swing doors in a number of different setups with and without a vestibule. Furthermore the vestibules were configured so that the doors had different angles in relation to each other. Measurements were conducted for several different operation positions of the doors such as half open and nearly closed. Additionally a doll was placed in the door opening to simulate a person in order to measure the effect of people passing through the door. The experiments were performed over a range of differential pressures from 5 to 50 Pa. In total 1456 tests were conducted of 151 door positions in 15 door setups (Yuill et al, 1996).

For swing doors the discharge coefficient was measured for different opening angles;  $30^\circ$ ,  $60^\circ$  and  $90^\circ$ , see figure 3.4. For the sliding doors the discharge coefficient was measured for the opening ratio of  $1/8$ ,  $3/8$ ,  $1/2$  and  $3/4$ , see figure 3.5.



Figure 3.4. Door positions of which discharge coefficients were measured for swing doors.

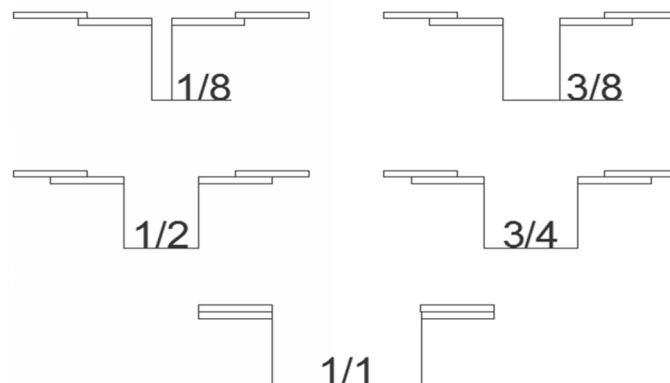


Figure 3.5. Door positions of which discharge coefficients were measured for sliding doors.

The second study conducted was a field study where times for the different stages in door operation were measured. The study was made on 109 doors which included 15800 door openings. The measured times are illustrated in figure 3.6 and are described below:

- Base open time, the minimum time a door would be open if no person passed through it.
- Time to reach fully open position(a)
- Duration of the fully open position(b)
- Time to close to the “slow close gap” position(c)
- Time to close the slow close gap” position(d)

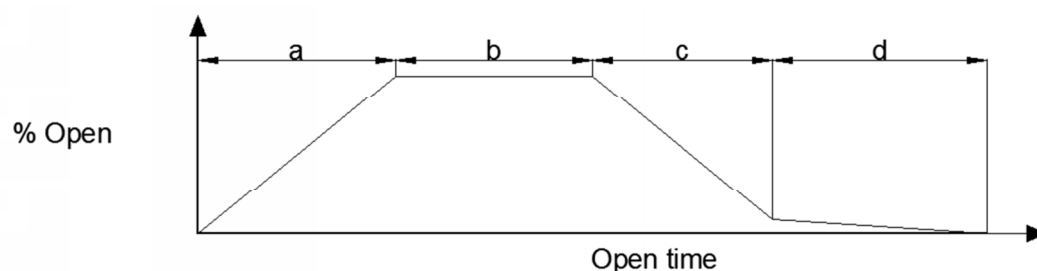


Figure 3.6. Illustration of different door opening positions related to time

When the discharge coefficient and the different operation times have been measured an average discharge coefficient was obtained by integrating over the door operation curve as in equation 36.

$$C_{d,avg} = (C_{d,a} * a + C_{d,b} * b + C_{d,c} * c + C_{d,d} * d) / (a + b + c + d) \quad (36)$$

Where

$C_{d,avg}$  is the average discharge coefficient  $\left[ \frac{m^3}{m^2 * s * Pa^n} \right]$

$C_{d,a}$  is the discharge coefficient for sector a

$C_{d,b}$  is the discharge coefficient for sector b

$C_{d,c}$  is the discharge coefficient for sector c

$C_{d,d}$  is the discharge coefficient for sector d

It was found that the “base open time” is an important factor in estimating the total time a door would be open. “Base open time” in combination with the number of people using the door per hour and the number of door openings per hour resulted in good correlating results.

The number of people passing through the door every hour and the number of people passing through during the opening time was also statistically measured. This combined with the time measurements resulted in a total open time per hour. When the total open time per hour is determined the averaged discharge coefficient is adjusted by taking into count what happens when a person is passing through the door. The resulting averaged discharge coefficient is therefore depending on the number of people per use. When the averaged discharge coefficient has been adjusted to the influence of people passing through it can be multiplied with the open time per hour. The result is the flow coefficient  $C_A$ .

### 3.4.1 Vestibules

For the cases where the different doors were set up in a vestibule configuration the base method is the same but the determination of the discharge coefficient became complicated. The complication occurred due to the fact that the coefficients depended on the openness of both doors. This was solved by using fourth order regression over two variables. The different times in operation was broken down to more sections, see figure 3.7.

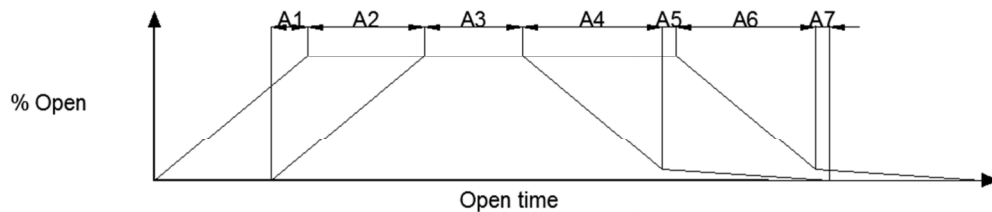


Figure 3.7. Illustration of different door opening positions related to time.

### 3.4.2 Results

The final results of this study were expressed in a couple of graphs where the airflow coefficient or adjusted discharge coefficient is plotted against the people flow through the door. The results for swing doors are found in figure 3.8 and the results for sliding doors are found in figure 3.9, the original results were expressed in  $\frac{cfm}{ft^2 \cdot \sqrt{in. of water}}$  and have been converted in to  $\frac{m^3}{m^2 \cdot s \cdot \sqrt{Pa}}$ .

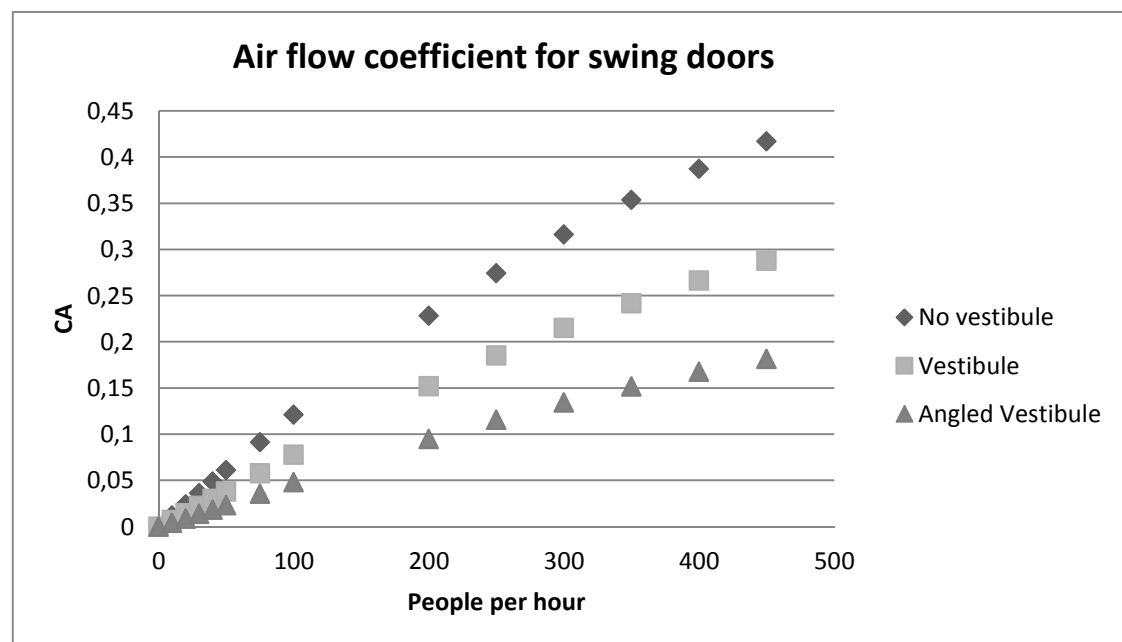


Figure 3.8. Graph of the air flow coefficient for swing doors as a function of the people flow.



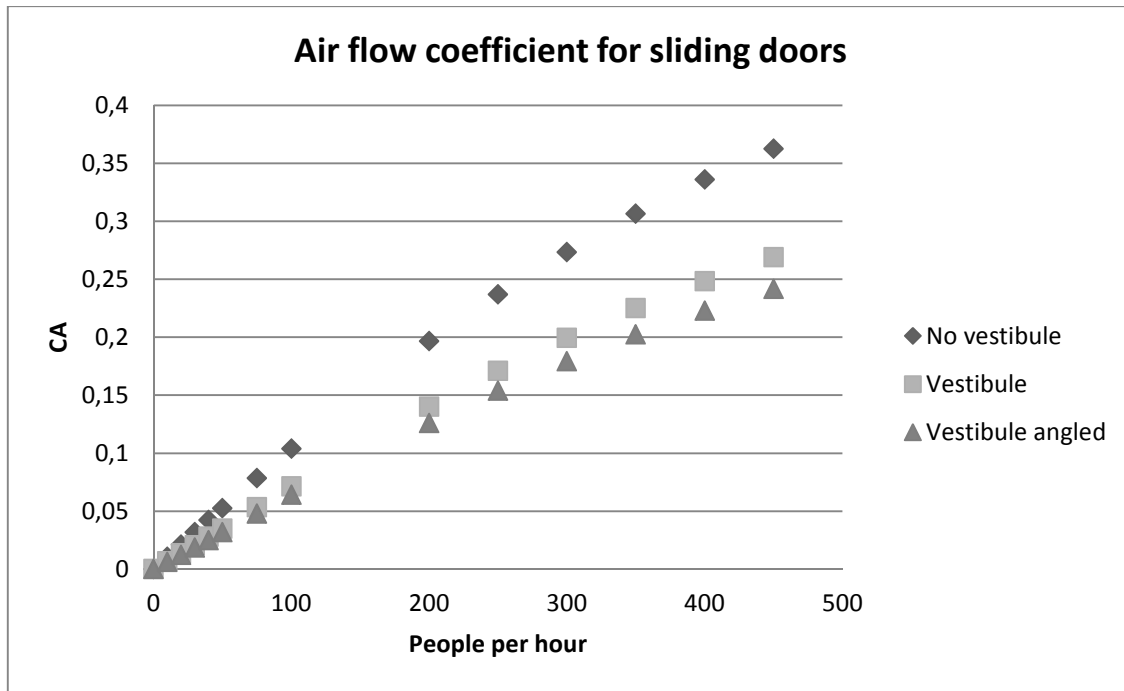


Figure 3.9. Graph of the air flow coefficient for sliding doors as a function of the people flow.

Other interesting results from the research project were the discharge coefficients for fully open doors in different door configurations. These discharge coefficients are found in table 3.3.

Table 3.3 Table of measured discharge coefficients for different door configurations (Yuill et al, 1996)

Door configuration:	$C_{d, \text{ fully open }} \left[ \frac{m^3}{m^2 \cdot s \cdot P_a^{0,5}} \right]$
Single swing door	0,62
Single sliding door	0,62
Swing doors with vestibule, inward opening	0,51
Swing doors with vestibule, outward opening	0,67
Sliding doors with vestibule	0,62
Swing doors with 90° vestibule	0,35
Sliding doors with 90° vestibule	0,35

### 3.5 Selected model for open type doors

The Yuill study was the most thorough report and the only report where discharge coefficients have been studied in laboratory experiments. In this thesis the resulting air flow coefficient  $C_A$  is considered as more accurate than the use of the standard discharge coefficient  $C_d = 0,65$  which is given by ASHRAE. The results of the Yuill study is based on averaged values from hundreds of measured entrances. Even though averaged values are used, the results of an energy calculation using  $C_A$  instead of  $C_d$  are considered as more accurate.

The Yuill study also provides a method in how to construct a more specific  $C_A$  for a specific door. By measuring the operation times for that unique door as explained in chapter 3.4 and then combine with the discharge coefficients presented in table 3.3 will result in a  $C_A$  for that specific door.

Equations of the air flow coefficients for the different entrance types are extracted from the result graphs of the Yuill study by the trend line function in Excel. The second order polynomial trend line was found to be best suited to these graphs. The coefficient of determination,  $R^2$  for these graphs proved to be 0,999 which indicate a well predicted model. Graphs with applied trend lines are found in figure 3.10 for swing doors and figure 3.11 for sliding doors. The extracted equations for swing doors are found in table 3.4 and for sliding doors in table 3.5.

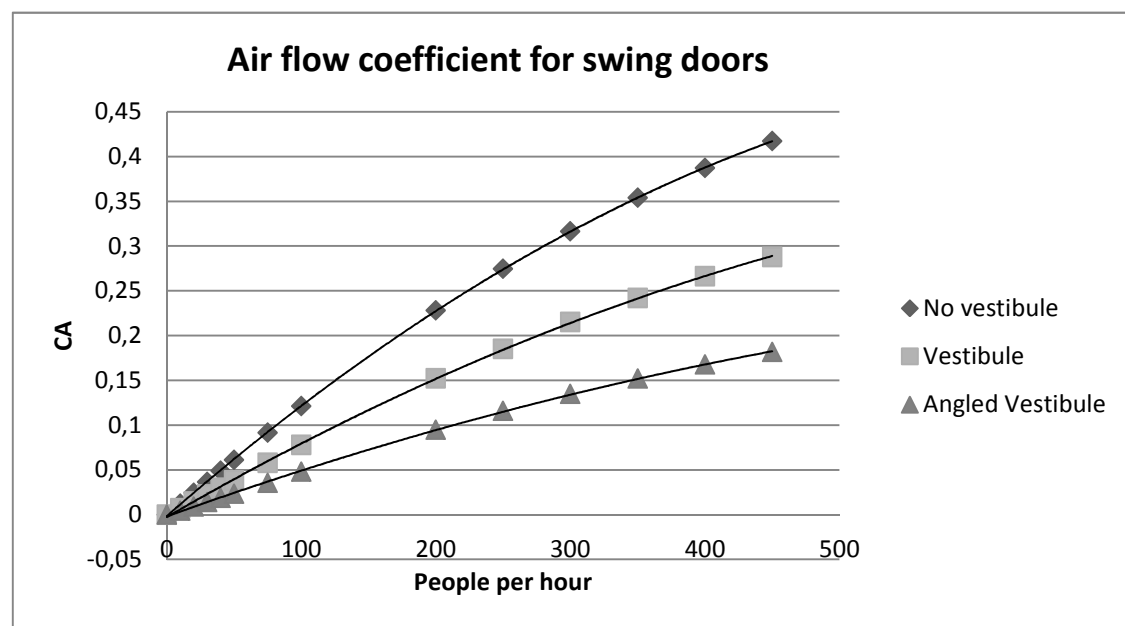


Figure 3.10. Graph of the air flow coefficient for swing doors as a function of the people flow, trend lines included.

Table 3.4. Equations for calculating the air flow coefficient for swing doors up to 450 PPH.

Equations for swing doors		
Door Type:	Air flow coefficient, $C_A$	
Single Door	$-9 * 10^{-7} * F_p^2 + 0,0013 * F_p - 0,0016$	(37)
Doors with vestibule	$-5 * 10^{-7} * F_p^2 + 0,0009 * F_p - 0,0028$	(38)
Doors with 90° vestibule	$-3 * 10^{-7} * F_p^2 + 0,0005 * F_p - 0,0019$	(39)

Where  $F_p$  is the flow of people [PPH]

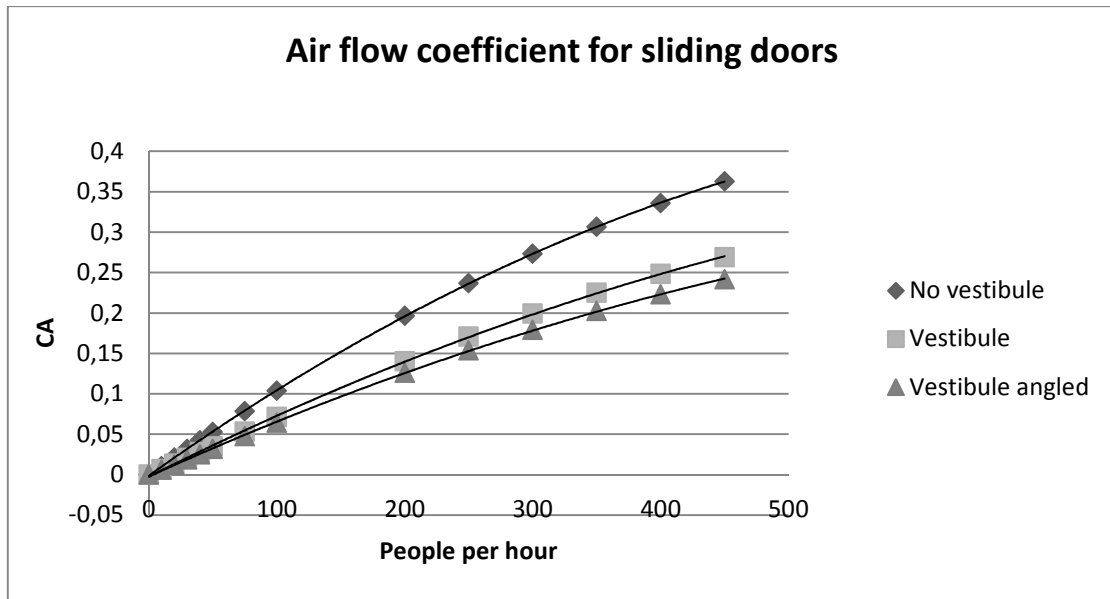


Figure 3.11. Graph of the air flow coefficient for swing doors as a function of the people flow, trend lines included.

Table 3.5. Equations for calculating the air flow coefficient for swing doors up to 450 PPH

Equations for slide doors	
Door Type:	Air flow coefficient, $C_A$
Single Door	$-7 * 10^{-7} * F_p^2 + 0,0013 * F_p - 0,0016$ (40)
Doors with vestibule	$-4 * 10^{-7} * F_p^2 + 0,0008 * F_p - 0,0024$ (41)
Doors with 90° vestibule	$-4 * 10^{-7} * F_p^2 + 0,0007 * F_p - 0,0021$ (42)

Where  $F_p$  is the flow of people [PPH]

NOTE: Equations 37-42 are misleading at very low flows of people. At 1-3 PPH the equations can result in a negative  $C_A$ .

The acquired equations for swing and sliding doors are to be considered as the chosen model which will be implemented into the BES and used to calculate the infiltration rate through entrances with swing and sliding doors.

## 4 Revolving doors literature study

This chapter will begin with a short introduction to revolving doors. Further on different studies concerning air infiltration through revolving doors will be presented. Finally selected calculation models based on these studies will be introduced.

### 4.1 Introduction of revolving doors

Revolving doors is an alternative to open-type doors. The operation of revolving doors is different from open-type doors in the way that they always maintain a physical separation between the indoor and outdoor climate. There are three common types of revolving doors which are illustrated in figure 4.1.

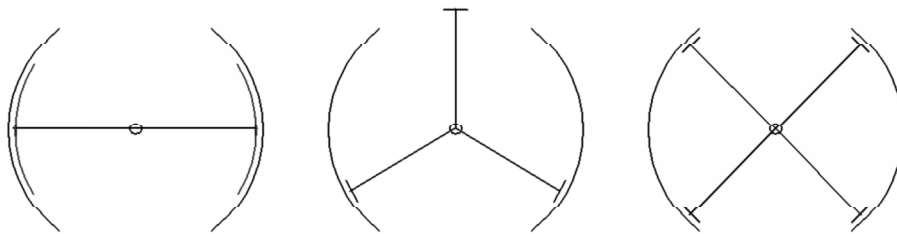


*Figure 4.1. To the left: 2-winged revolving door. In the middle: 3-winged revolving door. To the right: 4-winged revolving door.*

The two-winged door offers the largest volume of the segments and is therefore most suited where not only people but also larger objects need access. Such buildings can be supermarkets, shopping malls and airports where people use trollies and carry luggage. The four-winged door can be designed very compactly and still allow a high flow of people. Such doors are most suited where the floor space is very exclusive. A compromise between the two-winged and four-winged door is the three-winged. It allows a moderate flow of people while still enabling larger items to pass through. (Allgayer, 2007)

In 1888 Theophilus Van Kannel got his patent for a revolving door approved in the US. The door was announced as a new type of door which was storm proof. The door was claimed to have the following advantages:

- Noiseless operation, since there was no risk that moving parts of the door knocked in to each other
- Reduced ingress of wind, dust, snow and noise.
- Smooth operation since simultaneous traffic flow in 2 directions is possible
- Storm/Draught proof, since the wind is distributed on two wings resulting in zero net momentum which prevents the door from revolving due to strong wind.

Today it's well known that entrances with revolving doors are more energy efficient than the ones with swing or sliding doors. But until 1930 it was thought that the revolving door forced a greater air exchange per use than for a swinging door except under the worst conditions possible. However it is still quite unclear exactly how efficient the revolving doors are and the manufacturers fail to provide scientific data to support their products. It is however clear that revolving doors are more efficient than the open-type doors. (Allgayer, 2007)

## 4.2 Studies

The energy efficiency of revolving doors has been demonstrated in independent studies in the 1930s and 1960s. The physics behind air exchanges of open-type doors are considered to be well understood while the physics behind air exchanges of revolving doors has not been examined until 2007 when David Allgayer conducted his research. (Allgayer, 2007)

In 1961 Schutrum et al conducted experiments on a full scale four winged door. Leakages through door seals and air exchanges due to the revolving motion of the door were measured under various pressure and temperature differences (Schutrum et al, 1962). 42 years later in 2001 Zmeureanu et al reviewed the work of Schutrum and conducted new measurements on revolving doors which seals were worn in different degrees (Zmeureanu et al, 2001). In 2007 Allgayer made a real attempt to map the mechanisms of air exchanges due to the revolving motion of the door. Allgayer concluded that there are three operating regimes which decide the transfer rate of air through a revolving door. In 2009 Lin Du conducted experiments on a 1:10 scale model of a revolving door.

### 4.2.1 The Schutrum et al study

Schutrum et al conducted full scale experiments on a four bay revolving door. A sealed test room was connected with the outdoor environment see figure 4.3. The leakage through seals and the air exchange due to the revolving motion of the door were measured under various combinations of pressure and temperature differences. As a measuring method they used Hydrogen ( $H_2$ ) gas whose thermal conductivity was monitored. The experiments were carried out at different revolution rates of the door and also for different indoor and outdoor wind movements. The study resulted in several interesting graphs. In figure 4.2 the air infiltration through the seals is shown and in figure 4.3 the air infiltration due to the motion of the door is shown (Schutrum et al, 1962).

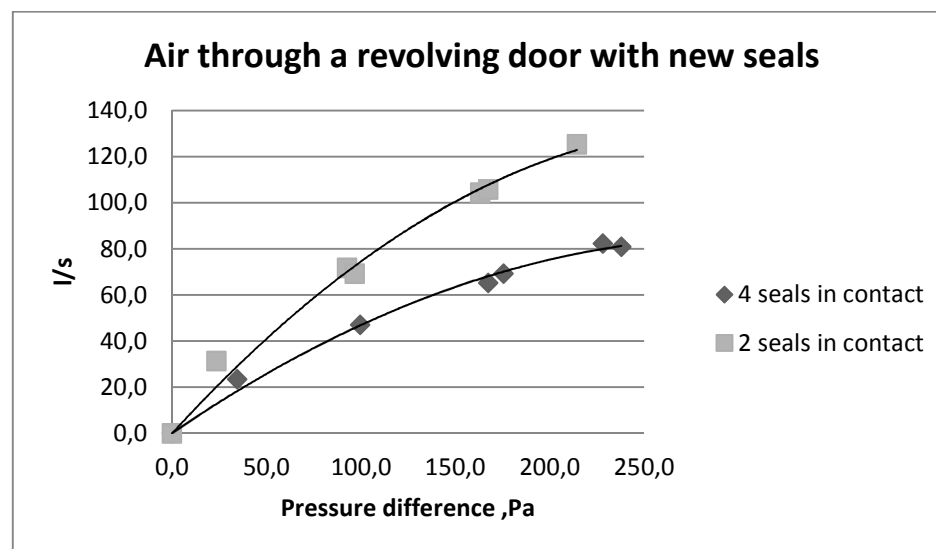


Figure 4.2. The air leakage through the seals of a revolving door as a function of the pressure difference over the door. (Schutrum et al, 1962).

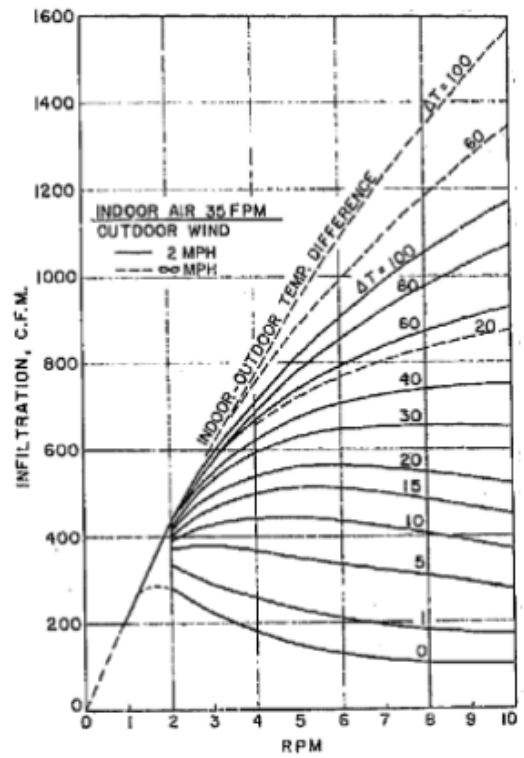
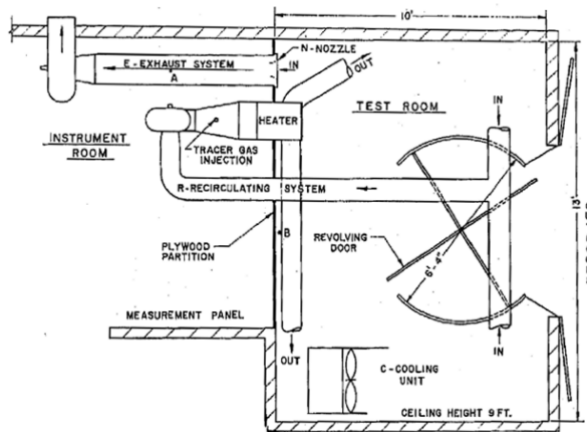


Figure 4.3. At the left: Setup of the experiment. At the right: Air exchange depending on temperature difference and revolution of the door (Schutrum et al, 1962).

#### 4.2.2 The Zmeureanu et al study

In the Zmeureanu et al study the air leakages of four revolving doors of a university building have been studied. These four doors shared the dimensions of 2,1m in diameter and 2m in height and they were all the four winged type of door. In addition they were all made by the same manufacturer in the 1970s. The differences between these doors were the state of their seals. Some doors lacked one seal while others had all 4 vertical seals intact. The physical state of the doors from the experiments is found in table 4.1.

Table 4.1. Physical state of the revolving doors in the experiment (Zmeureanu et al, 2001).

Door No	No of seals	Contact to the housing
1	4	Poor
2	3	Poor
3	3	Poor
4	4	Good

The experiment was carried out by using an aluminum box which was placed outside the building working as a test chamber. The depressurization of the test chamber was done with a fan from blower door equipment. The indoor air was drawn through the revolving door into the test chamber. Data of the pressure difference over the door and the airflow through the fan was collected. The resulting air leakages through the seals of the revolving doors were described by using the power law model. The results are shown in table 4.2.

Table 4.2. Results from the Zmeureanu study (Zmeureanu et al, 2001).

Door and position	Measured		Calculated	
	$C$ [L/(s · Pa <sup>n</sup> )]	$n$	Equivalent leakage area at 10 Pa (m <sup>2</sup> )	Air leakage at 75 Pa (L/s)
Door 1, four wing	15.7–17.7	0.72–0.74	0.034–0.038	366.8–402.4
Door 1, two wing	20.6–27.9	0.71–0.77	0.049–0.059	568.3–626.7
Door 2, four wing	8.0–12.6	0.70–0.76	0.019–0.025	217.5–256.4
Door 2, two wing	8.9–145.0	0.61–0.72	0.023–0.236	198.2–1984.1
Door 3, four wing	20.8–53.6	0.68–0.84	0.048–0.102	522.1–997.3
Door 3, two wing	21.1–114.8	0.62–0.78	0.051–0.191	609.4–1640.6
Door 4, four wing	19.8–20.9	0.65–0.67	0.037–0.038	348.6–350.6
Door 4, two wing	18.2–19.2	0.65–0.67	0.034–0.035	311.2–323.5



### 4.2.3 The Lin Du study

In 2009 Lin Du finished her thesis called “Air infiltration through Revolving Doors” (Du, 2009). The purpose of the thesis was to measure the infiltration due to the motion of a 1:10 scale model of a revolving door and to develop a methodology for calculating the exchange rate due to the motion of the door.

A method to scale up the results from the scale 1:10 door to a door of 2.1 m in diameter and 2 meter in height were introduced as defined in equation 43. In figure 4.4 the air exchange due to the motion of a full size door is presented. Additionally it was concluded that the temperature difference between indoor and outdoor air does not affect the air exchange due to the motion of the door (Du, 2009).

$$V_{\text{inf\_prototype}} = 0.61 * N_{\text{rpm}} + 2.15 \left[ \frac{\text{l}}{\text{s}} \right] \quad (43)$$

Where

$V_{\text{inf\_prototype}}$  is the air exchange induced by the motion of the door  $\left[ \frac{\text{l}}{\text{s}} \right]$

$N_{\text{rpm}}$  is the rotation speed of the door  $[\text{RPM}]$

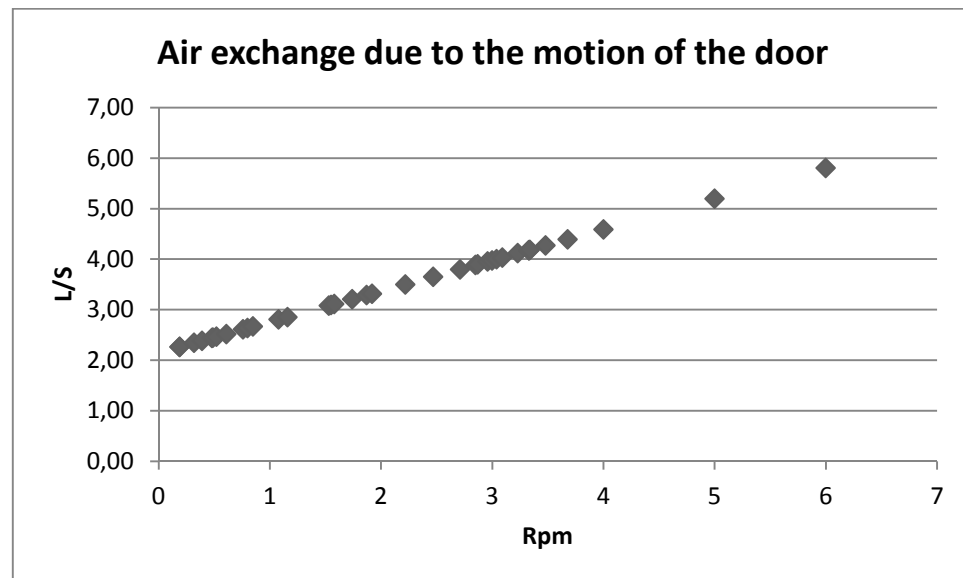


Figure 4.4 Air exchange due to the motion of a full scale revolving door (Du, 2009).

#### 4.2.4 The Allgayer study

David Allgayer have conducted an in depth study of the air and heat transfer mechanism induced by the revolving motion of the door (Allgayer, 2007). His report starts with a summary of all previous published reports in the field of air infiltration through revolving doors. He concludes that even though studies on infiltration through revolving doors have been done there's much about the physics of the air transfer that is unknown. He also implies that door manufacturers know very little about how their products work and perform. To gain more knowledge about the air transfer mechanism of a revolving door he conducted a series of experiments.

The experiment was conducted on a 1:3 scale model of a revolving door using water as the working medium. Saline solutions were used to replicate the density differences across the door. Digital image analysis was used to measure the density stratification of the water. The results of these experiments proves that the air transfer depend on the temperature difference, the geometry of the door way and the revolution rate.

Additionally it is concluded that a revolving door work under two transfer regimes; buoyancy limited and revolution limited transfer. The buoyancy limited regime is restricted by the time it takes for the air to exchange across the door under gravity. The revolution limited regime is restricted by the time it takes for the door to complete one revolution. With this knowledge it's possible to either increase or decrease the rate of infiltration by changing the revolution speed or the geometry of the door. This would result in either lower energy losses or increased ventilation (Allgayer, 2007).

#### 4.2.5 Studies made by manufacturers

The studies conducted by Zmeureanu et al and Schutrum et al are made on doors produced in the 1960's and the 1970's. These studies are the only ones made on full scale revolving doors by scientists. Due to the fact that society has become far more energy minded especially in recent years, obtaining measured data for more modern doors is crucial. Zmeureanu are mentioning a measurement made on a revolving door from the manufacturer Crane door. The measurement was made by the independent consultant WJE. The measurements were made according to the ASTM E 283 standard. The air leakage through the seals was determined to be 20-23 l/s at 75 Pa. (WJE, 1997). This gives a good indication of the performance of a modern door in perfect condition.

Except for the Allgayer study no more recent study of the air exchange rates due to the revolving motion of the door has been done since the Schutrum study. One of the leading revolving door manufacturers Boon Edam has shared their tool which is used to calculate the infiltration rate due to the revolving motion of the door. The model is based on several reports conducted at the TU Delft University. Unfortunately Boon Edam failed to provide these reports. Therefore the results of the calculation tool are only to be considered as indicators and to reflect the manufacturer's view of the performance. The tool is a sophisticated Excel document with the following user defined parameters:

- Diameter [m]
- Height under Canopy [m]
- Canopy height [m]
- Speed of the door set  $\left[\frac{m^2}{s}\right]$
- $\Delta T [^{\circ}C]$

In order to provide an example of the results produced by the calculation tool a 4-winged door with identical dimensions as the door used in the Schutrum and Zmeureanu studies is defined. The resulting infiltration flow is shown in the figure 4.5.

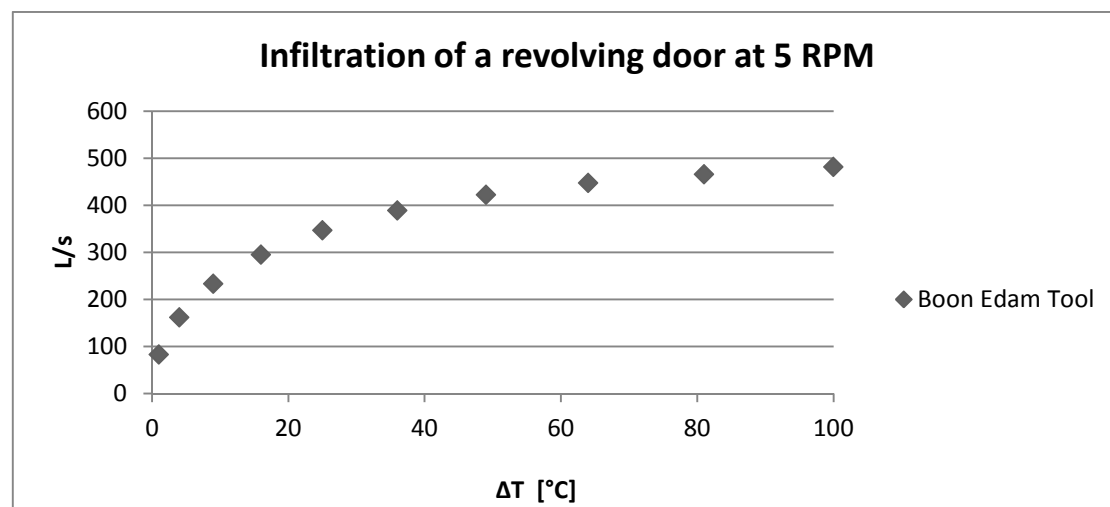


Figure 4.5. The air exchange induced by the temperature difference and revolution of a revolving door. (Boon Edam Tool, 2013).

### 4.3 Selected models for revolving doors

Even though only a few published studies are available it's a fact that the air infiltration through a revolving door occurs in two ways. By leakage through the seals and by air exchange due to the revolving motion of the door. Concerning the leakage through the seals the results from the Schutrum and Zmeureanu reports are based on doors manufactured in the 1960's and 1970's. Therefore there was a need to construct a model representing the performance of a modern door.

Concerning the air exchange due to the revolving motion of the door some reports have contradicted each other when it comes to the dependency on differences in air temperature. It is after some reasoning concluded that the air exchange is temperature dependent. Lin Du concluded otherwise but there are several factors of her experiment that are questionable. First of all the model is small 1:10 in scale, in order to simulate a full scale door Du chooses to increase the revolution rate 100 times. When simulating a full scale door revolving with a speed of 3 RPM the door in the experimental model is set to revolve at a speed of 300 RPM. It is hard to see that any temperature difference would make any large impact on a small volume at these high speeds. The door would work under what Allgayer calls the revolution limited regime.

Another problem in creating a model of a revolving door is the fact that all previously full scale studies have been conducted on a revolving door with the dimensions of 2,1 meters in diameter and 2 meters in height. The benefit of using the same dimensions of the door is that the studies can be compared. But in reality only a few doors will have these exact dimensions. As a result a reference door for the study cases has been defined, see table 4.3.

*Table 4.3. Specifications of the reference door.*

Reference Revolving Door	
Type:	4-wing
Height:	2,0 [m]
Diameter:	2,1 [m]
Operation Speed:	5 [RPM]

### 4.3.1 Model for calculating leakage through the seals of a revolving door

The leakage through the seals was first measured in the Schutrum report. The measurements were made on a new door in a laboratory environment. These results can be used to simulate a revolving door in perfect condition. The results from these measurements are shown in figure 4.2. The original results were plotted for a range of 0 to 250 Pa in pressure difference. Since 250 Pa is a very high pressure difference the range was lowered to 100 Pa to get a more fair view. As a simplification the mean value of the results for 2-wing contact and 4-wing contact was calculated resulting in figure 4.6.

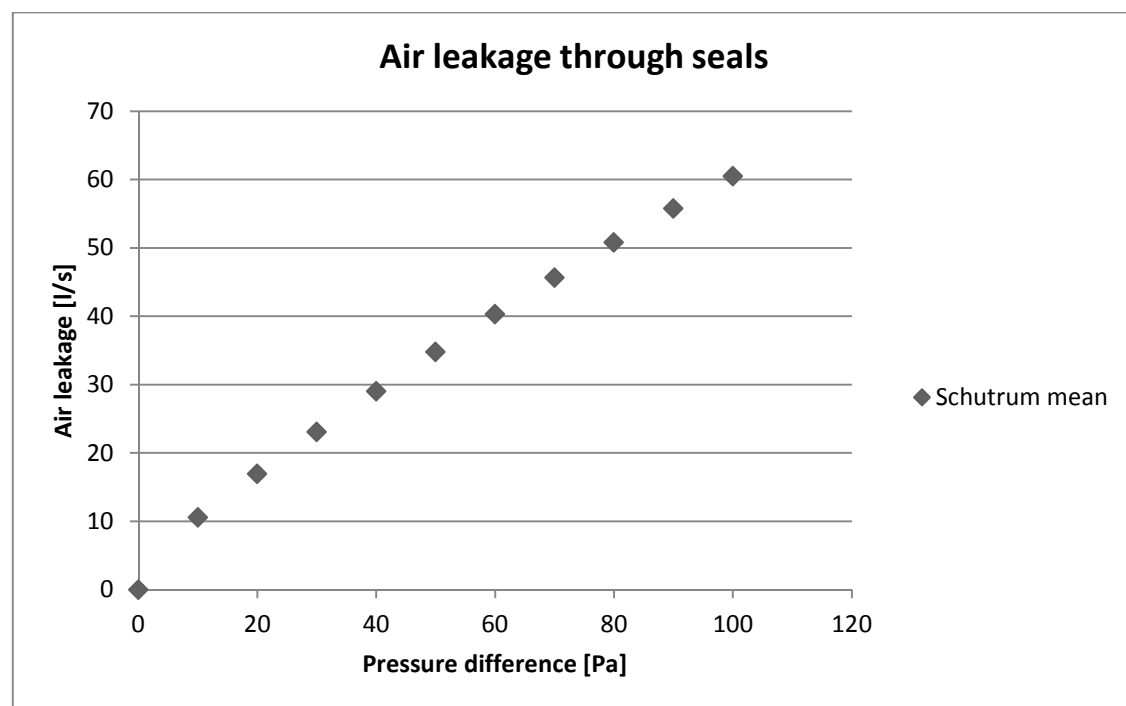


Figure 4.6. Air leakage through the seals of a revolving door as a function the pressure difference over the door.

In the Zmeureanu study the air leakage through the seals was measured on 30 year old doors. Some of them were lacking a seal. Focus was put on door number 4, see table 4.1. Door number 4 still had all seals intact and the seals were in good contact with the housing. This door is found suitable to represent a worn revolving door. As for the data from Schutrum a mean value was calculated from the results for 2-wing and 4-wing contact. See figure 4.7.

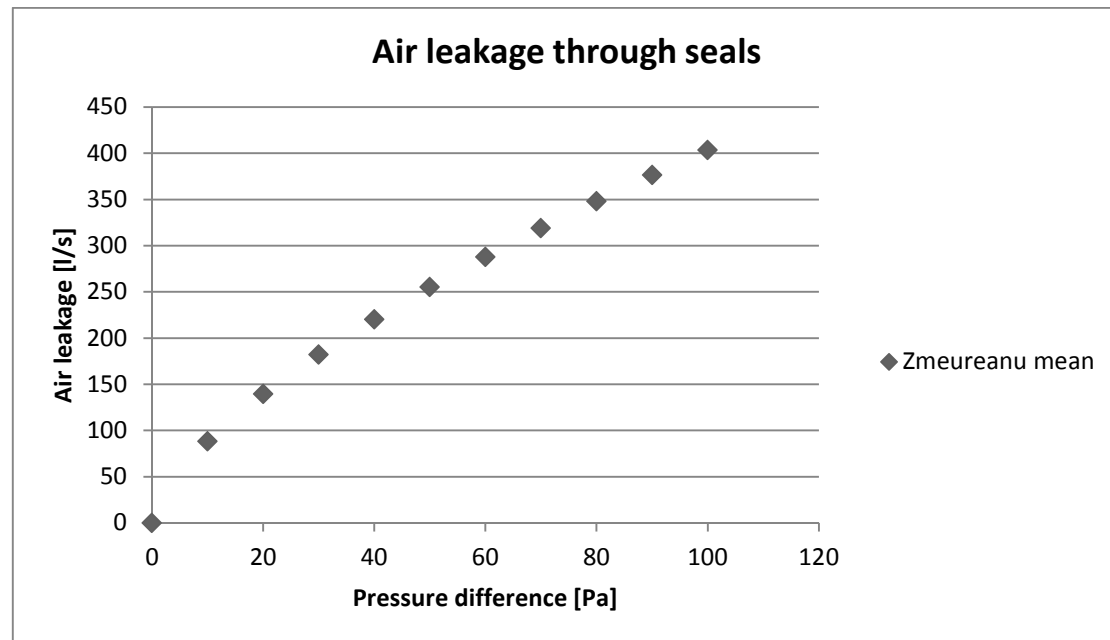


Figure 4.7. Air leakage through the seals of a revolving door as a function the pressure difference over the door.

Even though the design curves from both Schutrum and Zmeureanu would be suitable to represent revolving doors in the final calculation model the fact that they represent doors manufactured in the 1960's and 1970's can't be neglected. Due to the increased energy mindedness in the world it is reasonable to assume that revolving doors today are more energy efficient than ones from the 1960's and 1970's. The measurements on the door from (WJE, 1997) with identical dimensions as the doors from Schutrum and Zmeureanu are good indications on the performance of a modern door. The results of the measurements conducted on the revolving door from Crane door are just given for 75 Pa pressure difference. An estimated design curve will be based on the results from Schutrum. The resulting design curve is found in figure 4.8.

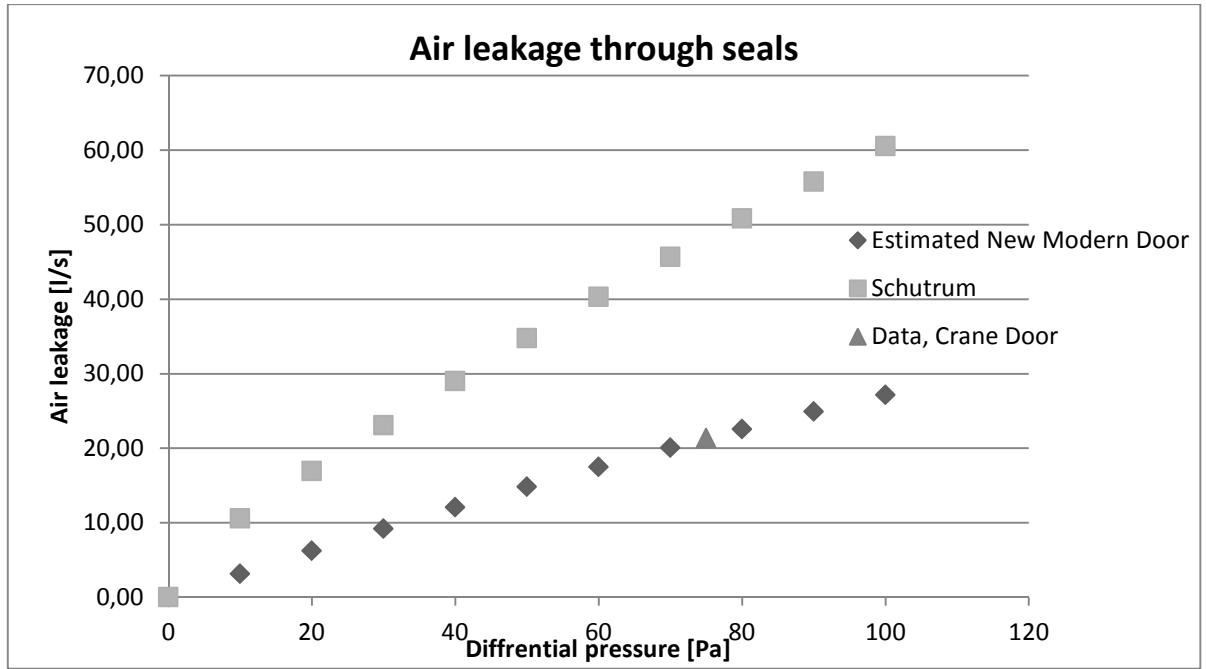


Figure 4.8. Air leakage through the seals of revolving doors as a function the pressure difference over the doors.

In order to estimate the performance of a modern door in a worn state the relation between the curves for Schutrum and Zmeureanu is applied on the curve for a modern door. Additionally a curve for a maintained modern door is created. The concept of a maintained door is that it is maintained on a regular basis. The design curve of a modern maintained door is close to equal the door from Schutrum. The design curve is found in figure 4.9.

The following relationships apply:

$$\dot{V}_{modern,worn}(\Delta P) = \left( \frac{\dot{V}_{Z,mean}(\Delta P)}{\dot{V}_{S,mean}(\Delta P)} \right) * \dot{V}_{modern door,new}(\Delta P) \quad (44)$$

$$\dot{V}_{modern,maintained}(\Delta P) = \left( \frac{\dot{V}_{Z,mean}(\Delta P)}{3 * \dot{V}_{S,mean}(\Delta P)} \right) * \dot{V}_{modern door,new}(\Delta P) \quad (45)$$

Where

$\dot{V}_{modern,worn}(\Delta P)$  is the leakage of a worn modern door at  $\Delta P \left[ \frac{l}{s} \right]$

$\dot{V}_{modern door,new}(\Delta P)$  is the leakage of a new modern door at  $\Delta P \left[ \frac{l}{s} \right]$

$\dot{V}_{modern,maintained}(\Delta P)$  is the leakage of a maintained modern door at  $\Delta P \left[ \frac{l}{s} \right]$

$\dot{V}_{Z,mean}(\Delta P)$  is the leakage of the door from the Zmeureanu study at  $\Delta P \left[ \frac{l}{s} \right]$

$\dot{V}_{S,mean}(\Delta P)$  is the leakage of the door from the Schutrum study at  $\Delta P \left[ \frac{l}{s} \right]$

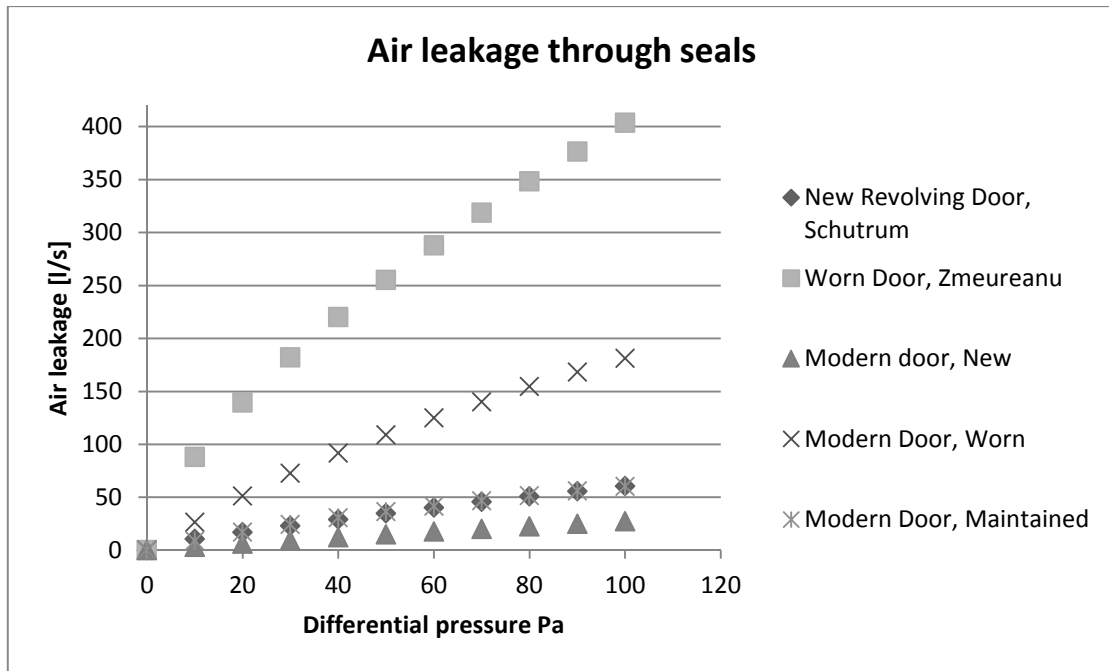


Figure 4.9. Air leakage through the seals of revolving doors as a function the pressure difference over the doors.

Now three performance curves have been obtained for a modern revolving door in three physical states. These curves will be implemented in the BES to calculate the infiltration rate through the door seals.



### 4.3.2 Model for calculating the air exchange induced by the revolving motion of a door

Schutrum et al presented the infiltration rate due to the revolving motion of the door in their report. In the results the indoor air movement is set to 0,18 m/s and a mean outdoor wind to 0,9 m/s. The outdoor wind and the indoor air movement have impacts on the infiltration due to the revolving motion of the door. But any data or model concerning this issue has not been found. Additionally in the calculation tool from Boon Edam there is no input for indoor or outdoor air movements. Therefore indoor and outdoor air movement has been neglected in this report. Data of the infiltration rate depending on the temperature difference and revolution rate have been extracted from figure 4.10. A graph presenting the infiltration rate at a fixed RPM of 5 for different temperatures is found in figure 4.11.

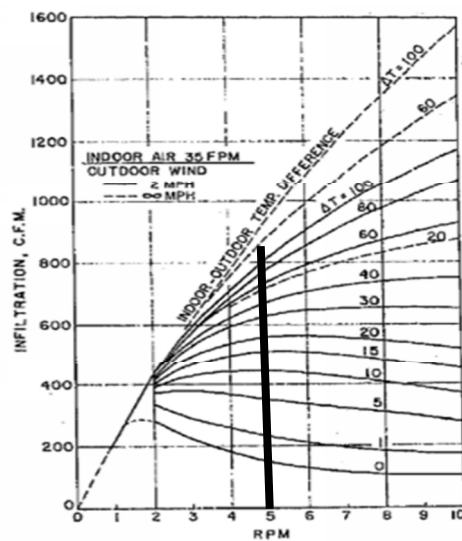


Figure 4.10. Air infiltration depending on temperature difference and revolution of the door. The vertical line indicates the values obtained for a revolution rate of 5 RPM (Schutrum et al, 1992).

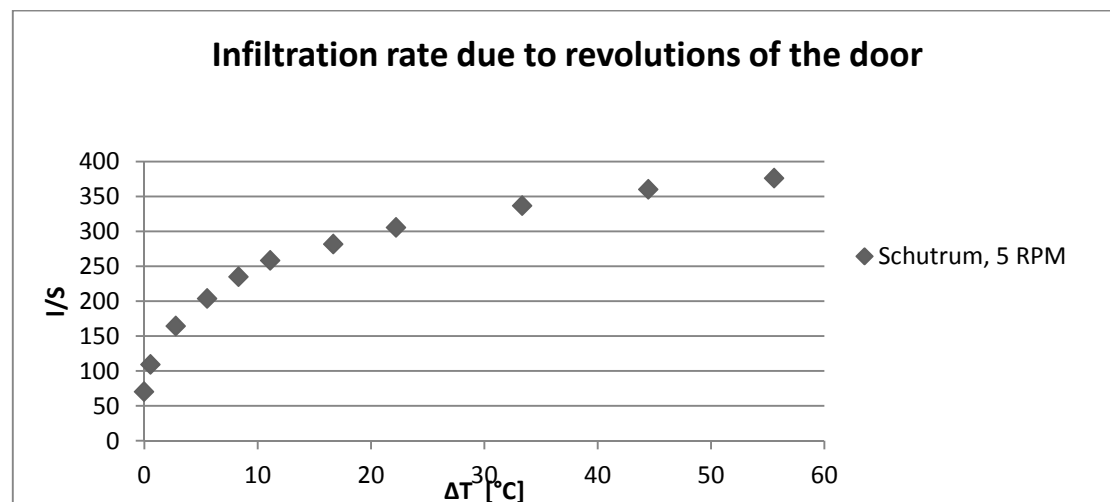


Figure 4.11. Air infiltration induced by a door revolving at 5 RPM depending on the temperature difference.

Even though it's hard to use data from the Boon Edam calculation tool due to the absence of scientific data it's still interesting to see the manufacturer's view of the performance. The complexity of the equations in the calculation tool indicates that studies have been done but not been published. In figure 4.12 the results from Schutrum is compared to the results of Boon Edam. The infiltration rate from the Boon Edam calculation tool is lower than Schutrum up to  $\Delta T = 12^\circ\text{C}$  above that it is higher. It's clear though that the curves are similar in shape and that no greater deviations occur until approx.  $\Delta T = 35^\circ\text{C}$ .

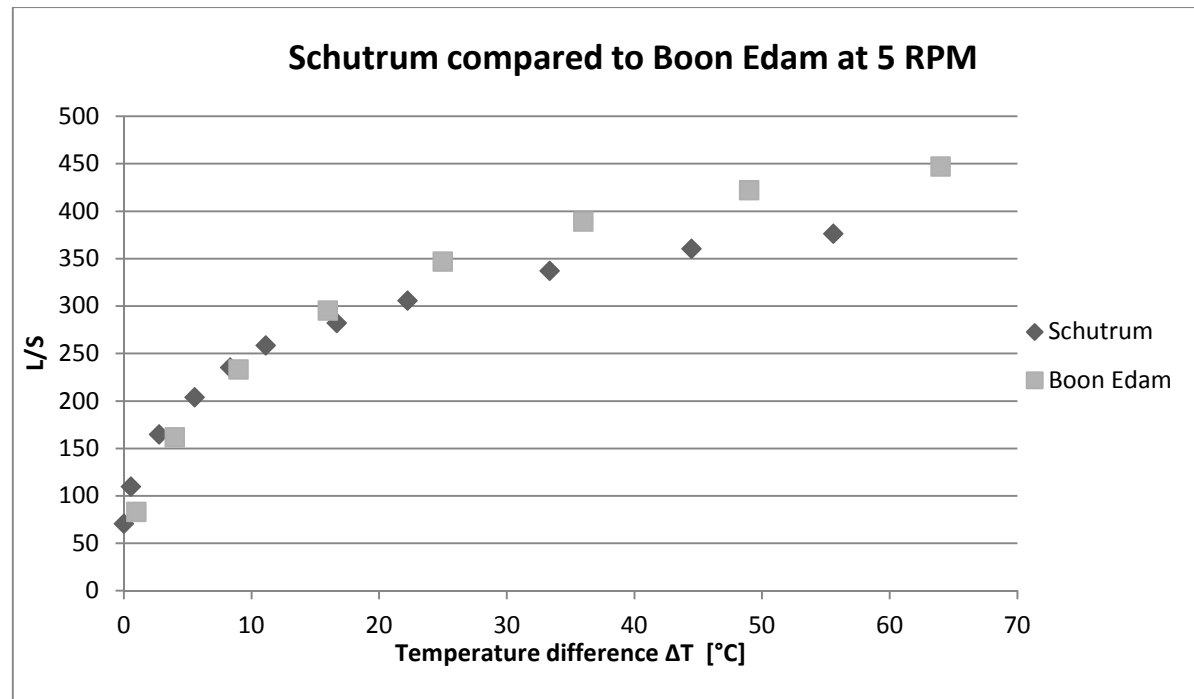


Figure 4.12. Air infiltration induced by a door revolving at 5 RPM depending on the temperature difference. A comparison between Schutrum and Boon Edam.

The data from the Schutrum et al study correlates good with the Boon Edam tool and since there are no other full scale studies conducted on the infiltration rate due to the revolving motion of the door the curve in figure 4.11 is to be considered as the chosen model to be implemented in BES to calculate the infiltration rate due to the revolving motion of the door.

### 4.3.3 Model for door usage

A revolving door is not revolving all the time. It will stop when it's not used. During the opening hours of the building where the door is installed the door will be revolving for a certain amount of time. When using building energy simulation software it is common that you work with calculations in an hourly resolution. The grade of door usage for a specific hour can be described with a ratio where 1 equals a door which is revolving the whole hour. The grade of usage is not only a matter of people flow and capacity. It's a complex probability problem, depending on sensors and the shape of the flow.

There was no space in this study to do any refined probability model. The grade of usage is therefore very simplified. For small revolving doors up to 3 meters in diameter it is common that every compartment of the revolving door can hold one person (BESAM, 2013). The door operates under a certain RPM and flow of people is allowed in two directions. Equation 46 shows how to calculate the capacity of a revolving door and equation 47 describes how the usage ratio is calculated.

$$Capacity = N_c * N_{PPC} * RPM * 60 [People\ per\ hour] \quad (46)$$

$$R_{usage} = \frac{F_p}{Capacity} \quad (47)$$

Where

$N_c$  is the number of compartments

$N_{PPC}$  is the number of people per compartment

$F_p$  is the flow of people, [People per hour]

A 4 winged revolving door allowing one person per compartment, revolving at a speed of 5 RPM has a capacity of 1200 people per hour.

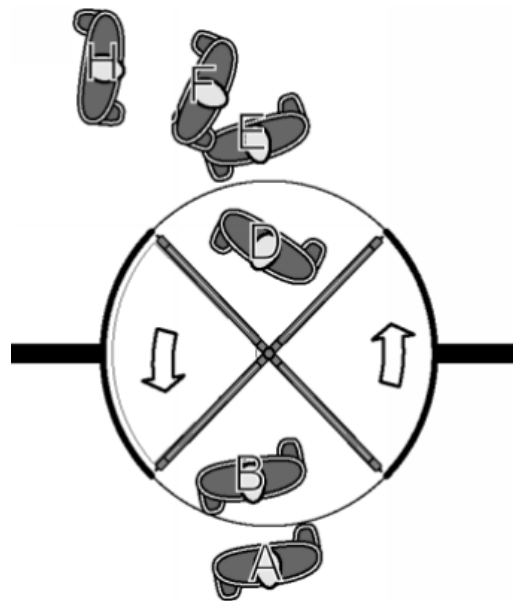


Figure 4.13. Illustration a flow of people through a revolving door (BESAM, 2013).

## 5 Implementation of selected models in IDA-ICE

In this chapter it will be explained how the chosen calculation models and design curves from 3 and 4 are implemented in the building energy software IDA-ICE. An introduction to the models for airflow through openings in IDA-ICE was presented in chapters 2.2 and 2.3.

### 5.1 Open type doors

The chosen model for open-type doors was presented in chapter 3.5 where different equations for the flow coefficient  $C_A$  were presented. The purpose of  $C_A$  is to replace  $C_D$  when calculating the air infiltration through exterior doors.  $C_A$  depends on the number of people that passes through the opening per hour and is to be considered a variable. In IDA-ICE the discharge coefficient  $C_d$  is a fixed parameter set to 0,65 by default. This provides a problem since  $C_A$  need to change with the time.

The first approach was to edit the code of the door model CELVO making  $C_d$  a variable instead of a parameter. This proved to be a time demanding process for a beginner when it comes to creating component models in IDA. During the process of editing the code it was found that instead of editing the whole model the out signal from the opening schedule could be used to manipulate  $C_d$ . A principal function diagram over the implementation is shown in figure 5.1.

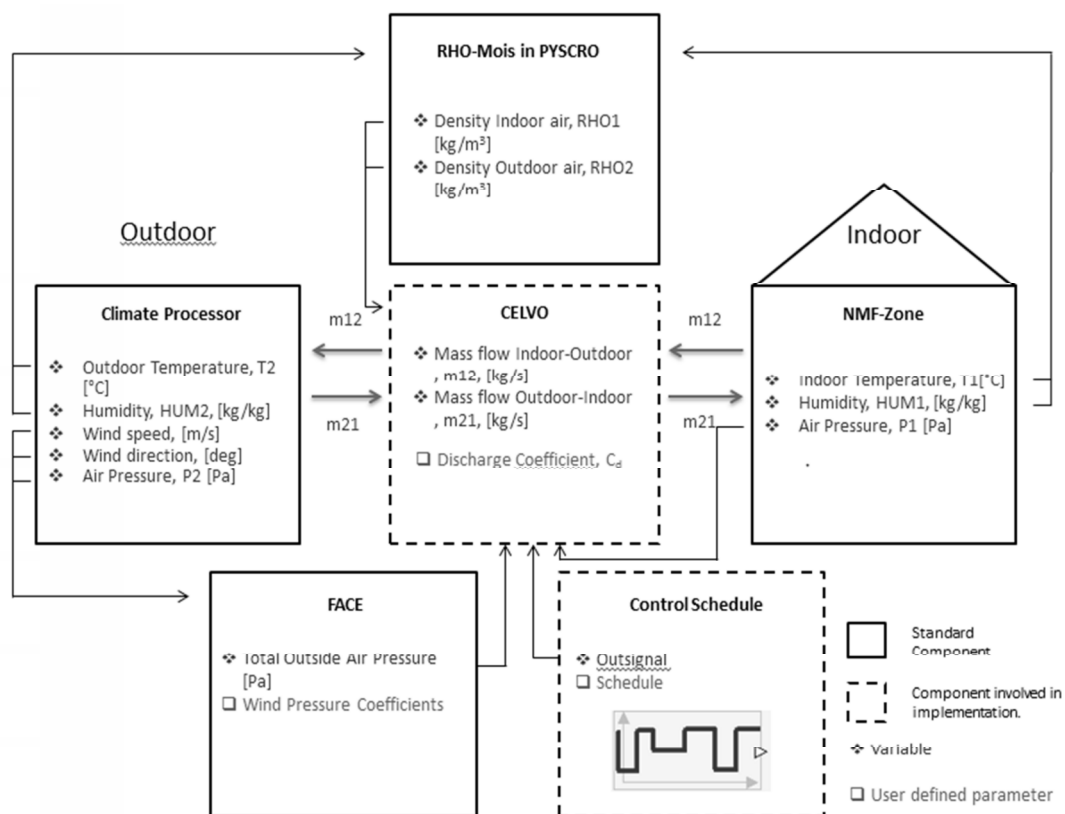


Figure 5.1. Principal function diagram over the implementation into IDA-ICE.

The manipulation of  $C_d$  is possible since the out signal from the opening schedule connected to CELVO controls the width of the opening. And since the area of the opening is multiplied with  $C_d$  in every mass flow equation it is possible to edit the area instead of  $C_d$ . The width depends on the out signal of the opening schedule as defined in equation 48.

$$W(t) = \max(A_{Leak}, S_{Control}) * w [m] \quad (48)$$

Where

$W(t)$  is the width of the opening at the time  $t$  [m].

$A_{Leak}$  is the minimum leak relative to the area, set to 0 by default.

$S_{Control}$  is the control signal from the opening schedule, ranges from 0 to 1.

$w$  is the width of the door when fully open [m]

With this connection known the opening schedule for the door can be used to manipulate the discharge coefficient. This is possible since the mass flow calculated by CELVO always uses the operation  $W(t) * C_d$

If  $S_{Control}$ , the out signal of the opening schedule is defined as in equation 49.  $C_d$  will be effectively changed to  $C_A$

$$S_{Control} = \frac{C_A}{C_d} \quad (49)$$

As an example. At the time  $t$  the people flow through the door is 450 PPH which with the equation for a single sliding door gives a  $C_A$  of 0,44. To implement this value in IDA-ICE you divide 0,44 with 0,65 resulting in the value of 0,68 which is then defined in the opening schedule for the time  $t$ .

## 5.2 Revolving doors

From the Schutrum and Zmeureanu study it is known that infiltration through a revolving door occur in two ways. From pressure driven leakage through the seals and from revolution speed and temperature driven air exchange due to the revolving motion.

### 5.2.1 Infiltration due to the motion of the door

As described in chapter 4.3.2 a design curve with the air exchange depending on the temperature difference at a specific RPM was acquired. The idea was that this air exchange can be simulated by an air handling unit which basically consists of two fans. One fan is supplying outdoor air and the other one exhausts indoor air. The flows of these fans are decided by the design curve presented in chapter 4.3.2. The energy use of these fans was not measured, and the temperature rise due to the fans needed to be put to zero. The performance of these fans was unlimited; their only function was to provide the air exchange which is described in the performance graph. A principal function diagram over the implementation is shown in figure 5.2.

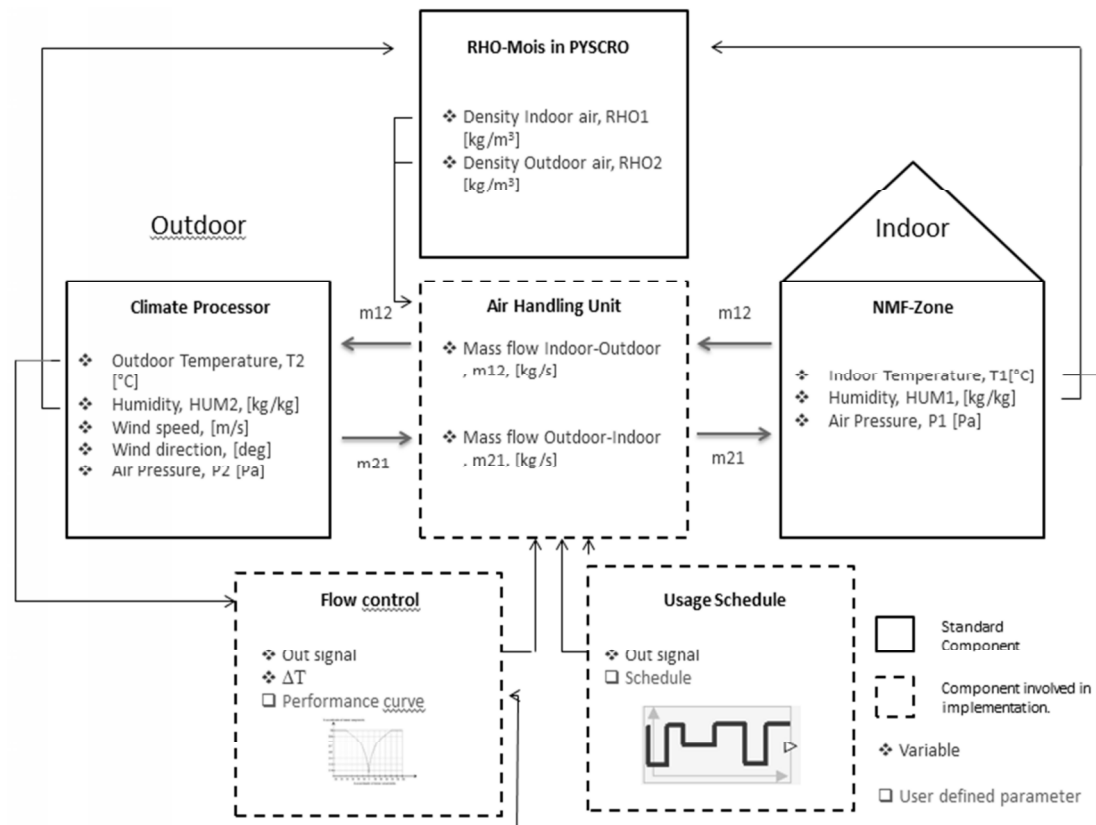


Figure 5.2. Principal function diagram over the implementation into IDA-ICE.

First a local AHU was created in the zone where the door is located. Even though it's not a CAV system a CAV supply and return flow need to be defined. It's only possible to define it in  $\text{L/s}\cdot\text{m}^2$ . Therefore the maximum flow from the calculation model needs to be divided by the area of the zone. See figure 5.3

L/(s.m2)

Add AHU...

Remove



Name	Central air handling unit	System type	Return air for CAV	Supply air for CAV	Return terminal height
 CENTRAL-AHU	Air Handling Unit	VAV, temp+CO2 con...	n.a.	n.a.	2.6
 Revolving Door	Air Handling Unit	CAV	0.235	0.235	1

Figure 5.3. AHU form for a zone in IDA-ICE.

When the local AHU has been created and the air flows were defined an advanced energy model was created. The AHU can now be found under the schematic tab in the zone. Now all the standard components and controls were deleted and only the supply and return fan were left. The default temperature rise of  $1^\circ\text{C}$  of the fans was put to 0. The return and supply fan have to be reconnected to the ambient air and to the zone. In order to explain the control of the AHU the final schematic is shown in figure 5.4.

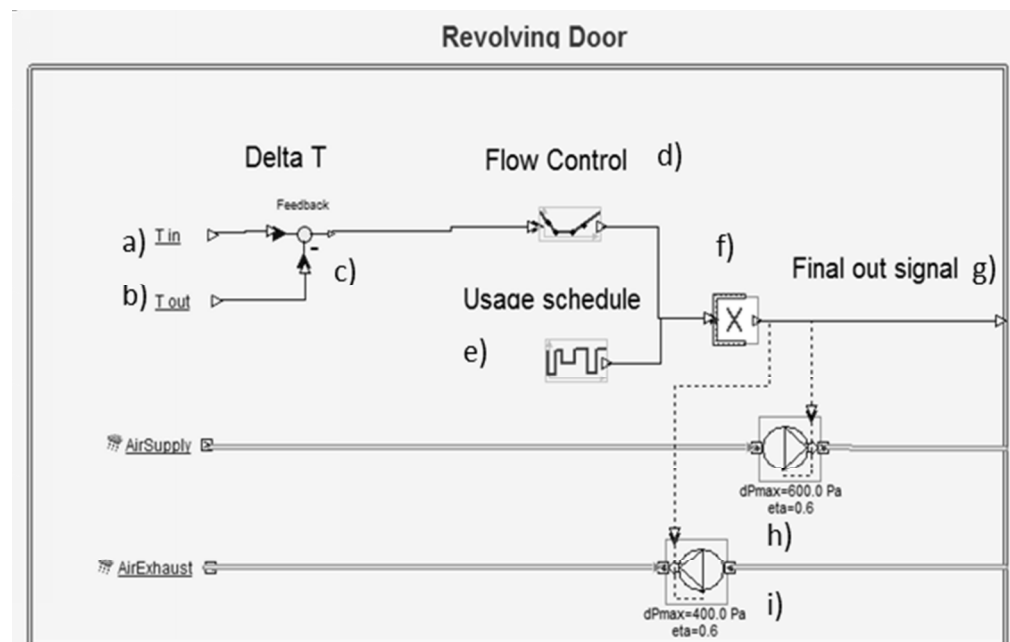


Figure 5.4. Revolving door model based on an AHU model in IDA-ICE.

The air exchange induced by the revolving door depends on the temperature difference between the indoor and outdoor air. In order to access these parameters and calculate the difference two reference links have to be created (a and b). One is connected to the outdoor air temperature (b) and the other is connected to the indoor temperature in the zone (a). To calculate the difference the reference links were connected a component called feedback (c) which subtracts one value from the other.

In order to simulate the grade of usage of the revolving door a usage schedule (e) was created. The usage schedule of the AHU will work in the following way. An out signal of the range 0-1 will be created. The out signal depends on how much people that will walk through the door during 1 hour and the capacity of the door. As mentioned in chapter 4.3.3. An example of a usage schedule can be found in figure 5.5. The following equation is used to define the out signal.

$$\frac{F_p}{Max\ capacity} = S_{control}$$

Where

$F_p$  is the flow of people, [People per hour]

$S_{control}$  is the control signal from the opening schedule, ranges from 0 to 1.

$Max\ capacity$  is the maximum flow of people that the door can handle, [People per hour]

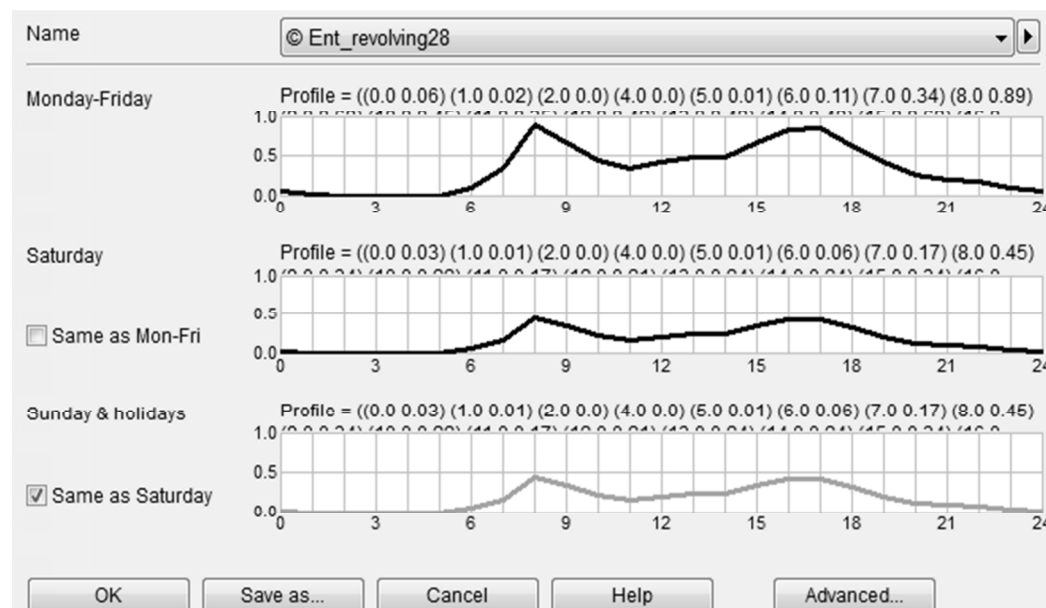


Figure 5.5. Usage schedule in IDA-ICE based on data from the Nils Ericson terminal.



The maximum flow of air to and from the zone due to the revolving door was defined when adding the AHU. The revolving door will be simulated with a performance curve where the air flow depends on the temperature difference. This curve is defined in the AHU with the component called *Linear Segment Controller- PLINSEGM* (d). An out signal of 1 from the *Linear Segment Controller* will result in the maximum flow while 0 will result in no flow. Therefore the graph in the *Linear Segment Controller* must be defined so that the maximum value in the performance curve corresponds to the value of 1. An example of a performance curve translated into a graph in the *PLINSEGM* is found in figure 5.6. The out signal of the *PLINSEGM* is described by 49.

$$\frac{\dot{V}_{\Delta T=x}}{\dot{V}_{max}} = S_{flow} \quad (49)$$

Where

$S_{flow}$  is the signal which controls the air exchange

$\dot{V}_{\Delta T=x}$  is the air flow at the temperature  $x$  according to the performance curve.

$\dot{V}_{max}$  is the maximum air flow in the performance curve.

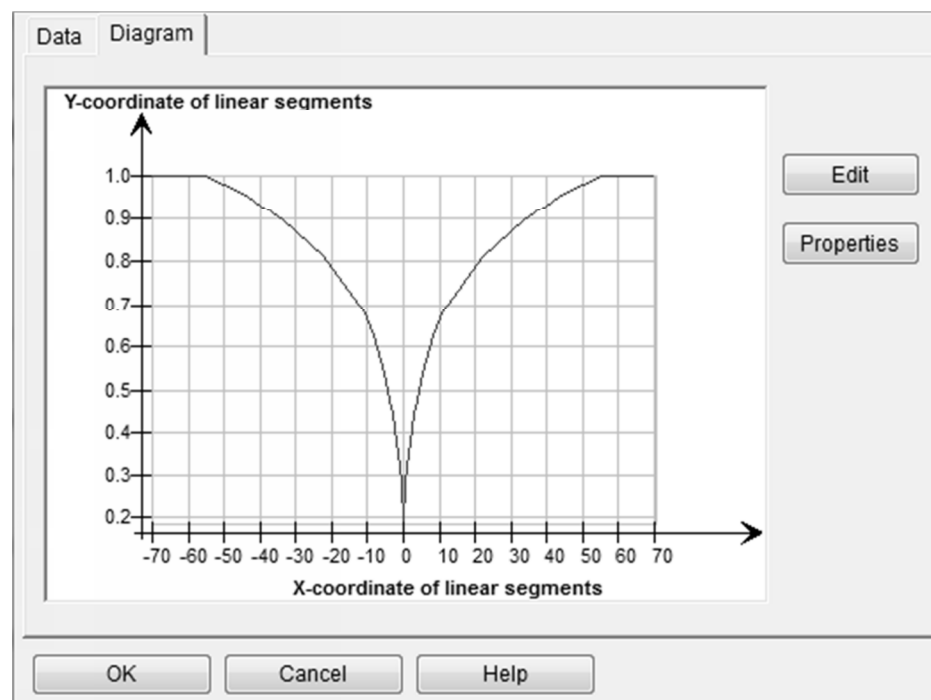


Figure 5.6. Control graph of the component *PLINSEGM* in IDA-ICE.

The final air exchange induced by the simulated revolving door is decided by the performance curve multiplied with the usage ratio. The result will be an average in and out flow from the zone which will change every hour. This operation is done with the multiplier (f). The following equations describes how the resulting average flow is obtained.

$$S_{final} = S_{flow} * S_{control} \quad (50)$$

$$\dot{V}_{average} = V_{max} * S_{final} \quad (51)$$

Where

$S_{final}$  is the final out signal which decides the air exchange

$\dot{V}_{average}$  is the average air exchange induced by the revolving motion of the door

To measure the energy loss of the infiltration due to the revolving motion of the door the energy meter for mechanical ventilation in the zone must be edited. The energy from all other AHUs is set to zero as in the figure 5.7.

close Object name **EMETER\_VENTIL** Object type **EMETER**

Calculates monthly power consumption and cost (in selected currency)

Input powers [W]

- INPOWER[1] <— 0.0 W
- INPOWER[2] <— MECH\_SUP.QS[2]

Connect all

Parameters

N_IN	2	Number of input links
FIXED COST	0.0	Fixed yearly cost
PRICE	[1..4]	Prices, per kwh; up to four different rates

Interfaces

PRICENOLINK

Figure 5.7. Input form of a ventilation energy meter in IDA-ICE.

The energy loss is then presented in the energy report for the zone to which the revolving door is connected. The result will be presented as mechanical ventilation see 5.8.

Energy for "Waiting hall"											
kWh (sensible only)											
Month	Envelope & Thermal bridges	Internal Walls and Masses	Window & Solar	Mech. supply air	Infiltration & Openings	Occupants	Equipment	Lighting	Local heating units	Local cooling units	Net losses
1	-6950.0	-5623.0	-51410.0	-3682.0	-31.3	4954.0	2171.0	7285.0	68160.0	0.0	0.0
2	-5879.0	-6402.0	-41175.0	-3055.0	-19.4	4281.0	1961.0	6580.0	55998.0	0.0	0.0
3	-5062.0	-7901.0	-25389.0	-2654.0	-19.0	4198.0	2171.0	7285.0	45814.0	0.0	0.0
4	-3421.0	-8673.0	-1951.0	-1963.0	-20.6	3603.0	2101.0	7050.0	26892.0	-0.4	0.0
5	-2516.0	-9462.0	11215.0	-1581.0	-18.5	3357.0	2171.0	7285.0	15505.0	-137.1	0.0
6	-1245.0	-8930.0	23764.0	-1005.0	-16.5	2919.0	2101.0	7050.0	4825.0	-386.8	0.0
7	-415.0	-9556.0	32308.0	-592.4	-10.2	2862.0	2171.0	7285.0	552.4	-873.8	0.0
8	-1165.0	-8220.0	16765.0	-742.6	-14.6	3290.0	2171.0	7285.0	2312.0	-481.1	0.0
9	-2205.0	-7202.0	1306.0	-1053.0	-16.9	3696.0	2101.0	7050.0	12850.0	-59.3	0.0
10	-3652.0	-6840.0	-18561.0	-1662.0	-14.9	4458.0	2171.0	7285.0	29615.0	0.0	0.0
11	-4763.0	-6231.0	-33948.0	-2184.0	-36.3	4716.0	2101.0	7050.0	48125.0	0.0	0.0
12	-7059.0	-7566.0	-52887.0	-3615.0	-27.9	5005.0	2171.0	7285.0	71499.0	0.0	0.0
Total	-44332.0	-92606.0	-139963.0	-23789.0	-246.2	47339.0	25562.0	85775.0	382147.4	-1938.5	0.0
During heating	-8030.6	-6352.8	-67805.6	-5091.7	-50.5	7161.1	2537.2	8513.9	89861.1	0.0	0.0
During cooling	-2650.0	-25052.8	118916.7	-2621.7	-23.9	7213.9	4013.9	13469.4	2994.4	-1471.4	0.0
Rest of time	-33651.4	-61200.4	-191074.1	-16065.6	-171.8	32864.0	19010.9	63791.7	289291.9	-467.1	0.0

Figure 5.8. Result report in IDA-ICE. The marked field shows the resulting energy impact of the air exchange that occurs due to the motion of the door.

## 5.2.2 Infiltration through the door seals

In chapter 4.3.1 three leakage curves for the doors called new, maintained and worn were presented. The new door performed the best and the worn door performed the worst. In order to consider the leakage part of the revolving doors in the IDA-ICE simulation the leakage curves had to be implemented in the software.

The first approach was to use an edited CELVO model described in chapter 2.2, where the pressure difference over the door was to be connected to a *Linear Segment Controller- PLINSEGM*, a graph where the discharge coefficient were plotted against the pressure difference. This approach resulted in numerical errors since the two variables discharge coefficient and pressure difference depended on each other. It was also concluded that this was a wrong approach since the CELVO model is designed for large vertical openings and not against leaks trough narrow corridors such as the leaks through the door seals.

The second approach was to use the CELEAK model described in chapter 2.3. The CELEAK model has no support to variable input, in the meaning that no schedule and no performance curve can be connected to it. There is input in the form of constants where a power law exponent is combined with either a mass flow coefficient or an equivalent leakage area. The equivalent leakage area is defined as the area which in combination of a discharge coefficient set to 1.0 result in the same leakage as the real area and the real discharge coefficient at the pressure difference of 4 pa. A principal function diagram over the implementation is shown in figure 5.9.

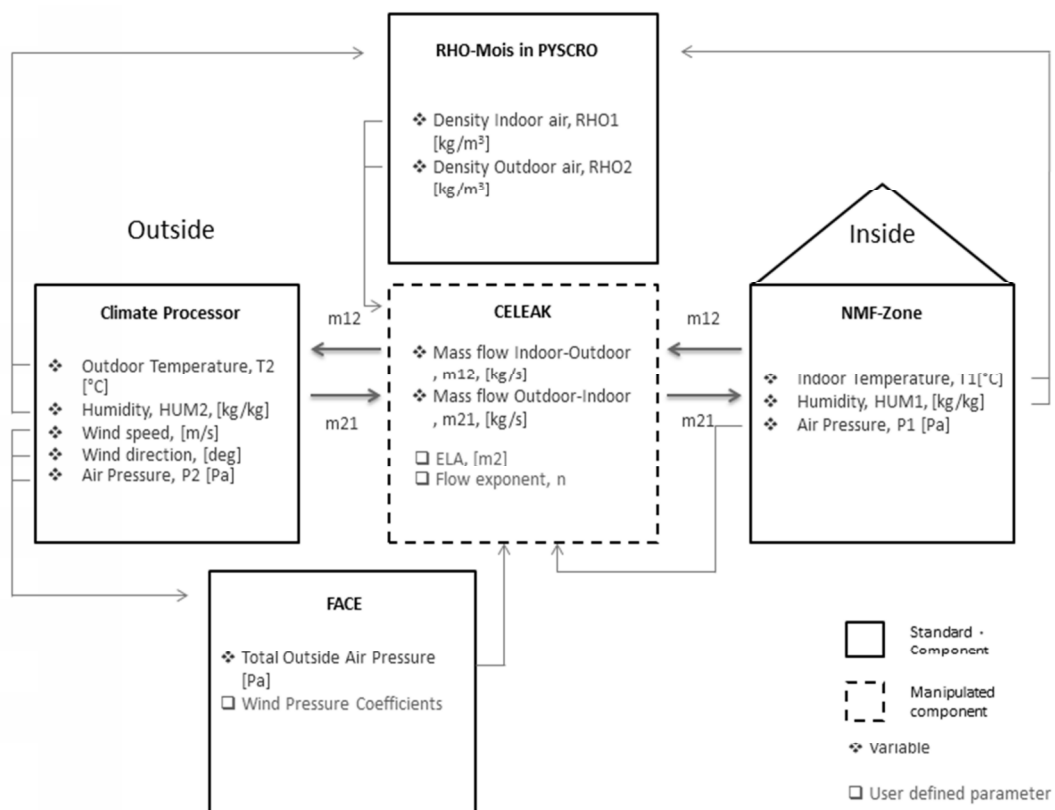


Figure 5.9. Principal function diagram of the infiltration model.

In order to obtain the ELA and flow exponent for the reference door in the conditions; new, maintained and worn a curve fitting method has been applied. The results for a new door are seen in figure 5.10, for a maintained door in figure 5.11 and for a worn door in figure 5.12. The resulting ELAs and flow exponents are shown in table 5.1.

Table 5.1. ELAs and flow exponents for a revolving door in different physical states.

Door:	ELA [ $m^2$ ]	Flow exponent
New	0,00034	1
Maintained	0,00175	0,82
Worn	0,0049	0,82

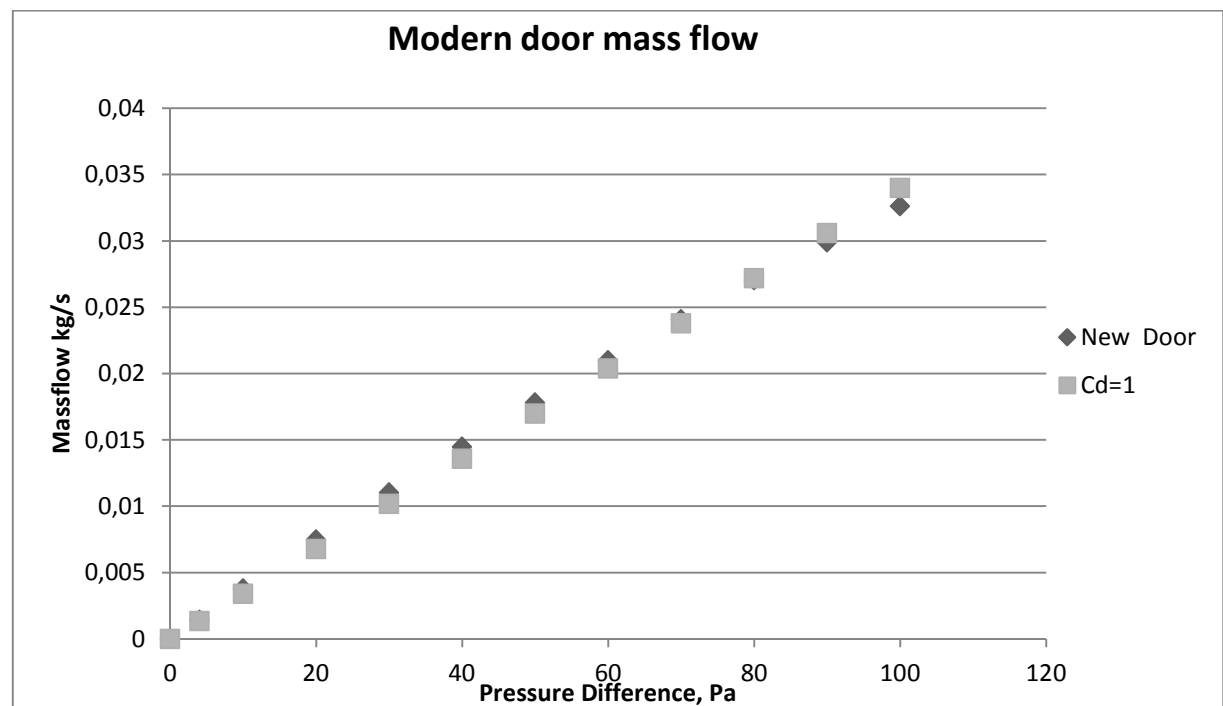


Figure 5.10. Performance curve of a new modern revolving door compared to a power law curve with a flow coefficient of 1 and a flow exponent of 1.

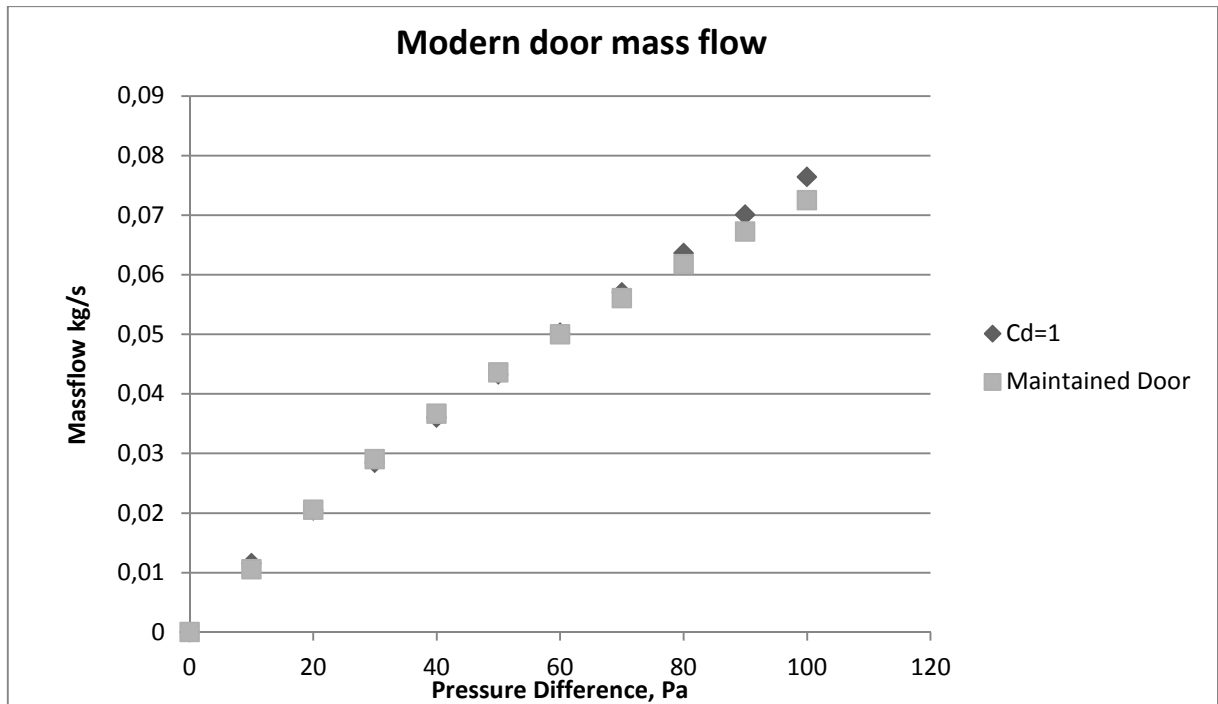


Figure 5.11 Performance curve of a maintained modern revolving door compared to a power law curve with a flow coefficient of 1 a flow exponent of 0,82.

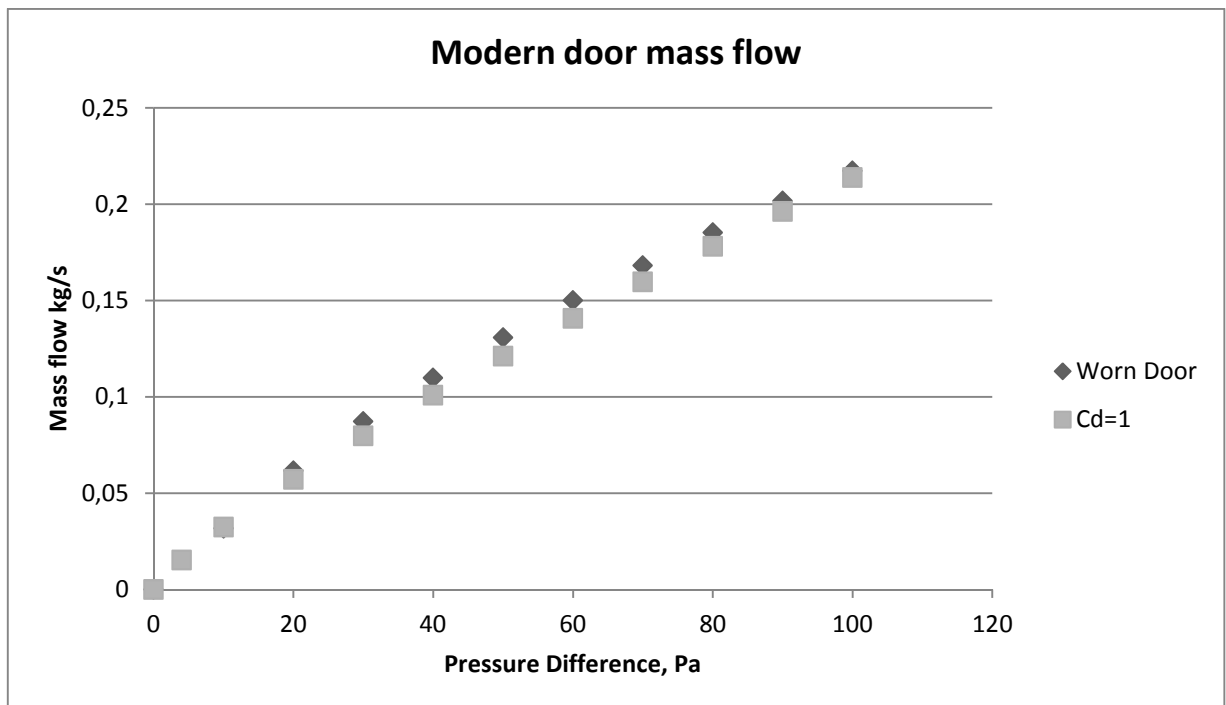


Figure 5.12 Performance curve of a worn modern revolving door compared to a power law curve with a flow coefficient of 1 a flow exponent of 0,82.

When the leakage parameters for the specific door are determined they can be defined in the CELEAK model. The CELEAK model has to be linked with the zone model and to the specific face of the building where the door is located. These are found in the outline tab of the CELEAK model. Terminal 1 is to be connected to the zone and Terminal 2 to the face, see figure 5.13.

Name	Value	Start	Unit	Connected to	Description
TERMINAL_1				NMFZONE.TERM[50]	
TERMINAL_2				/RevolvingMainEntranceDoor4.f3\$Building body 3.OUT2LEAK	
DP_LINK[1:0]	0				dP monitor link

Figure 5.13. Interface form of the CELEAK component in IDA-ICE.

In order to measure the infiltration through the new leak was added to the energy meter for leaks in the zone. If only the infiltration through the door is to be measured all other leaks have to be deleted in the energy meter. If the total air leakage is to be measured the other leaks are kept and the new leak is added. See figure 5.14 where only the new leak is measured.

Object name **EMETERLEAKAIRING**
Object type **EMETER**

Calculates monthly power consumption and cost (in selected currency)

Input powers [W]

☒ INPOWER[1] <— Leaks\_2.QS21

Parameters

N_IN	<input type="text" value="1"/>	Number of input links
FIXED COST	<input type="text" value="0.0"/>	Fixed yearly cost
PRICE	<input type="text" value="[1..4]"/>	Prices, per kwh; up to four different rates

Interfaces

PRICENOLINK

Figure 5.14. Input form of a ventilation energy meter in IDA-ICE.

The energy loss is then presented in the energy report for the zone to which the revolving door is connected. The result will be presented under infiltration and openings see figure 5.15. The total infiltration though the door due to the leakage through the seals is obtained by adding the “mechanical ventilation” and “infiltration, as seen in figure 5.8 and 5.15.

Energy for "Waiting hall"											
kWh (sensible only)											
Month	Envelope & Thermal bridges	Internal Walls and Masses	Window & Solar	Mech. supply air	Infiltration & Openings	Occupants	Equipment	Lighting	Local heating units	Local cooling units	Net losses
1	-6950.0	-5623.0	-51410.0	-3682.0	-31.3	4954.0	2171.0	7285.0	68160.0	0.0	0.0
2	-5879.0	-6402.0	-41175.0	-3055.0	-19.4	4281.0	1961.0	6580.0	55998.0	0.0	0.0
3	-5062.0	-7901.0	-25389.0	-2654.0	-19.0	4198.0	2171.0	7285.0	45814.0	0.0	0.0
4	-3421.0	-8673.0	-1951.0	-1963.0	-20.6	3603.0	2101.0	7050.0	26892.0	-0.4	0.0
5	-2516.0	-9462.0	11215.0	-1581.0	-18.5	3357.0	2171.0	7285.0	15505.0	-137.1	0.0
6	-1245.0	-8930.0	23764.0	-1005.0	-16.5	2919.0	2101.0	7050.0	4825.0	-386.8	0.0
7	-415.0	-9556.0	32308.0	-592.4	-10.2	2862.0	2171.0	7285.0	552.4	-873.8	0.0
8	-1165.0	-9220.0	16765.0	-742.6	-14.6	2290.0	2171.0	7285.0	2212.0	-491.1	0.0
9	-2205.0	-7202.0	1306.0	-1053.0	-16.9	3696.0	2101.0	7050.0	12850.0	-59.3	0.0
10	-3652.0	-6840.0	-18561.0	-1662.0	-14.9	4458.0	2171.0	7285.0	29615.0	0.0	0.0
11	-4763.0	-6231.0	-33948.0	-2184.0	-36.3	4716.0	2101.0	7050.0	48125.0	0.0	0.0
12	-7059.0	-7566.0	-52887.0	-3615.0	-27.9	5005.0	2171.0	7285.0	71499.0	0.0	0.0
Total	-44332.0	-92606.0	-139963.0	-23789.0	-246.2	47339.0	23362.0	85775.0	362147.4	-1938.3	0.0
During heating	-8030.6	-6352.8	-67805.6	-5091.7	-50.5	7161.1	2537.2	8513.9	89861.1	0.0	0.0
During cooling	-2650.0	-25052.8	118916.7	-2631.7	-23.9	7313.9	4013.9	13469.4	2994.4	-1471.4	0.0
Rest of time	-33651.4	-61200.4	-191074.1	-16065.6	-171.8	32864.0	19010.9	63791.7	289291.9	-467.1	0.0

Figure 5.15. Result report in IDA-ICE. Where the highlighted field presents the energy impact of the infiltration through the door seals.



## 6 Case study: Simple office model

In this chapter the simple office model will be described. In addition to the specification of the model itself various considerations concerning door usage and wind will be presented. Finally the different simulation cases will be explained and presented.

### 6.1 The IDA-ICE model

In order to evaluate the chosen calculation models a simple model of an office building has been created. The building has been given a very simple geometry which can be resembled as the one of a shoe box, see figure 6.1. The area and height of the building have been inspired by the building who currently hosts the company ÅF AB in Gothenburg. The focus of the simulations conducted on this building was to be entirely on the infiltration through the entrance. Therefore elements such as windows and internal walls have been neglected. The heating and cooling system of the building have been given unlimited power to ensure that the temperature set points can be achieved. The specifications of the model are presented in table 6.1.

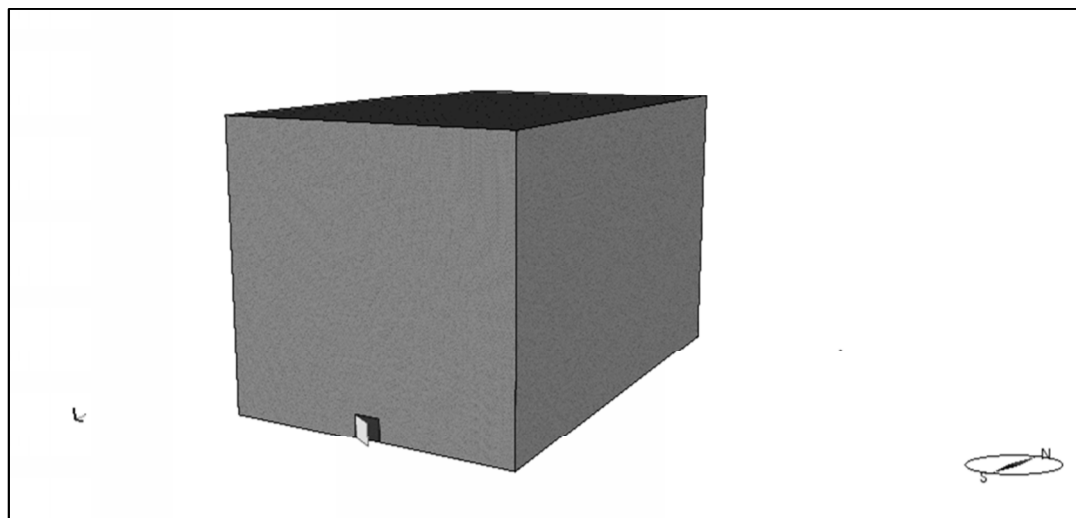


Figure 6.1. 3-D model of the simple office model.

Table 6.1. Specifications of the simple office model.

Dimensions:			
Height:	24 m	Floor area:	1000 m <sup>2</sup> /floor
Width:	25 m	Envelope area:	9335 m <sup>2</sup>
Length:	40 m	Volume:	27046 m <sup>3</sup>
No of entrances:	1	No of floors :	6
Climate:			
Min Temperature:	20C	Supply air flow:	2 L/s*m2
Max Temperature:	21C	Return air flow:	2 L/s*m2
Installations:			
Ideal heater	9999999 W	Ideal cooler	9999999 W

## 6.2 Evaluation of best and worst wind cases

In order to evaluate the energy performance for different entrance types, the worst and best wind direction has to be determined. If the entrance is or will be located at the worst side some entrance types might be very unsuitable. To determine the worst and best wind cases in an energy performance perspective can be rather complex. One factor is that the wind might blow strongly in one direction during the warm season when the temperature differences are low resulting in low energy flows, while it might change direction during the winter when the temperature differences are much higher.

Another factor is the wind variation during a 24 hour period. Since most entrance doors are used during daytime 06:00-18:00 the highest impact on energy losses due to the wind is received during this period. Night time wind might be strong and blow in one direction while it might be weaker and blow in another direction during daytime. This fact will be neglected but it's worth reflecting over.

The climate file "Gothenburg, S ve-1977" used in the IDA-ICE software uses a one hour resolution. The following parameters are given in the file: Hour, Dry bulb temperature, Relative humidity, Wind direction, Wind speed, Direct and diffuse solar radiation.

To decide the best and worst wind direction the data of wind speed and direction could be used. The wind speed is given in m/s with the accuracy of one decimal while the wind direction is given in 10s of degrees. To get an idea of the best and worst wind direction the hours were multiplied with the wind speed and the  $\Delta T(20\text{-Ambient temperature})$  for every 10s of degrees in direction. The study resulted in the figure 6.2.

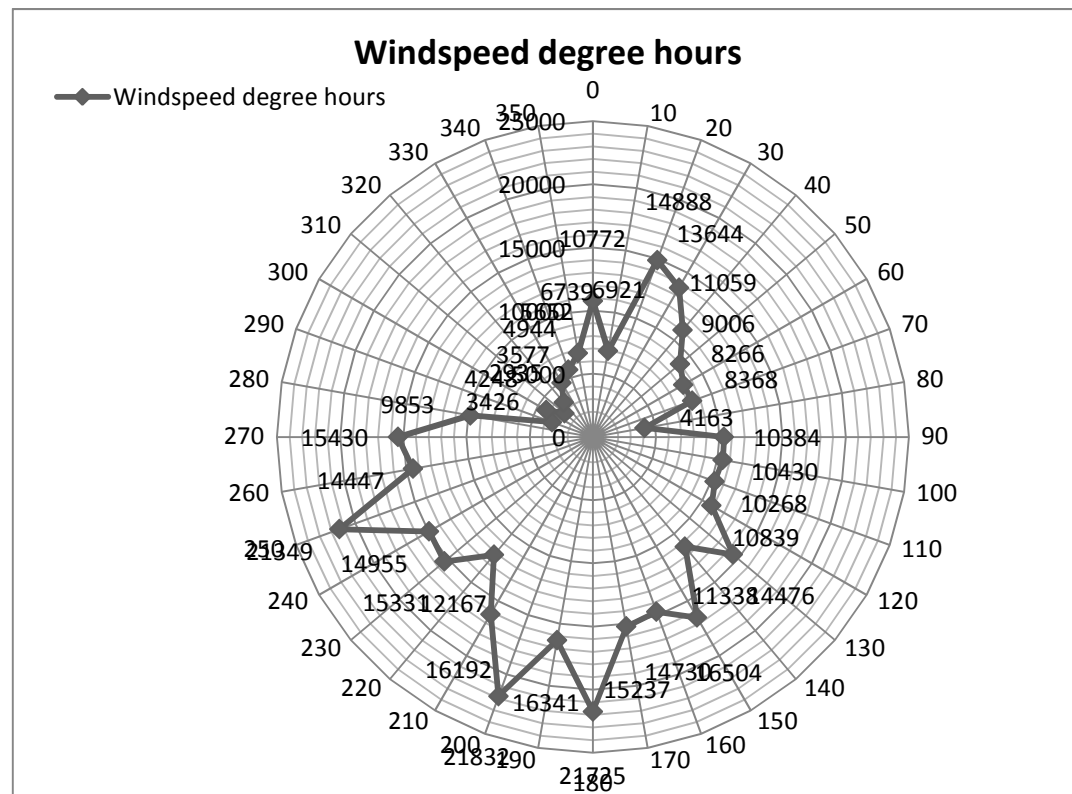


Figure 6.2. Diagram over wind speed degree hours for different wind directions.

From the study made on the climate file it is clear that the worst case would either be from the south-south west or west-south west. And the best wind case would be from the west northwest. When turning the building entrance in IDA-ICE towards these worst directions the result is lower than the case where the entrance is facing a wind coming straight from the south. The explanation to this fact is that IDA-ICE smooth the variations in wind direction according to the following equation.

$$W_{d,mean}(t) = W_d(t) + \frac{(W_d(t-1) - W_d(t))}{2} \quad (52)$$

Where

$W_{d,mean}(t)$  is the wind direction, which IDA-ICE calculates at the time t

$W_d(t)$  is the wind direction in the climate file at the time t

The worst wind direction is concluded to be straight south ( $180^\circ$ ). Since the entrance is located on the south side of the building the worst orientation of the building is  $0^\circ$

### 6.3 Door-usage schedules

In order to evaluate the energy performance of the various entrances types on an office building an office like door-usage schedule was created. This schedule is based on Swedish office times and office behavior. The base opening hours of the office are from 08:00 to 17:00. One hour of flex time is applied resulting in that some people arrive and leave up to one hour early or late. The flex time also apply at lunch time 12:00. Some flow of people between the peak hours is considered. The building is closed every weekend.

The calculation models for open type doors are valid up to a flow of 450 people per hour. Therefore the schedule called “High” (see figure 6.3) have a maximum flow of people set to 450 PPH. The schedule called “Medium” (see figure 6.4) have all flows of people reduced by 33%. And the schedule called “Low” (see figure 6.5) have all flows of people reduced by 66%.

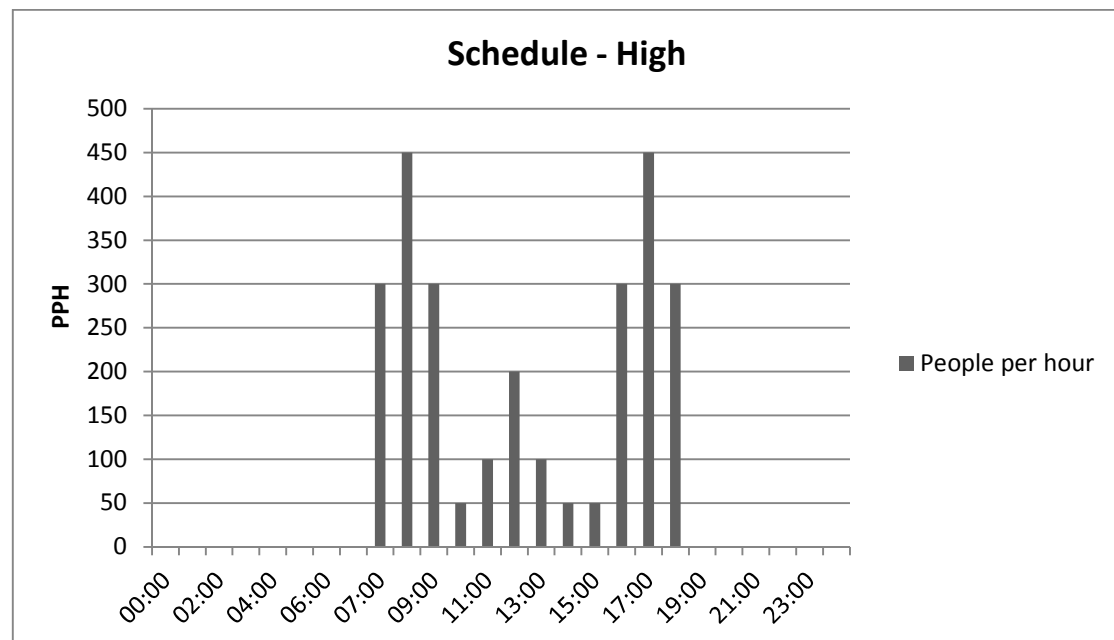


Figure 6.3. Door usage schedule of office style, denoted as Schedule-High.

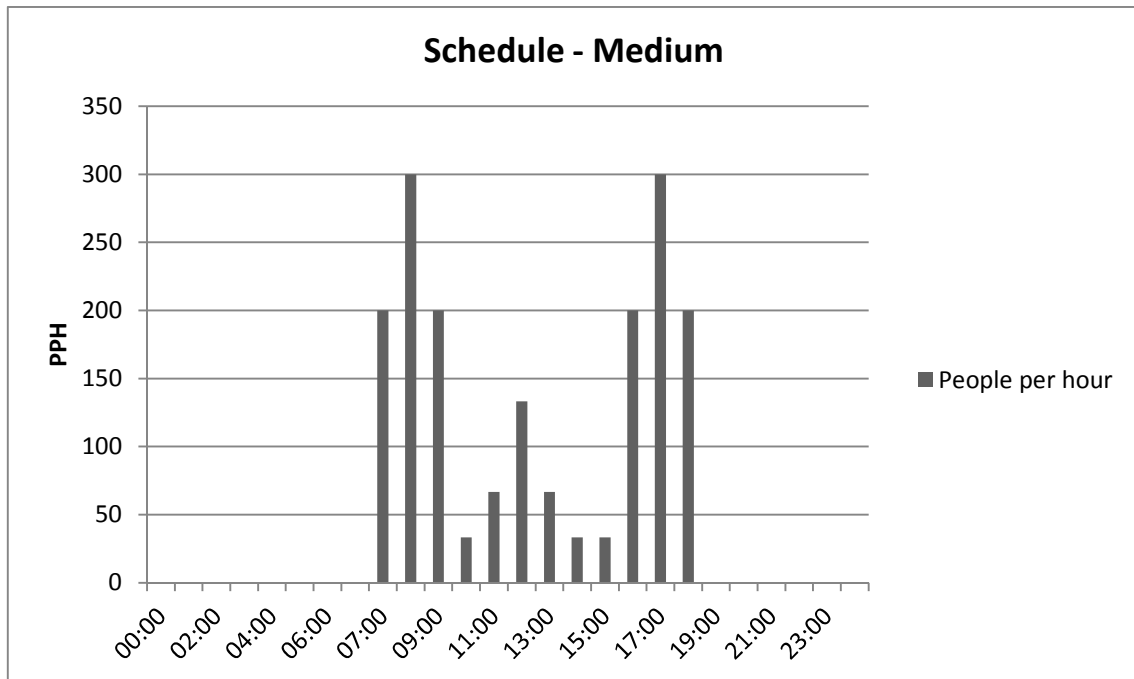


Figure 6.4. Door usage schedule of office style, denoted as Schedule-Medium.

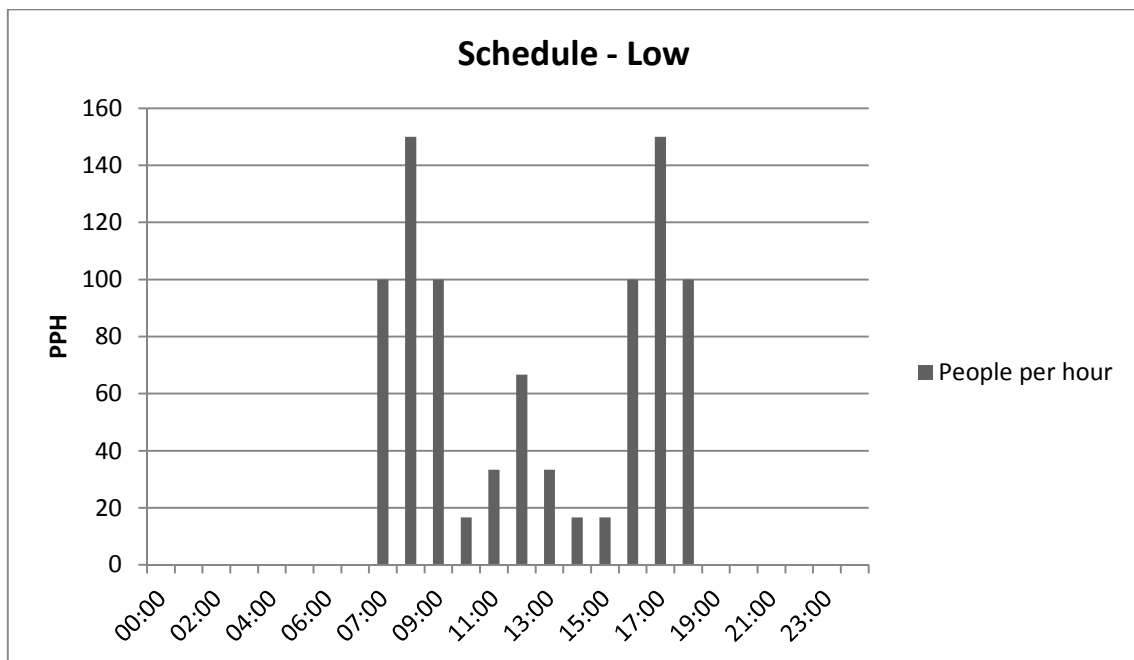


Figure 6.5. Door usage schedule of office style, denoted as Schedule-Low.

## 6.4 Simulation cases

A range of simulation cases have been created in order to analyze the entrance models under different conditions. The difference between the scenarios is flow of people, building geometry, variety of entrance solutions and pressurization of the building. The simulated entrance solutions for every case are seen in table 6.2 where the letters h, l, and m indicate what door usage schedule which was used for the simulation. See Appendix B for illustrations of the different entrance solutions. All simulations were simulated with a time period of 1 year.

Table 6.2. Entrances types simulated in the different cases.

	Reference h	Reference m	Reference l	Double Height h	+ 5 Pa pressure h	- 5 Pa pressure h
Single sliding door	X	X	X	X	X	X
Single swing door	X	X	X			
Sliding doors with vestibule	X	X	X			
Swing doors with vestibule	X	X	X	X	X	X
Sliding doors with 90 vestibule	X	X	X	X	X	X
Swing doors with 90 vestibule	X	X	X			
4-wing revolving door, new	X	X	X			
4-wing revolving door, maintained	X	X	X	X	X	X
4-wing revolving door, worn	X	X	X			

### 6.4.1 Reference Case

The energy performance of the various entrances was analyzed under 3 sets of usage schedules. The purpose of this simulation was to see that all entrance models worked in IDA-ICE and how the entrances performed at different flows of people. The preconditions to this simulation case are shown in table 6.3.

Table 6.3. Simulation settings for the reference case.

Simulation Settings			
Climate file:	Göteborg, Säve	Air-tightness	0,5 L/(s*m <sup>2</sup> )
Wind Coefficients:	Exposed	Height adjustment	None
Wind Profile:	Suburban	Pressurization:	None

### 6.4.2 Double height case

In this case the height of the building was doubled from 24m to 48m in order to increase the stack pressure. In this case only sliding and revolving door solutions were simulated. The purpose of the simulation was to determine the impact of an increased stack pressure and an increased area of the building envelope. The preconditions to this simulation case are shown in table 6.4.

Table 6.4. Simulation settings for the double height case

Simulation Settings			
Climate file:	Göteborg, Säve	Air-tightness	0,5 L/(s*m <sup>2</sup> )
Wind Coefficients:	Exposed	Height adjustment	+24 meters
Wind Profile:	Suburban	Pressurization:	None

### 6.4.3 Case with +5 Pa mechanically induced pressure difference

In this case the ventilation levels were adjusted to obtain a positive pressure difference of 5 Pa. This means that the pressure is higher inside the building than outside when no other pressure effects are present. In this case only sliding and revolving door solutions were simulated. The purpose of the simulation was to determine what impact pressurization of the building has on the infiltration through the different entrance types. The preconditions to this simulation case are shown in table 6.5.

Table 6.5 Simulation settings for case with +5 Pa mechanically induced pressure difference

Simulation Settings			
Climate file:	Göteborg, Säve	Air-tightness	0,5 L/(s*m <sup>2</sup> )
Wind Coefficients:	Exposed	Height adjustment	+24 meters
Wind Profile:	Suburban	Pressurization:	+5 Pa

#### 6.4.4 Case with -5 Pa mechanically induced pressure difference

In this case the ventilation levels were adjusted to obtain a negative pressure difference of 5 Pa. This means that the pressure is lower inside the building than outside when no other pressure effects are present. In this case only sliding and revolving door solutions were simulated. The purpose of the simulation was to determine what impact depressurization of the building has on the infiltration through the different entrance types. The preconditions to this simulation case are shown in table 6.6.

*Table 6.6 Simulation settings for case with -5 Pa mechanically induced pressure difference*

Simulation Settings			
Climate file:	Göteborg, Säve	Air-tightness	0,5 L/(s*m <sup>2</sup> )
Wind Coefficients:	Exposed	Height adjustment	+24 meters
Wind Profile:	Suburban	Pressurization:	-5 Pa



## 7 Case study: Nils Ericson Terminal, NET

In this chapter the Nils Ericson terminal also called NET will be introduced. Some modifications of the chosen calculation models from 3.5 will be presented. Additionally the different energy simulation cases will be described.

### 7.1 Introduction

An opportunity to implement the acquired calculation models for different entrance types on a high infiltration building has been made possible due to the cooperation with Cajsa Lindström. The building is the Nils Ericson bus terminal in Gothenburg for which Cajsa has made an energy model. This cooperation gave access to a detailed energy model and documented annual energy usage. With climate data for the specific year of 2010, a detailed building energy model and data for energy usage it was possible to in some degree validate the calculation models. See figure 7.1 for illustrations of the terminal.

All building specifications such as dimensions, ventilation system, heating system, cooling system, occupancy data, g-values, U-values and so on are described in (Lindström, 2013). Only data and specifications concerning flow of people and entrances will be described in this thesis.

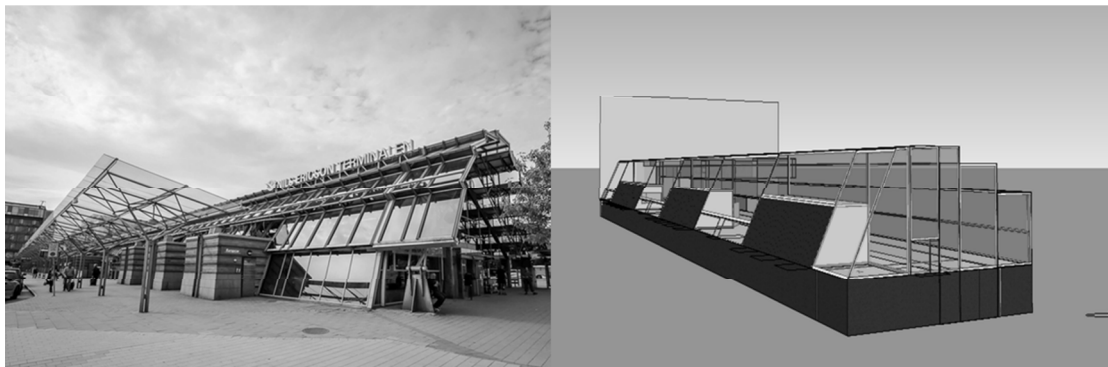


Figure 7.1 To the left NET in reality (Bengtsson, 2013) At the right energy model of NET (Lindström, 2013).

## 7.2 Entrances of NET

There are in total 23 entrances in NET of which 18 are gates and 5 are ordinary entrances. In figure 7.2 the locations of the different entrances are found. Entrance (A) is called the main entrance, B, C, and D are called back entrances and E is called side entrance. The 18 gates are marked with (F). The specifications for these entrances are found in table 7.1. Illustrations of all entrance solutions can be found in Appendix B.

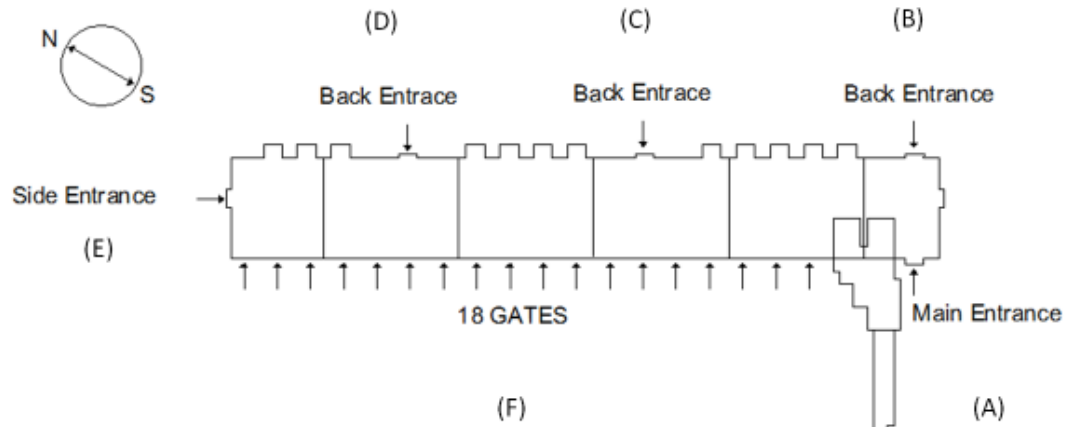


Figure 7.2. Overview of the entrances of NET.

Table 7.1. Entrance summary of the NET.

Entrances of the Nils Ericson Terminal			
Name	Number of entrances	Entrance type	Dimensions
Gates	18	Single slide door with air curtain	2 m x 2 m
Main Entrance	1	Slide door vestibule	2 m x 2 m
Back Entrance	3	Slide door vestibule	2 m x 2 m
Side Entrance	1	Slide door vestibule	2 m x 2 m

### 7.2.1 Door usage at NET

The most vital factor of energy modeling of entrances is the door opening frequency. Lindström has estimated the door usage from occupancy data in her report. The distribution of people flow for the different entrances according to Lindström is found in figure 7.3. The flow of people through the different entrances are presented in figures 7.4, 7.5 and 7.6.

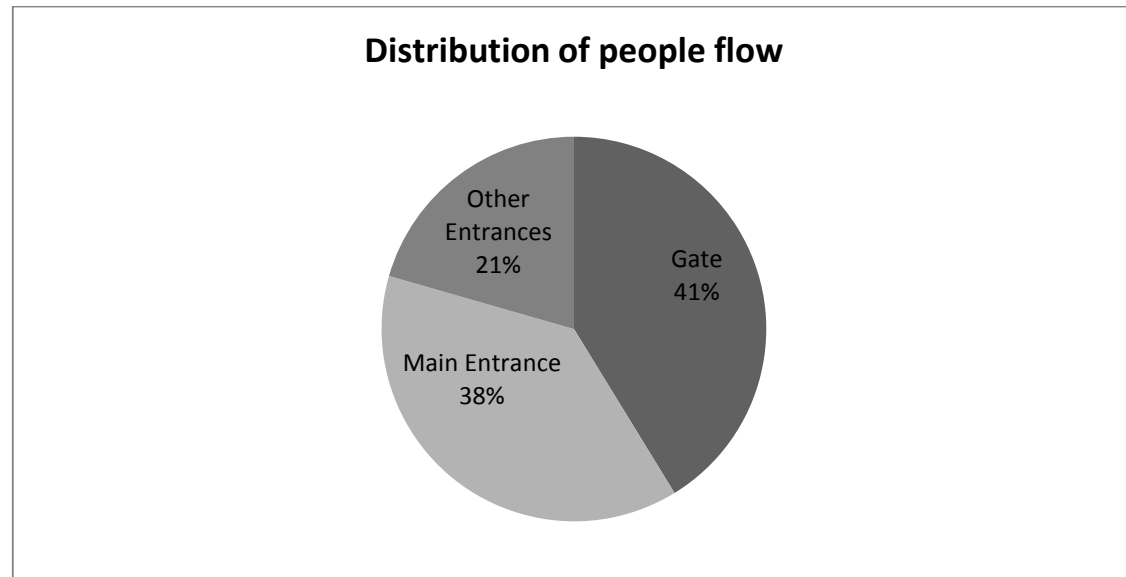


Figure 7.3. Distribution of people flow among the different entrance groups.

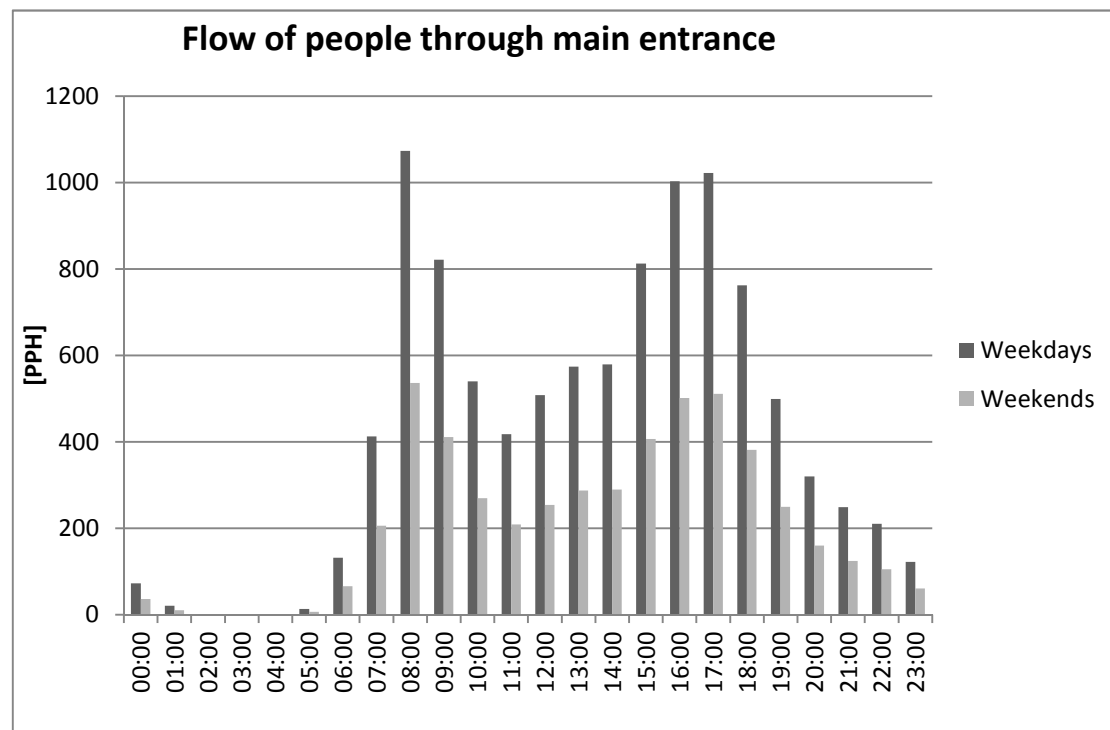


Figure 7.4. Flow of people through the main entrance during weekdays and weekends.

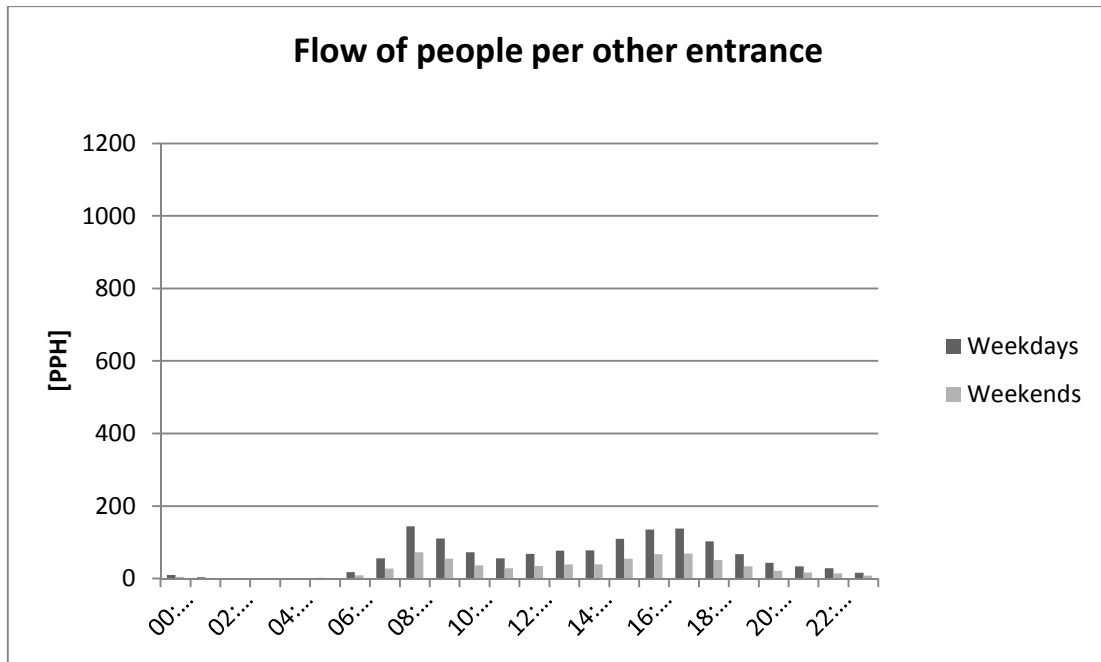


Figure 7.5. Flow of people through other entrances during weekdays and weekends.

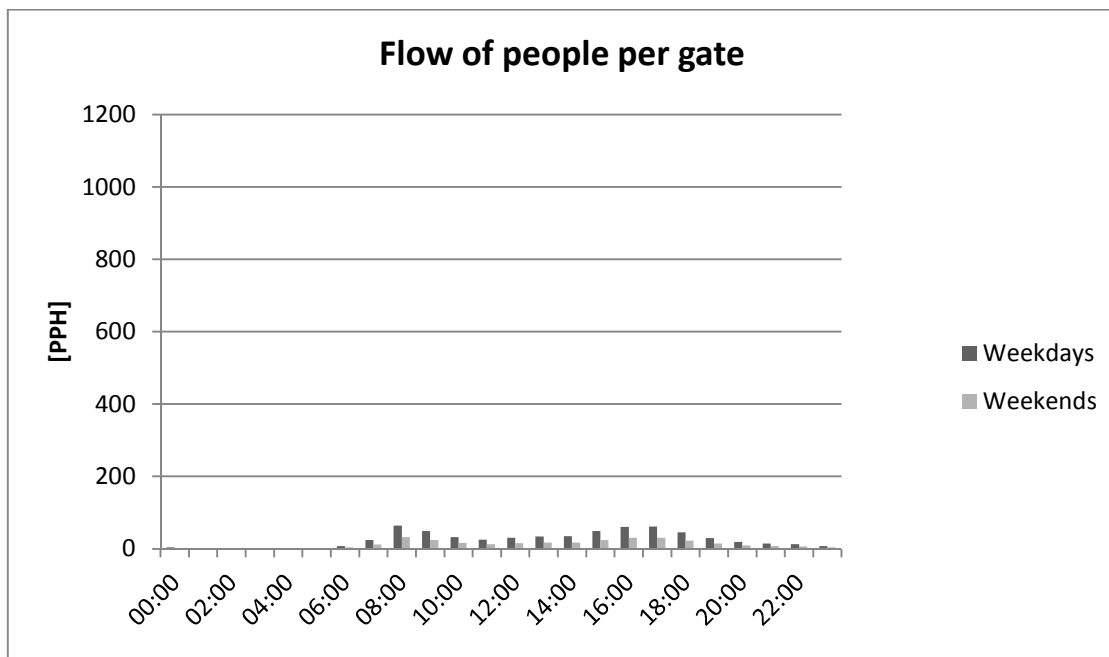


Figure 7.6. Flow of people through one gate during weekdays and weekends.

### 7.3 Extended model for open type doors

The maximum flow of people through the main entrance of NET exceeds 1000 PPH. Since the equations acquired for open-type doors are valid up to 450 PPH there is a need to create a model for people flows over 450 PPH. Since no data was available for people flows above 450 PPH some rough assumptions were made.

At 900 PPH and higher any door, vestibule or not is assumed to be fully open with an air flow coefficient equal to the maximum discharge coefficient for the specific entrance type. 0.62 for single doors and doors with straight vestibules and 0.35 for doors with 90° vestibules. For people flows in the range 450-900 PPH the curve fitting method was applied with 900 PPH defined as the endpoint.

For swing doors the curve fitting resulted in figure 7.7 with the equations valid for 450-900 PPH presented in table 7.2. For sliding doors the curve fitting resulted in figure 7.8 with the equations 450-900 PPH presented in table 7.3.

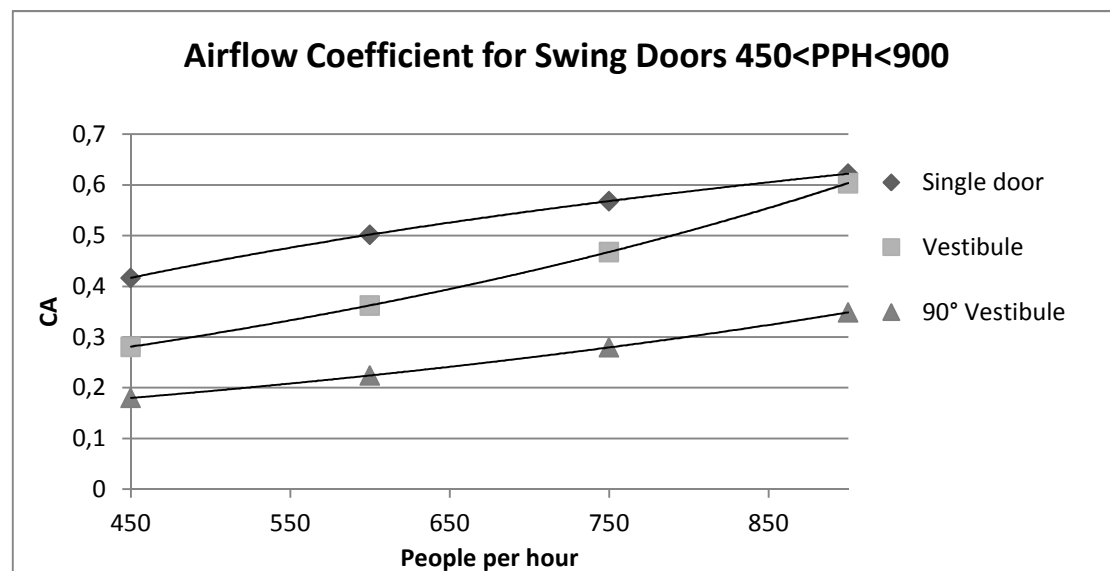


Figure 7.7. Estimated airflow coefficient for swing doors with people flows between 450 and 900 PPH.

Table 7.2. Air flow coefficient equations for swing doors valid for 450- 900 PPH

Equations for swing doors, 450<PHP<900		
Door Type:	Air flow coefficient, $C_A$	
Single Door	$0,2964 * \ln(F_p) - 1,3941$	(53)
Doors with vestibule	$0,137 * e^{0,0017 * F_p}$	(54)
Doors with 90° vestibule	$0,0928 * e^{0,00147 * F_p}$	(55)

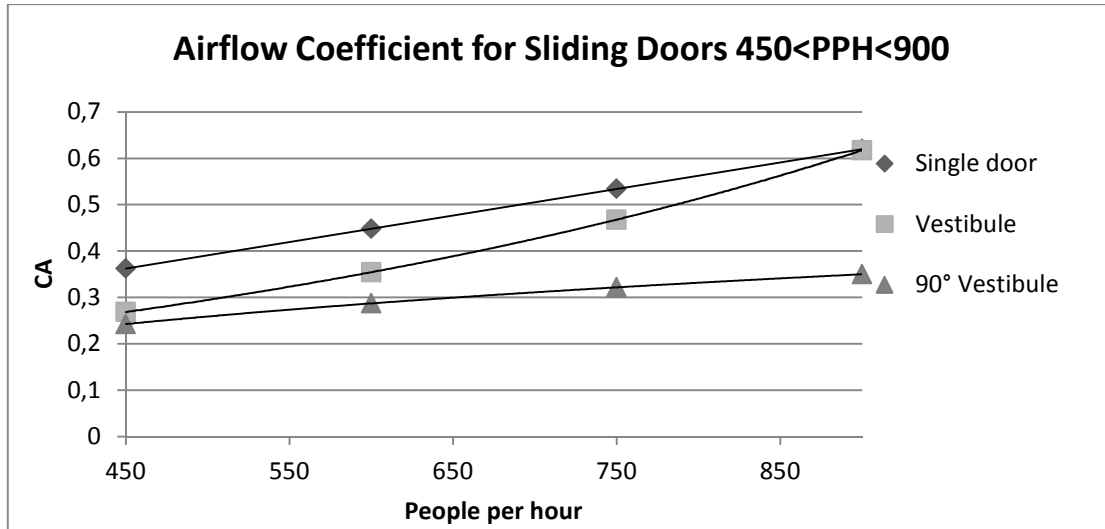


Figure 7.8. Estimated airflow coefficient for sliding doors with people flows between 450 and 900 PPH.

Table 7.3. Air flow coefficient equations for swing doors valid for 450- 900 PPH.

Equations for slide doors, 450<PPH<900		
Door Type:	Air flow coefficient, $C_A$	
Single Door	$0,000572 * (-450 + F_p) + 0,3626$	(56)
Doors with vestibule	$0,1168 * e^{0,00185 * F_p}$	(57)
Doors with 90° vestibule	$0,155 * \ln(F_p) - 0,7044$	(58)

## 7.4 Scale up of revolving door model

The chosen models for revolving doors are only valid on a 4-winged door with the reference dimensions of 2,1 m in diameter and 2 meter in height as described in chapter 4.3. The NET is a bus terminal and therefore it is natural that people will carry luggage. A 4-winged door with a diameter of 2,8m is the minimum diameter required for a door where people with large bags are to pass (Boon Edam, 2013). Usual for this kind of building are doors with a diameter around 4 m. In order to calculate on realistic door sizes the reference door has to be scaled up. To keep the margin of error as low as possible the revolving doors used in this case study are the smallest possible, 2,8 m in diameter.

The leakage through the door seals depends on the area of the door way. Therefore the ELA for a maintained revolving door will be scaled up by 1,333 resulting in a ELA of 0,00233 m<sup>2</sup>. See equation 59 and 60.

$$s_{area} = \frac{A_{\phi=2,8}}{A_{\phi=2,1}} = 1,333 \quad (59)$$

$$ELA_{\phi=2,8} = 0,00175 * s_{area} = 0,00233 [m^2] \quad (60)$$

The air exchange due to the revolving motion of the door depends on the volume of the door. Therefore the air exchange of the door will be scaled up by 1,78 according to equation 61. The resulting performance curve where the scaled up door is compared to an identical door calculated by the Boon Edam calculation tool, see figure 7.9

$$s_{volume} = \frac{V_{\phi=2,8}}{V_{\phi=2,1}} = 1,78 \quad (61)$$

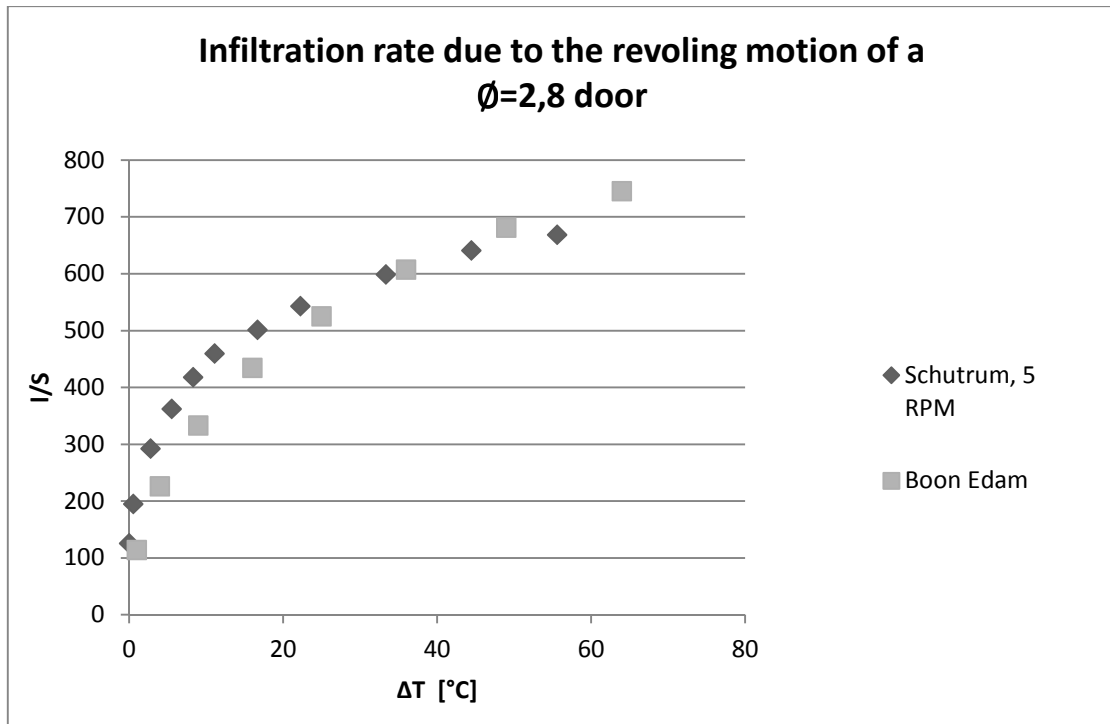


Figure 7.9. Comparison of infiltration between Schutrum and Boon Edam.

## 7.5 Simulation cases

Several simulation cases have been constructed. In order to keep the amount of simulations down the entrances of NET have been grouped in to 3 groups; Gates, Main Entrance and Other entrances. Different entrances and the variation of these differ between the study cases. Table 7.4 gives an overview of the different simulation cases and the entrances that are simulated in every case. All simulations will be one year simulations with a site specific climate file from 2010.

Table 7.4. Map over the simulation cases and the entrance types to simulate.

Study Case	Entrance groups		
	Gates	Main Entrance	Other Entrances
Reference case	Single sliding door	Sliding door vestibule	Sliding door vestibule
Gate study	Variation ↓ Single swing door Sliding door vestibule Swing door vestibule Sliding door 90° vestibule Swing door 90° vestibule 3x Revolving Doors Ø 2,8m	Sliding door vestibule	Sliding door vestibule
Main entrance study	Variation ↓ Single sliding door	Single swing door Sliding door vestibule Swing door vestibule Sliding door 90° vestibule Swing door 90° vestibule Revolving Door Ø 2,8m	Sliding door vestibule
Optimization studies			
Optimal open type case	Swing door 90° vestibule	Swing door 90° vestibule	Swing door 90° vestibule
All entrances revolving	Single sliding door	Revolving Door Ø 2,8m	Revolving Door Ø 2,8m
All entrances and gates revolving	3x Revolving Doors Ø 2,8m	Revolving Door Ø 2,8m	Revolving Door Ø 2,8m

### 7.5.1 Reference case

In this simulation case all entrance doors are defined as they are in reality. The purpose of this simulation was to obtain a reference case which all other simulations can be compared to. The results of the reference case will also indicate how accurate the door models are. Additionally simulations where all doors are either closed or fully opened will be conducted. The purpose of those simulations was to determine the impact the entrance door models have on the results. The entrance solutions for this case are defined in table 7.4.



### 7.5.2 Gate study

The purpose of this study is to see how different entrance solutions for the gates will affect the infiltration into the building. In this simulation study only entrance solutions for the gate doors are studied, all other entrances are kept as in the reference model. See the variations in table 7.4. The initial single slide door is calculated with half area due to the influence of the air curtain. All open-type door solutions for the gates are calculated with the influence of the air curtain. Changing to 18 revolving doors would be unrealistic and time demanding when it comes to modeling. Instead a solution with 3 revolving doors with an external roof was created see figure 7.10.

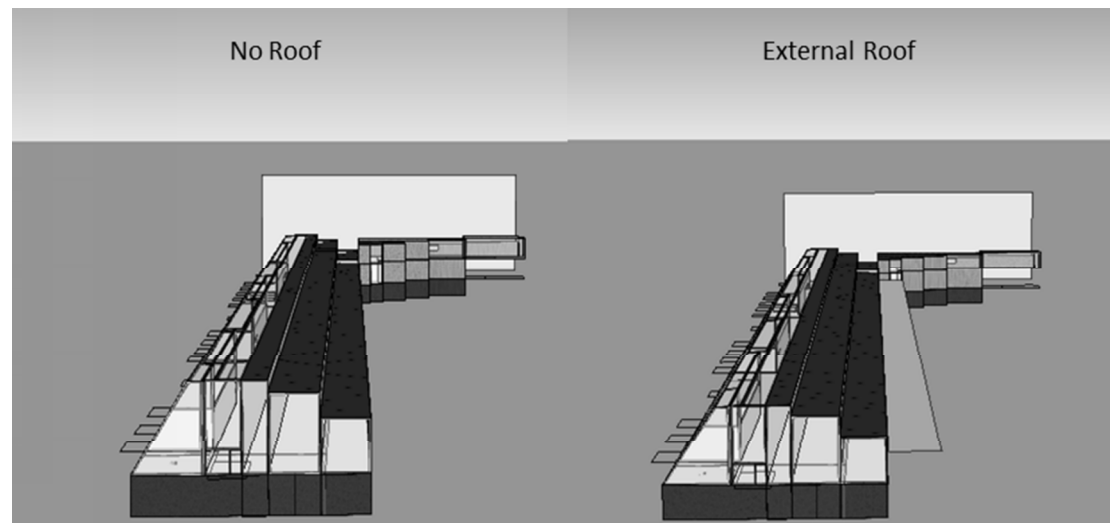


Figure 7.10. To the left a model without the external roof and to the right a model with an external roof.

### 7.5.3 Main entrance study

The purpose of this study is to see how different entrance solutions for the main entrance will affect the infiltration into the building. In this simulation study only entrance solutions for the main entrance are studied, all other entrances are kept as defined in the reference model, see table 7.4.

### 7.5.4 Optimization studies

In optimal open-type door case entrances and gates will be changed to swing doors with a 90° vestibule. This solution has proved to give the best energy performance for open-type doors. The purpose of this simulation is to determine how the energy performance of the building is affected and to show that a quite simple solution like this can save energy.

In the revolving entrances case all entrances have revolving doors except for the gates which are kept defined in the reference model. This simulation will show the energy performance of the building with a highly realistic entrance solution. Changing the sliding door vestibules to revolving doors won't affect the area used.

In the revolving entrances and gates case all entrances and gates have revolving doors. Where the gate doors have been converted to 3 revolving doors and an external roof have been added to allow people to wait outside. See figure 7.10. This case was assumed to be the most energy efficient solution.

## 8 Results from the study cases

This chapter will present the results of the simulation cases described in chapter 6 and 7. Simulation results of infiltration both through entrances and the total infiltration into the buildings will be presented. From the simulations conducted on NET results of delivered heating and cooling are presented to show what effect the infiltration has on the energy consumption for the whole building. The results of the simplified office model will focus entirely on the infiltration through the door and the total infiltration into the building.

### 8.1 Simple office model

In this chapter the results from the simulations conducted on the simple office model will be presented. The focus of the results is to present how the different entrance solutions are performing related to each other. Additionally how they are affected by changes of the flow of people, the building height and mechanically induced pressure differences.

#### 8.1.1 Reference case

In figure 8.1 the infiltration loss through the different entrances is presented. The results are presented for the three different schedules which were described in chapter 6.3. The best performing entrance is the revolving door and the worst is the one with a single slide door. It is also clear that the variations in people flow have a large impact on the infiltration losses.

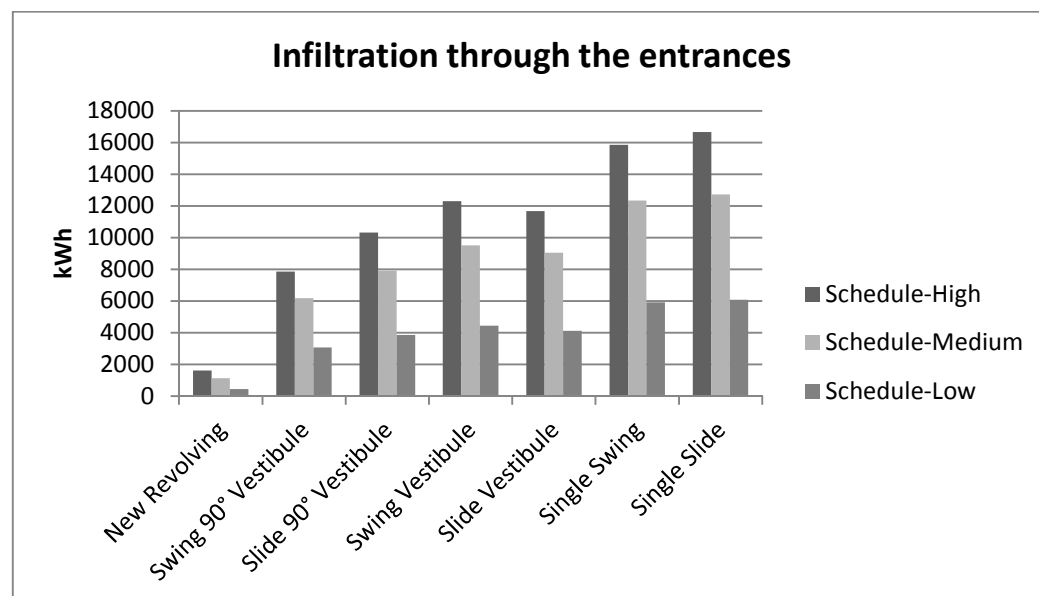


Figure 8.1. Infiltration through different entrances with different usage schedules.

In figure 8.2 the total infiltration into the building is presented. It is clear that the changes in people flow through the entrance has a smaller impact on the total infiltration into the building. In figure 8.3 the percentage of the total infiltration through the entrance is presented. Here it is clear that most entrance types stand for 20-40% of the total infiltration losses. While the revolving door only stand for 5-10%.

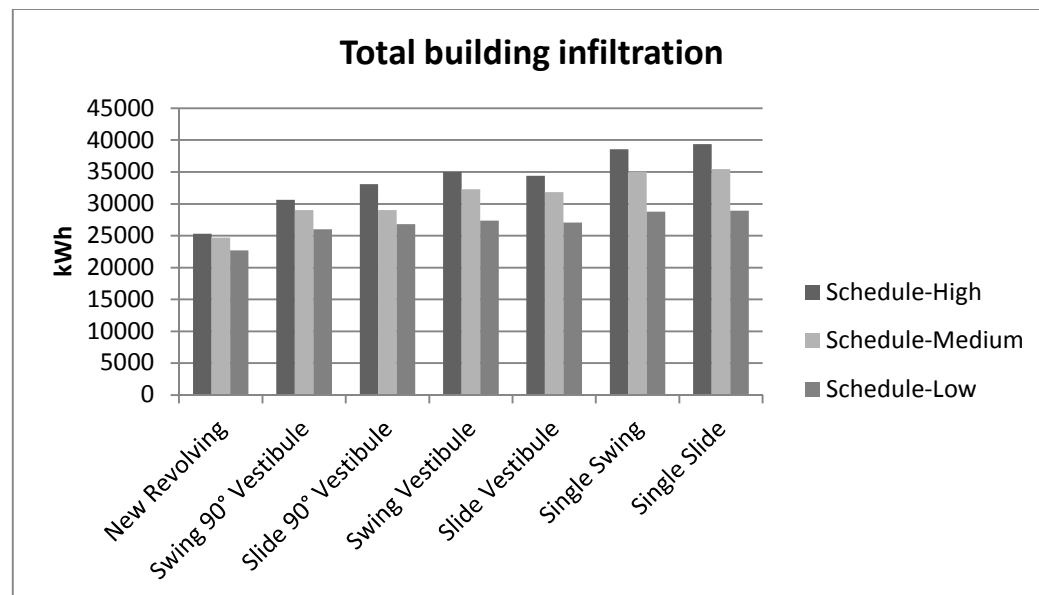


Figure 8.2. Total infiltration into the building with different entrances and different usage schedules.

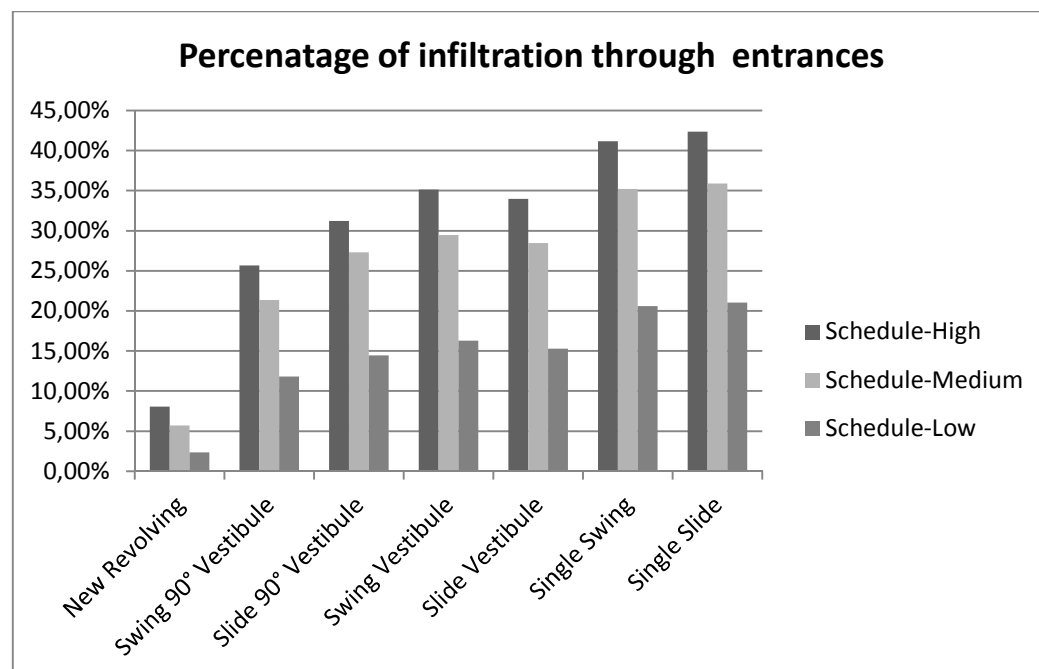


Figure 8.3. Percentage of the total infiltration from infiltration through entrances at different usage schedules.

It is clear that the flow of people through the entrance has a great impact on the infiltration. In figure 8.4 it is shown how sensitive different entrances are for changes in the people flow by presenting the impact of schedule changes from high to medium and from high to low. Additionally it is clear that the revolving door is more sensitive than the open-type entrance solutions.

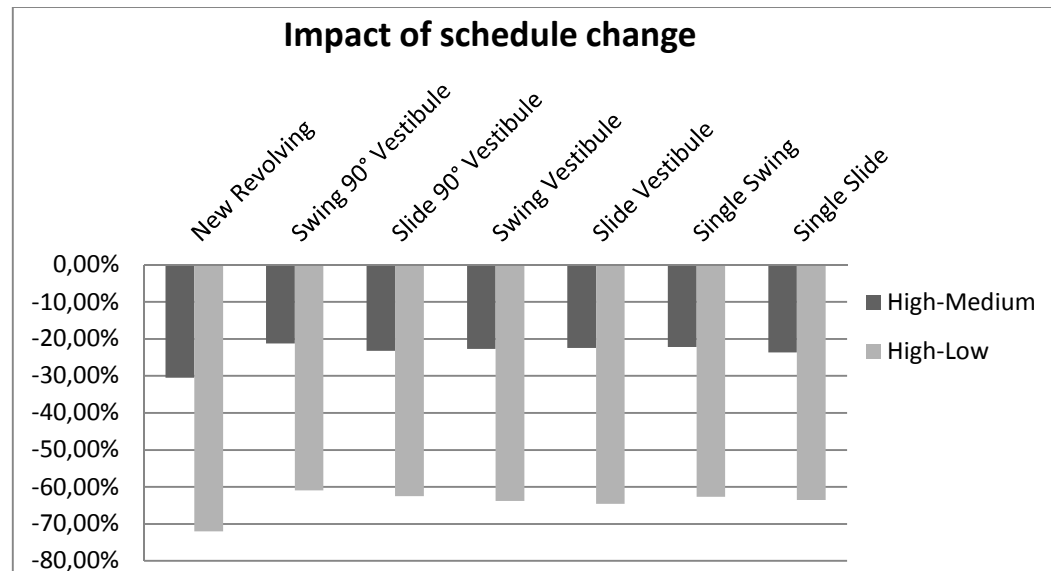


Figure 8.4. Impact of changes in door usage schedules on the infiltration through the entrances.

Three models representing a revolving door in the conditions new, maintained and worn were introduced in chapter 4.3.1. The annual infiltration through the door in different conditions with the high schedule is presented in figure 8.5. The infiltration through the worn door is 44% greater than through a new door. While the infiltration is only 13% greater for a maintained door than for a new one.

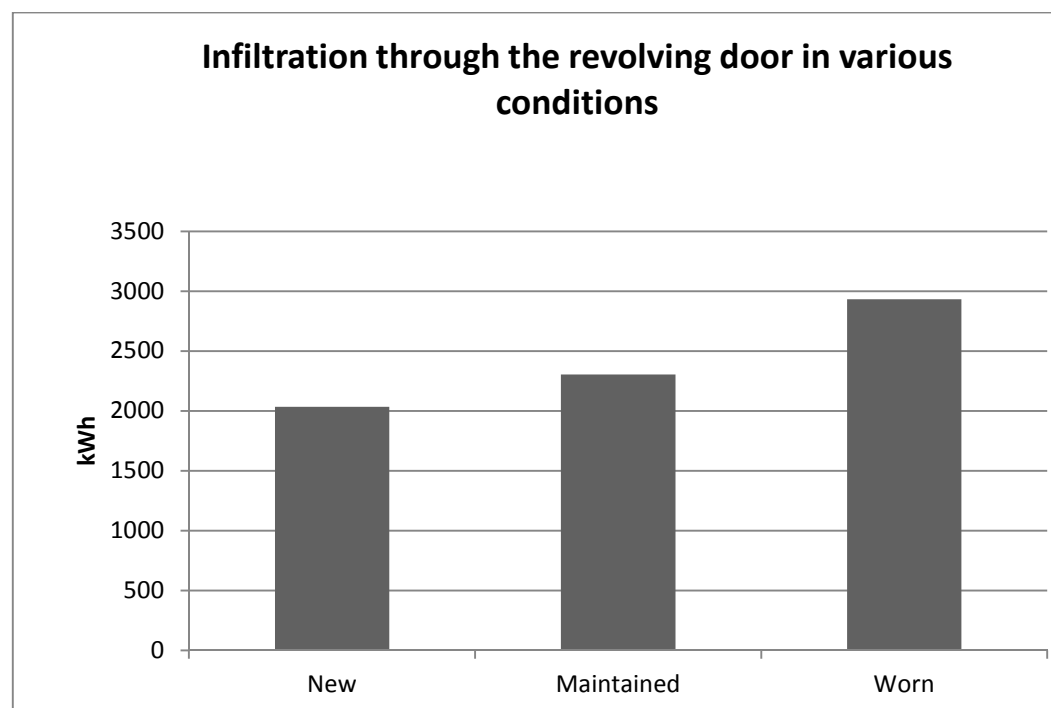


Figure 8.5. Infiltration through a revolving door in different physical states.

The infiltration through a revolving door is lower than any type or setup of open-type doors. By a fact the infiltration is reduced when replacing an existing open-type door to a revolving one. The reduction of infiltration can be described as a factor. This factor is presented for sliding doors at different schedules in figure 8.6. It shows that the effect of changing to a revolving door is the largest at low flows of people, although it is very high in general.

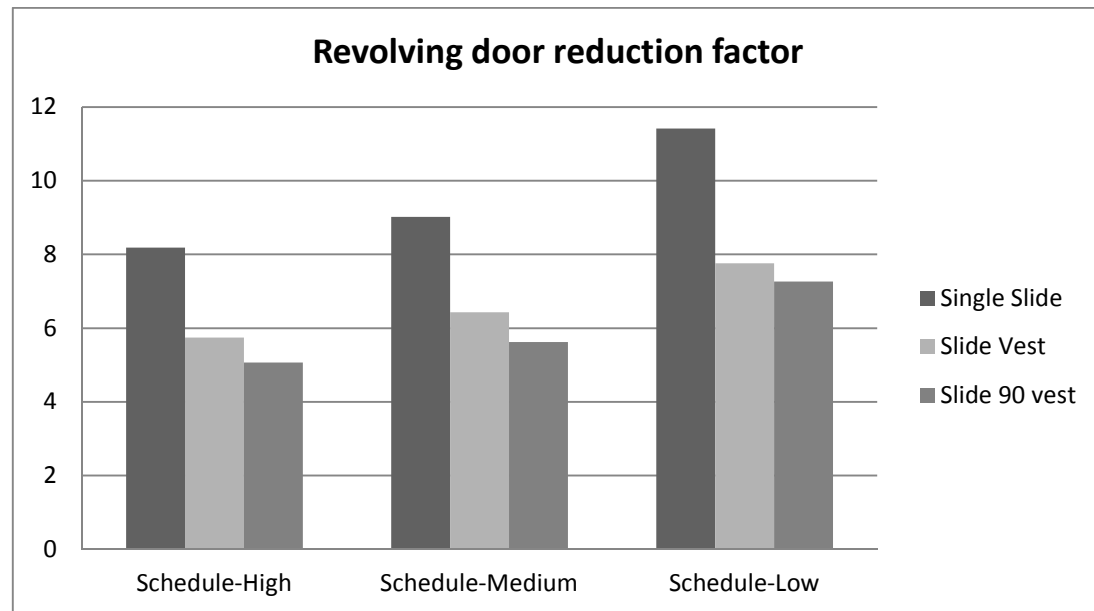


Figure 8.6. Reduction in infiltration by changing entrance to a revolving door.

### 8.1.2 Double height case

With the height of the building doubled both the total infiltration into the building and the infiltration through the entrance increased. The total infiltration into the building and the infiltration through the entrance are presented in figure 8.7. The percentage of the total infiltration through the entrance decreased for entrances compared to the reference building. See figure 8.8 for the percentage of the total infiltration through the entrance.

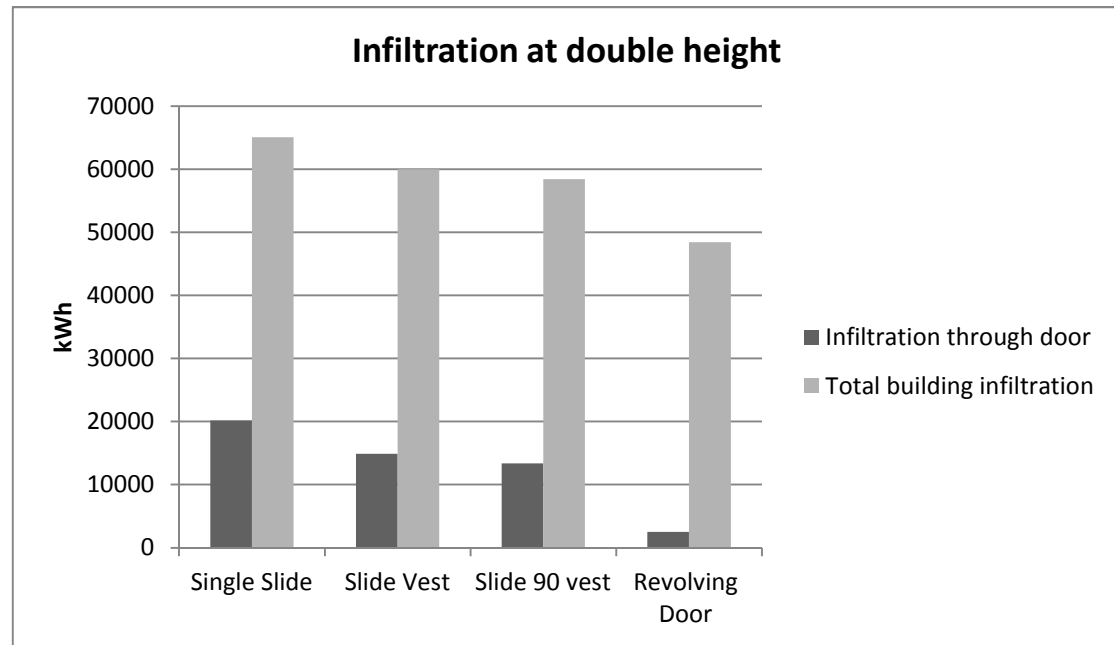


Figure 8.7. Total infiltration and infiltration through the entrances with double height on the building model.

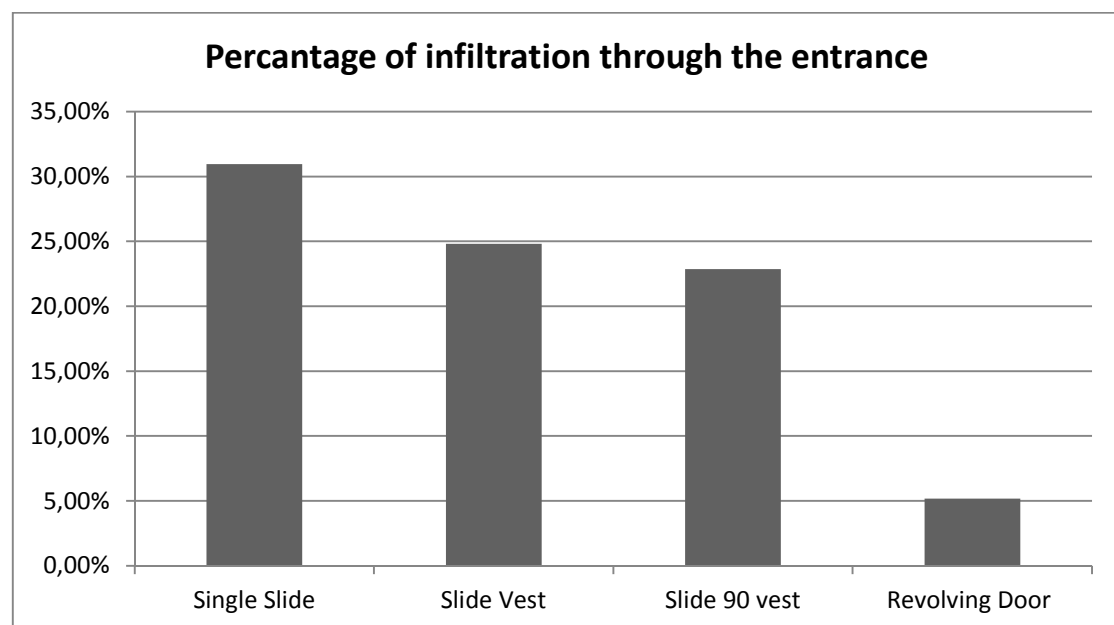


Figure 8.8. Percentage of the total infiltration from infiltration through entrances.

The impact on the amount of infiltration into the building from the height doubling is presented in figure 8.9. The impact of the height doubling was highest for the best performing open-type solution when looking at the increase of infiltration through the entrance. The increase of total building infiltration was highest with a revolving entrance.

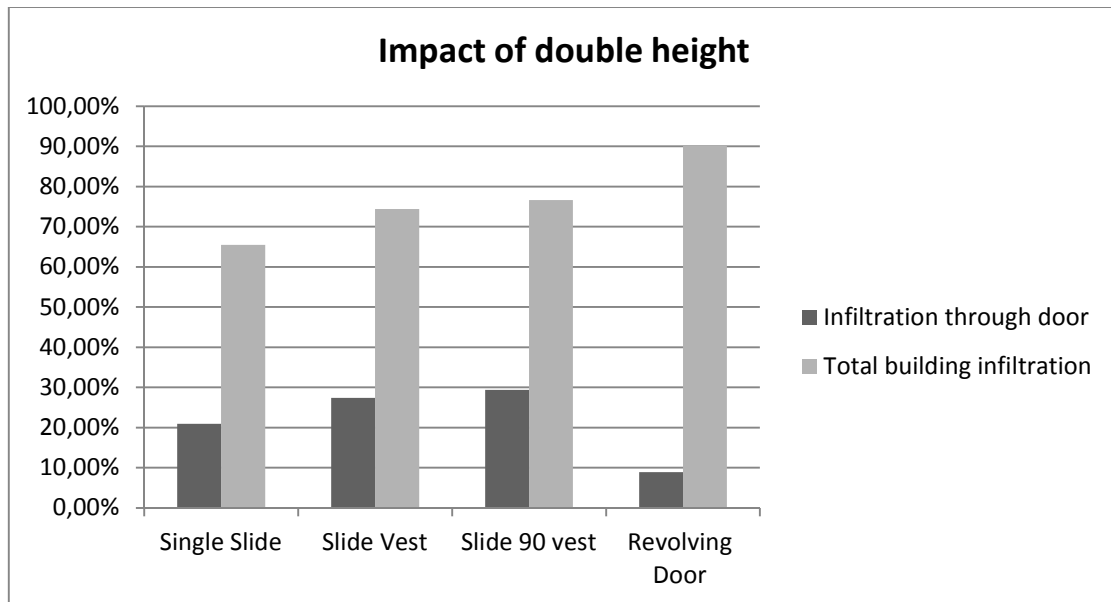


Figure 8.9. Impact on the total infiltration and infiltration through entrances caused by a doubling of the building height.

### 8.1.3 Mechanically induced pressure difference cases

In the case with a mechanically induced pressure difference of + 5 Pa the infiltration into the building is strongly decreased. The total infiltration into the building and the infiltration through the entrance are presented in figure 8.10. The percentage of the total infiltration through the entrance for all entrances are increased compared to the reference building. The largest increase is seen for the case with a revolving door. See figure 8.11 for the percentage of the total infiltration through the entrance.

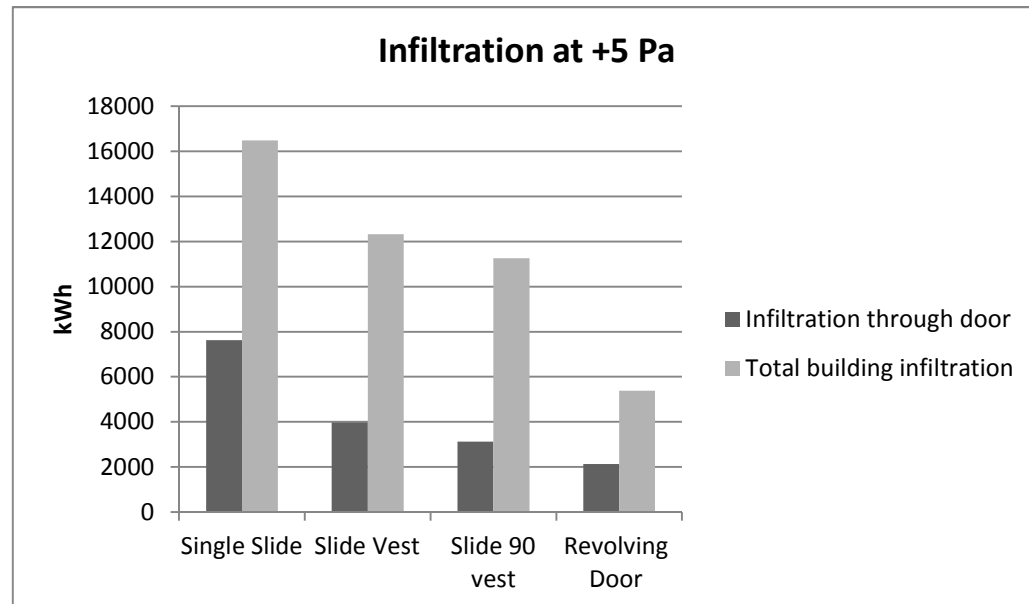


Figure 8.10. Total infiltration and infiltration through the entrances with +5 Pa mechanically induced pressure difference.

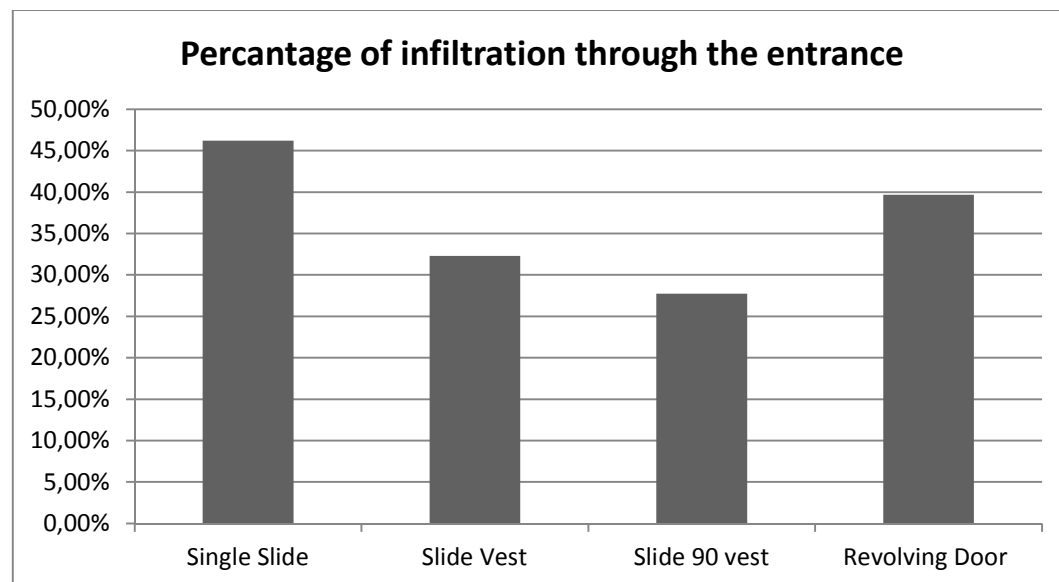


Figure 8.11. Percentage of the total infiltration from infiltration through entrances.



The impact on the amount of infiltration into the building due to the mechanically induced pressure of +5 Pa is presented in figure 8.12. The impact of the +5 Pa was highest for the revolving door entrance when looking at the decrease of total building infiltration. While the infiltration decrease through the revolving door was the lowest. The sliding door with 90 degree vestibule received the largest impact among the open-type doors.

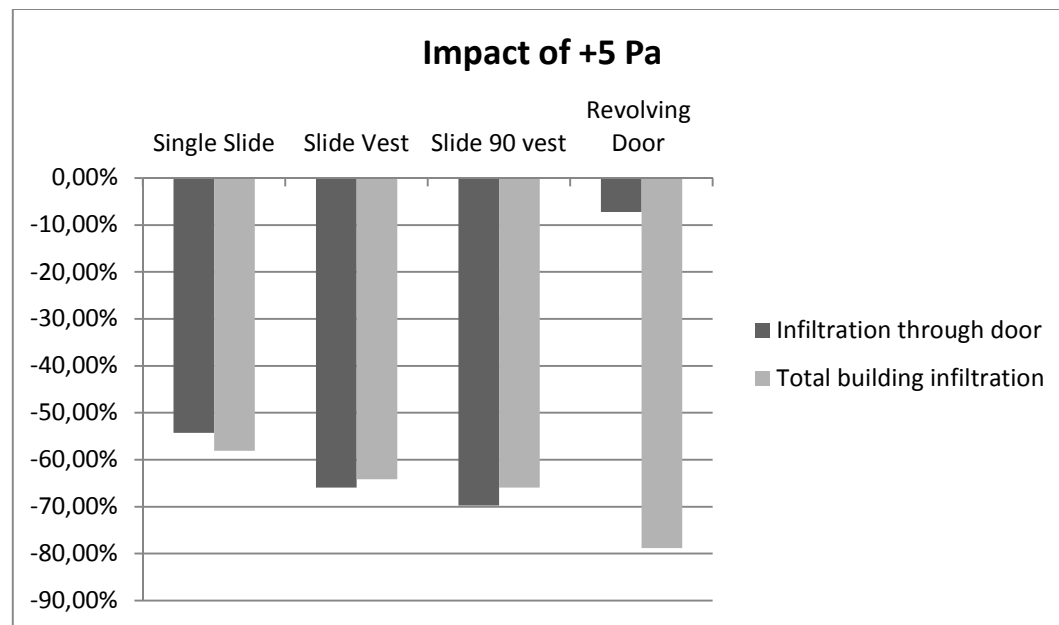


Figure 8.12. Impact on the total infiltration and infiltration through entrances caused by a +5 Pa mechanically induced pressure difference.

In the case with a mechanically induced pressure difference of - 5 Pa the infiltration into the building is strongly increased. The total infiltration into the building and the infiltration through the entrance are presented in figure 8.13. The percentage of the total infiltration through the entrance is decreased for all entrances compared to the reference building. See figure 8.14 for the percentage of the total infiltration through the entrance.

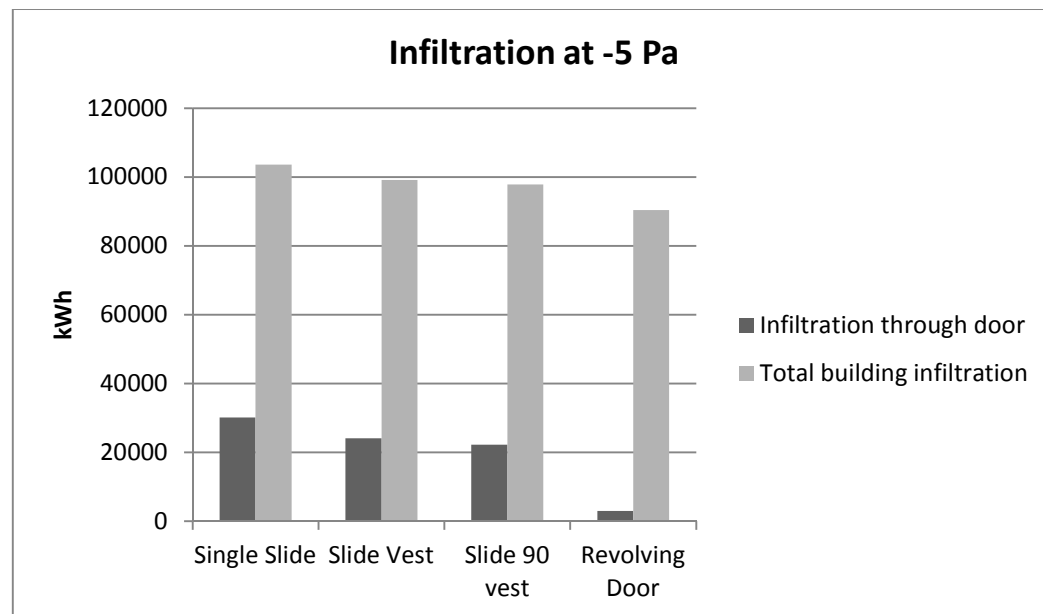


Figure 8.13. Total infiltration and infiltration through the entrances with -5 Pa mechanically induced pressure difference.

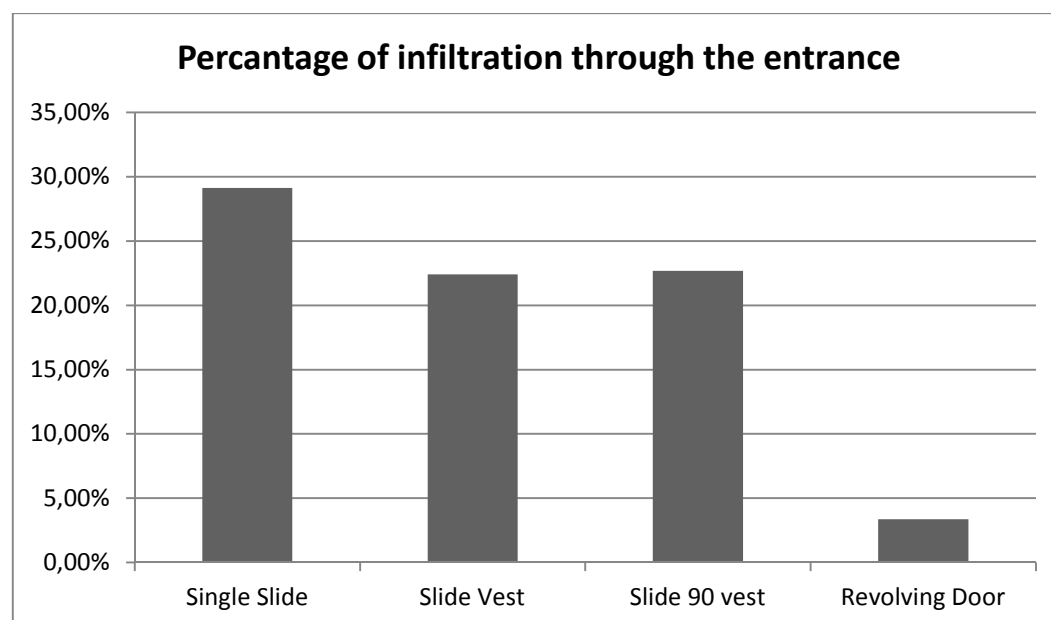


Figure 8.14 Percentage of the total infiltration from infiltration through entrances.

The impact on the amount of infiltration into the building due to the mechanically induced pressure of -5 Pa is presented in figure 8.15. The impact of the -5 Pa was highest for the revolving door entrance when looking at the increase of total building infiltration. While the infiltration decrease through the revolving door was the lowest. The sliding door with 90 degree vestibule received the largest impact among the open-type doors.

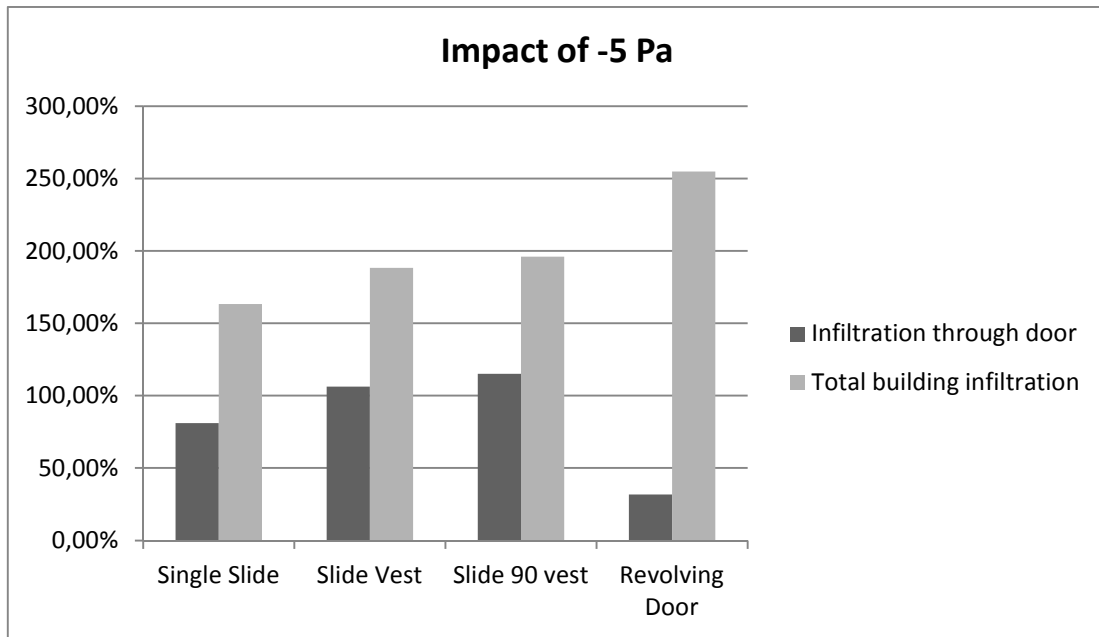


Figure 8.15. Impact on the total infiltration and infiltration through entrances caused by a +5 Pa mechanically induced pressure difference.

Due to a much larger impact of negative mechanically induced pressure compared to the impact of positive mechanically induced pressure the behavior due to mechanical pressure were further studied. Several different cases of mechanically induced pressure differences were simulated see figure 8.16. With a positive mechanically induced pressure difference the infiltration slowly converges towards zero. While with a negative induced pressure difference the infiltration increases rapidly, but the increase will eventually flatten out at very high pressure differences.

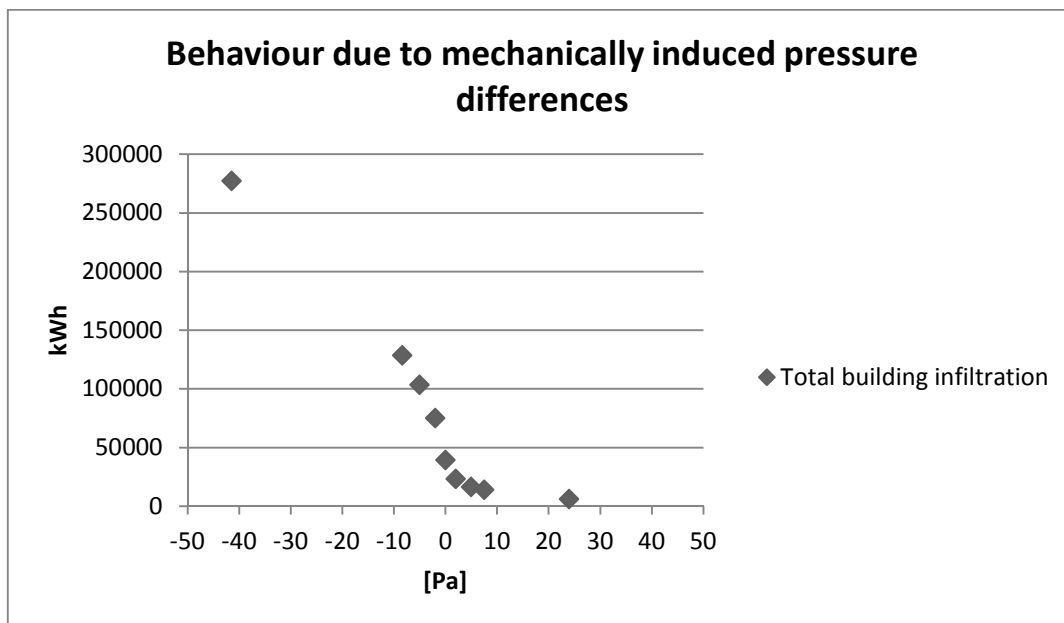


Figure 8.16. Behaviour of the infiltration due to mechanically induced pressure differences.

Finally it was of interest to see which of the cases where a change to a revolving door is the most efficient. The most efficient case is with a negative mechanically induced pressure difference. Here a revolving door would reduce the infiltration through the entrance by 10 times compared to a single sliding door. While only 3,5 times in the case with a positive mechanically induced pressure difference. See figure 8.17 for the results.

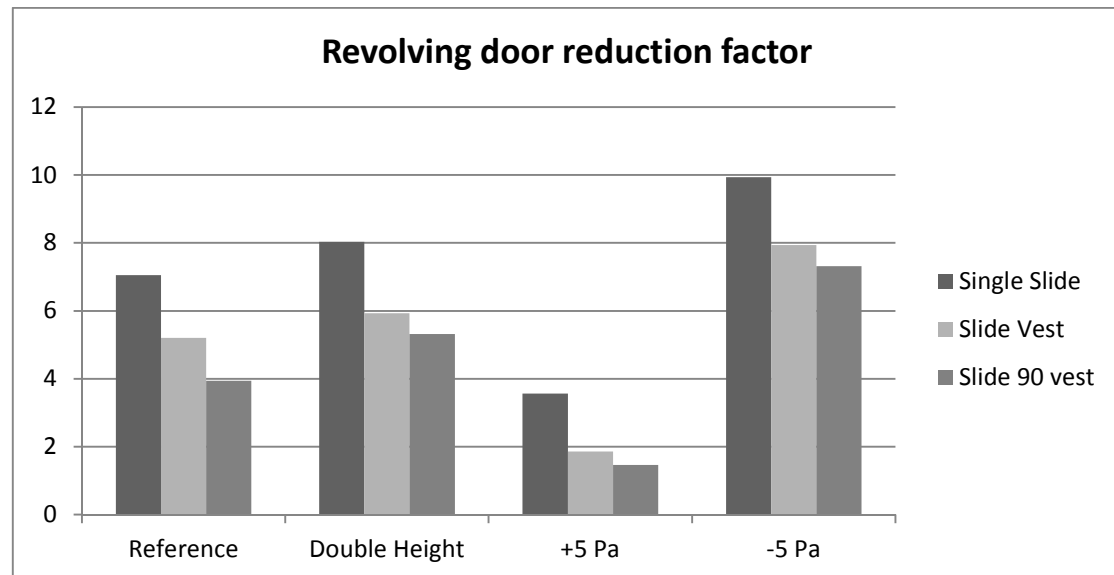


Figure 8.17. Reduction in infiltration by changing entrance to a revolving door.

## 8.2 Nils Ericson Terminal

In this chapter the results from the different simulation cases on the Nils Ericson terminal will be presented.

### 8.2.1 Reference study

A one year energy simulation of the reference model resulted in a heating consumption of 1084 MWh and a cooling consumption of 61 MWh. The total infiltration into the building was 238 MWh accounting for approximately 45% of the energy losses. The distribution of infiltration losses is illustrated in figure 8.18. Where the largest part of the infiltration goes through what has been denoted as other entrances (32%). While the amount that goes through the gates (23 %) and the main entrance (26 %) is rather equal. Only 19% goes through the leaks in the envelope.

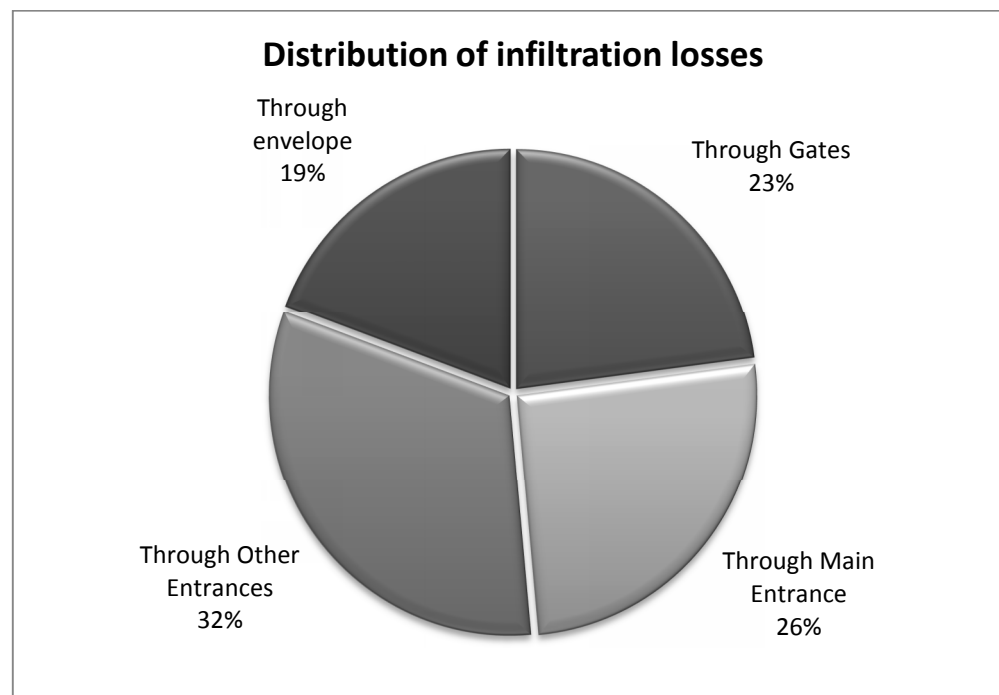


Figure 8.18. Distribution of infiltration losses at NET.

The results of the one year energy simulation with the year 2010 climate file have been compared with the actual consumption for that specific year, see table 8.1. Both the delivered heating and cooling were slightly low. The delivered heating was 89% accurate and the cooling 82%. Additionally results from the cases with doors always closed and always open were compared with the real case and reference model. The reference model had the overall highest accuracy while the case with doors always closed proved to be slightly more accurate for cooling.

Table 8.1. Comparison between measured energy and energy from simulations.

	Delivered Heating[MWh]	Delivered Cooling[MWh]	Accuracy Heating %	Accuracy Cooling %
Reality	1216,6	74,2	-	-
Reference model	1084	61	89,16	82,33
All doors closed	972,8	78,56	79,96	84,69
All doors fully open	1785	24,5	33,18	53,21

## 8.2.2 Gate study

In figure 8.19 the energy loss due to infiltration is presented for the varied entrance solutions. The highest infiltration is seen for the case with a single swing door and the lowest infiltration for the case with 3 revolving doors with an external roof. In figure 8.20 the heating consumption is presented for the variation of entrance solutions. Here the case with a single swing door has the highest consumption while the case of 3 revolving doors and no external roof has the lowest consumption. In figure 8.21 the cooling consumption is presented for the variation of entrance solutions. Here the case with 3 revolving doors and no external roof has the highest consumption while the case with 3 revolving doors and an external roof has the lowest.

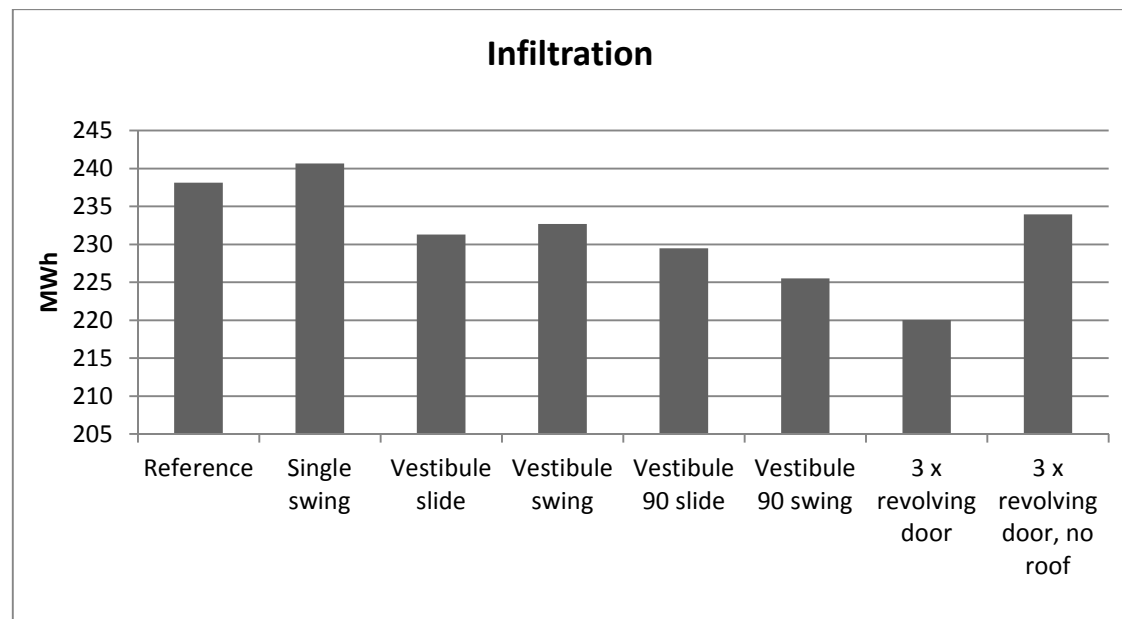


Figure 8.19. Total infiltration with different entrance solutions.

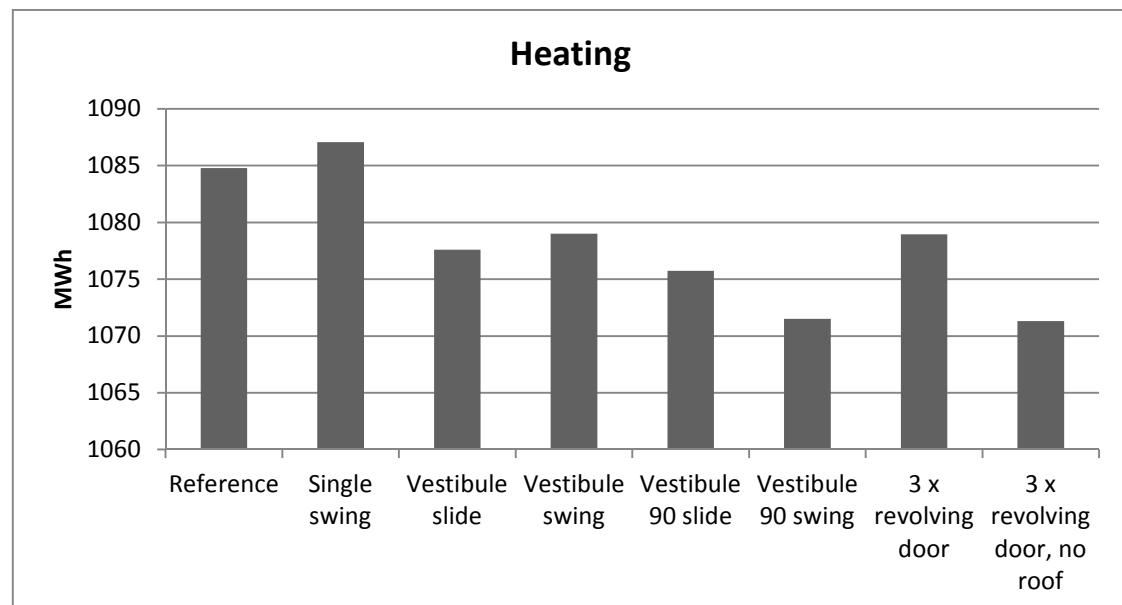


Figure 8.20. District heating use with different entrance solutions.

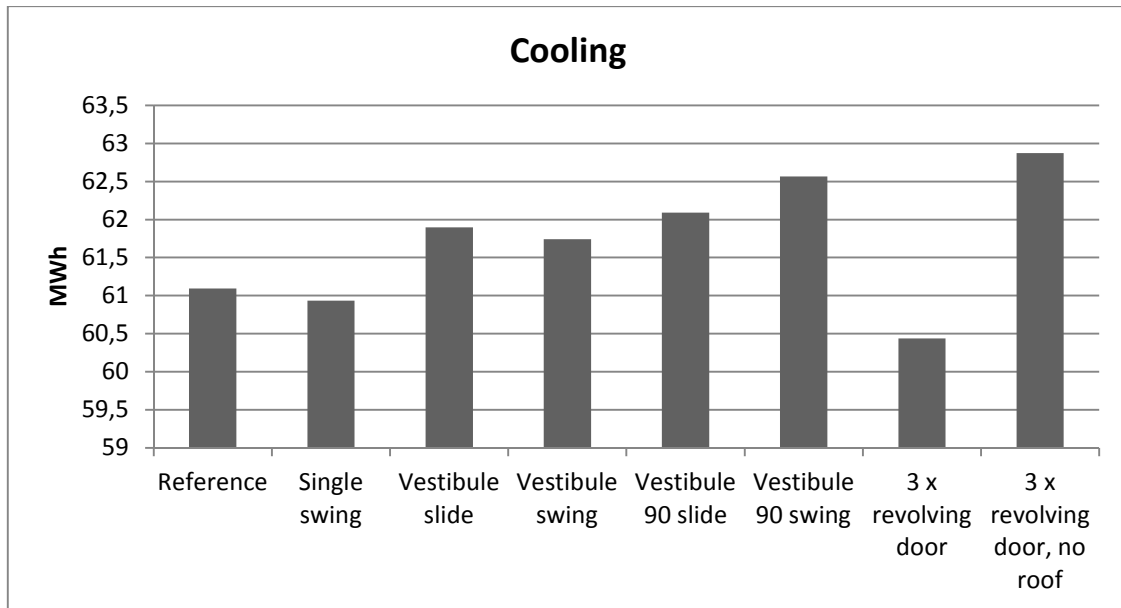


Figure 8.21. District cooling use with different entrance solutions.

In figure 8.22 the impact of the varied entrance solutions for the gates is presented. The figure shows the change of infiltration, cooling consumption and heating consumption relative to the reference model. The case with single swing doors was the only case increasing the infiltration. The trend among the open-type doors is that the heating consumption decreases with a decreased infiltration, with a magnitude of 105 % of the infiltration. While the cooling consumption increases by a magnitude of 12% of the infiltration. The revolving door case with an external roof provides the largest decrease of infiltration but does not affect the heating and cooling consumption in the same magnitude as for open-type doors. For the gates the entrance with swing doors in a 90° vestibule proves to be the most energy efficient.

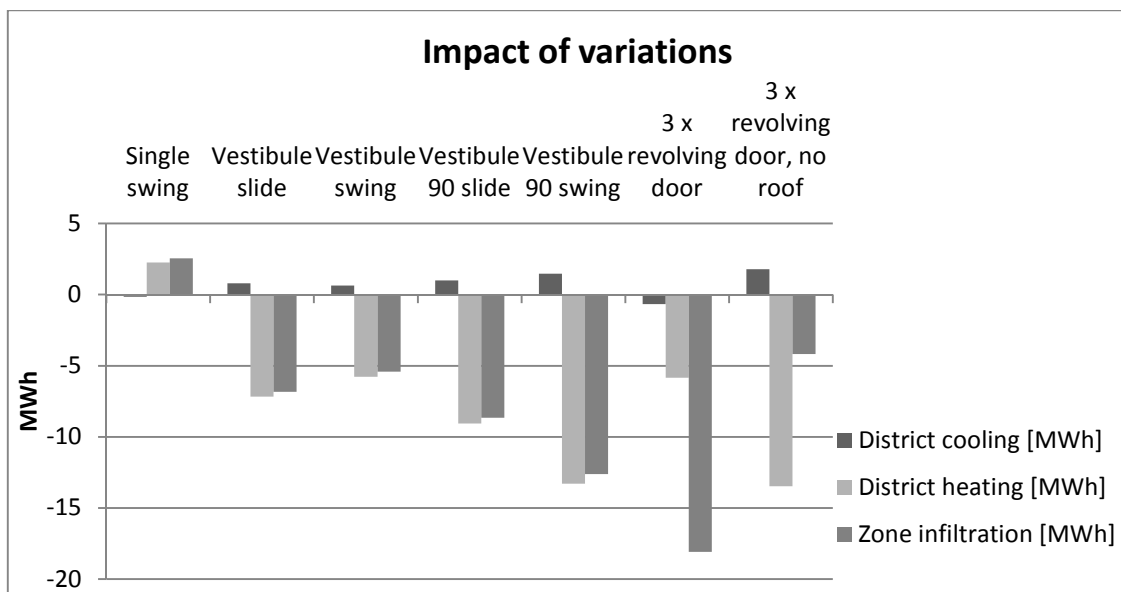


Figure 8.22. Impacts on infiltration, cooling and heating when changing the gate entrances.

### 8.2.3 Main Entrance Study

In figure 8.23 the energy loss due to infiltration is presented for the varied entrance solutions. The highest infiltration was seen for the case with a single swing door and the lowest infiltration for the case with a revolving door. In figure 8.24 the heating consumption is presented for the variation of entrance solutions. Here the case with a single swing door has the highest consumption while the case with a revolving door has the lowest consumption. In figure 8.25 the cooling consumption is presented for the variation of entrance solutions. Here the case with a revolving door has the highest consumption while the case with a single swing door has the lowest.

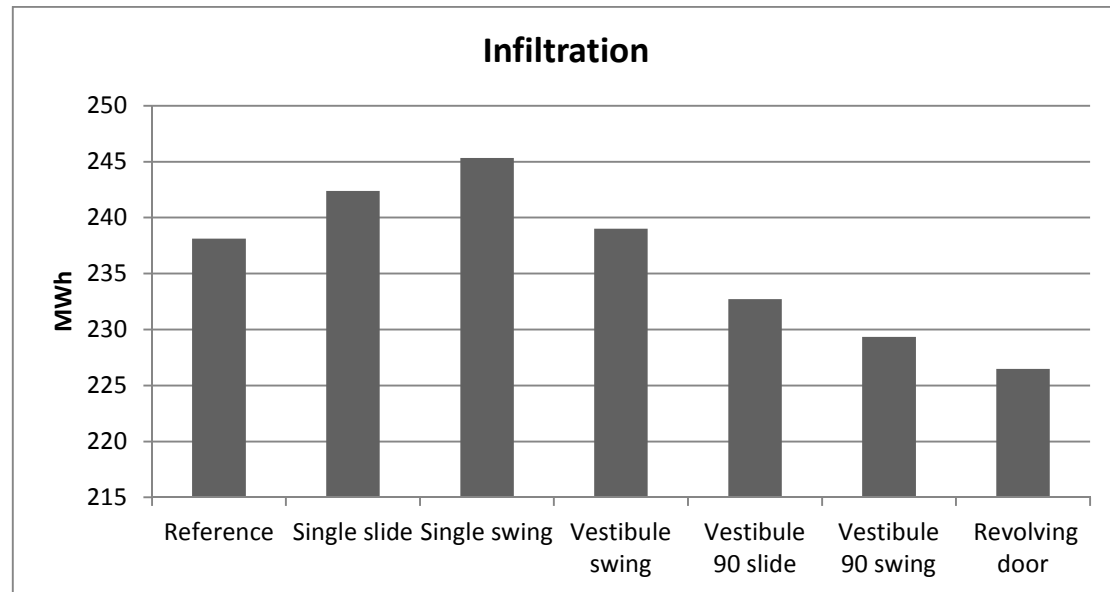


Figure 8.23. Total infiltration with different entrance solutions.

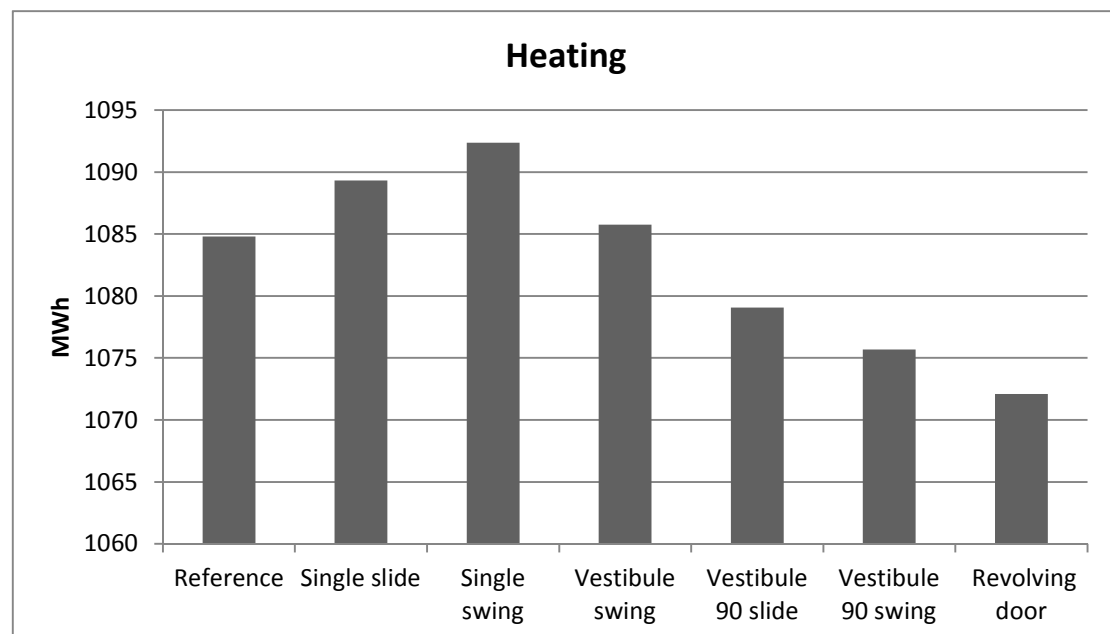


Figure 8.24. District heating use with different entrance solutions.



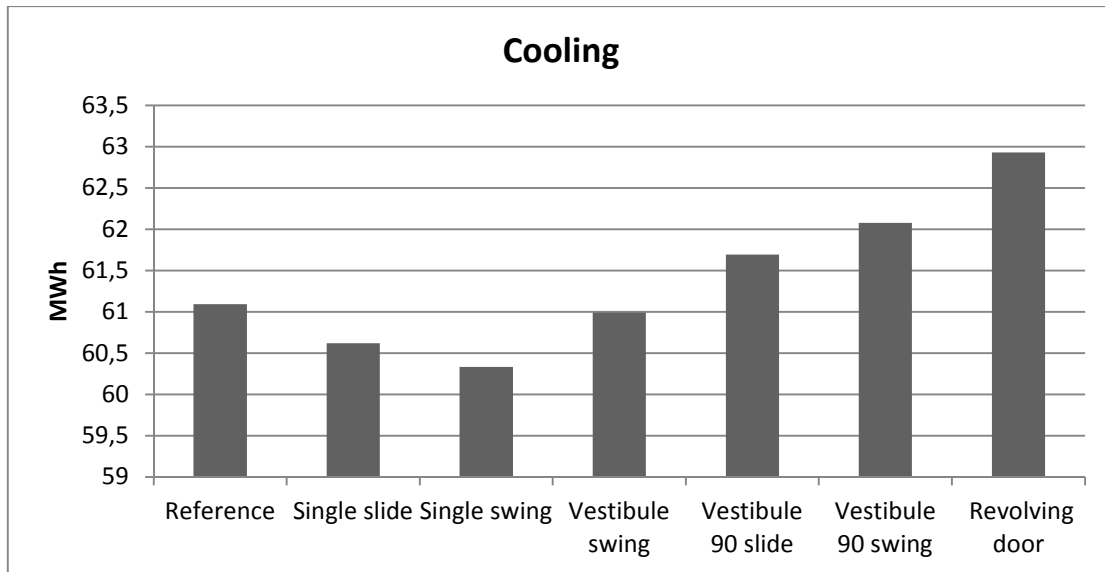


Figure 8.25. District cooling use with different entrance solutions.

In figure 8.26 the impact of the varied entrance solutions for the main entrance is presented. The figure shows the change of infiltration, cooling consumption and heating consumption relative to the reference model. The cases single swing, single slide and vestibule swing increased the infiltration. The trend among the open-type doors is that the heating consumption decreases with a decreased infiltration, with a magnitude of 106 % of the infiltration. While the cooling consumption increases by a magnitude of 12% of the infiltration. The revolving door case provides the largest decrease of infiltration and heating but at the same time it provides the highest increase in cooling. For the main entrance the revolving door proves to be the most energy efficient.

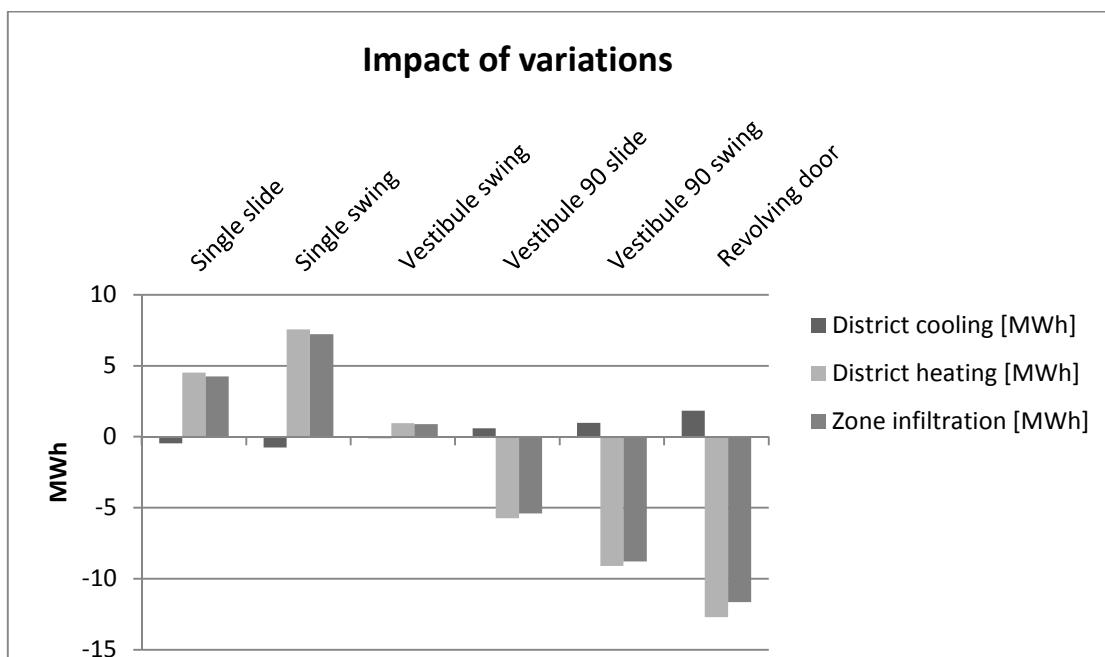


Figure 8.26. Impacts on infiltration, cooling and heating when changing the entrance type of the main entrance.

## 8.2.4 Optimization cases

The results of the optimization cases are presented in this chapter. In figure 8.27 the energy loss due to infiltration is presented for the varied entrance optimizing solutions. The solution where all entrances and gates have revolving doors provides the lowest infiltration while the solution where all entrances and gates have swing doors with 90° vestibules provides the highest infiltration. In figure 8.28 the heating consumption is presented for the variation of optimizing entrance solutions. Here the case where all entrances and gates have swing doors with 90° vestibules has the highest consumption while the solution where all entrances and gates have revolving doors provides the lowest heating consumption. In figure 8.29 the cooling consumption is presented for the variation of optimizing entrance solutions. Here the case where all entrances and gates have swing doors with 90° vestibules has the lowest consumption while the solution where all entrances have revolving doors provides the highest cooling consumption.

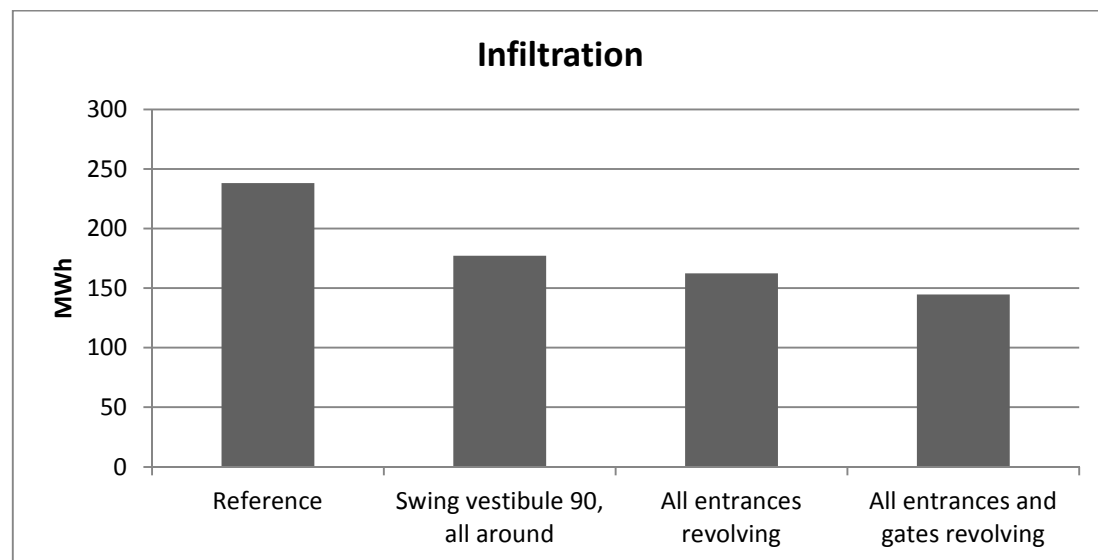


Figure 8.27. Total infiltration with different entrance solutions.

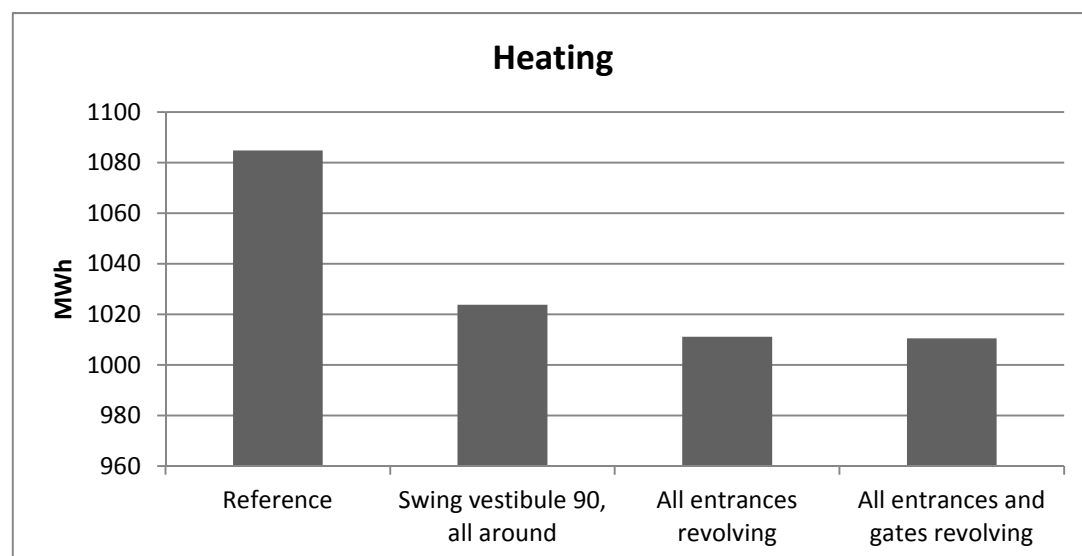


Figure 8.28. District heating use with different entrance solutions.

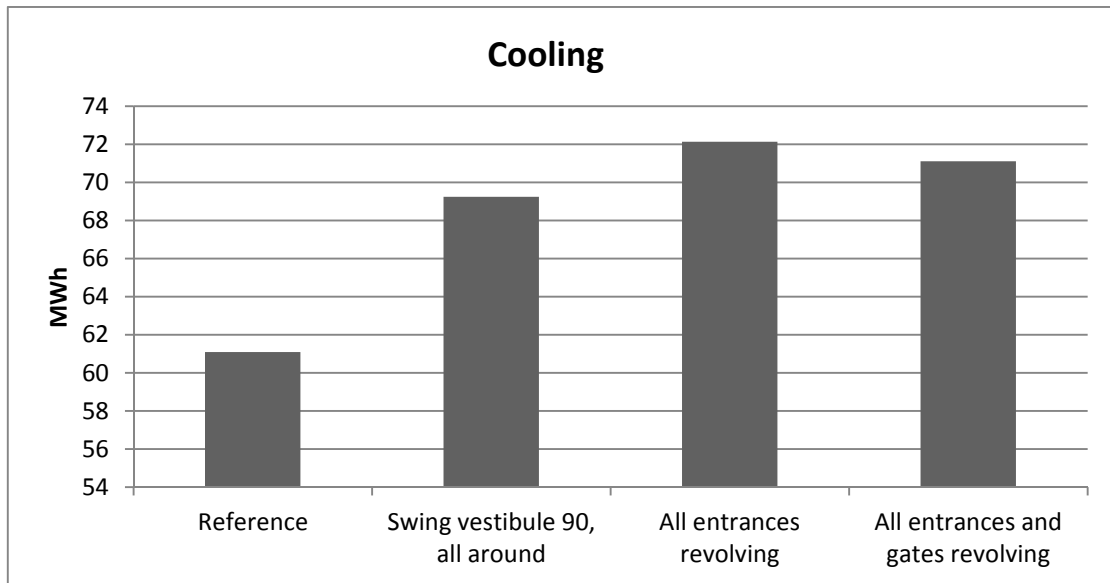


Figure 8.29. District cooling use with different entrance solutions.

In figure 8.30 the impact of the varied entrance optimizing solutions for the main entrance is presented. The figure shows the change of infiltration, cooling consumption and heating consumption relative to the reference model. All cases decreased the infiltration and heating but also increased the cooling. The cases with revolving door showed equal results in decreased heating consumption. The case where all entrances and gates have revolving doors gives a lower cooling consumption than the other revolving door case and therefore it is considered to be the best case.

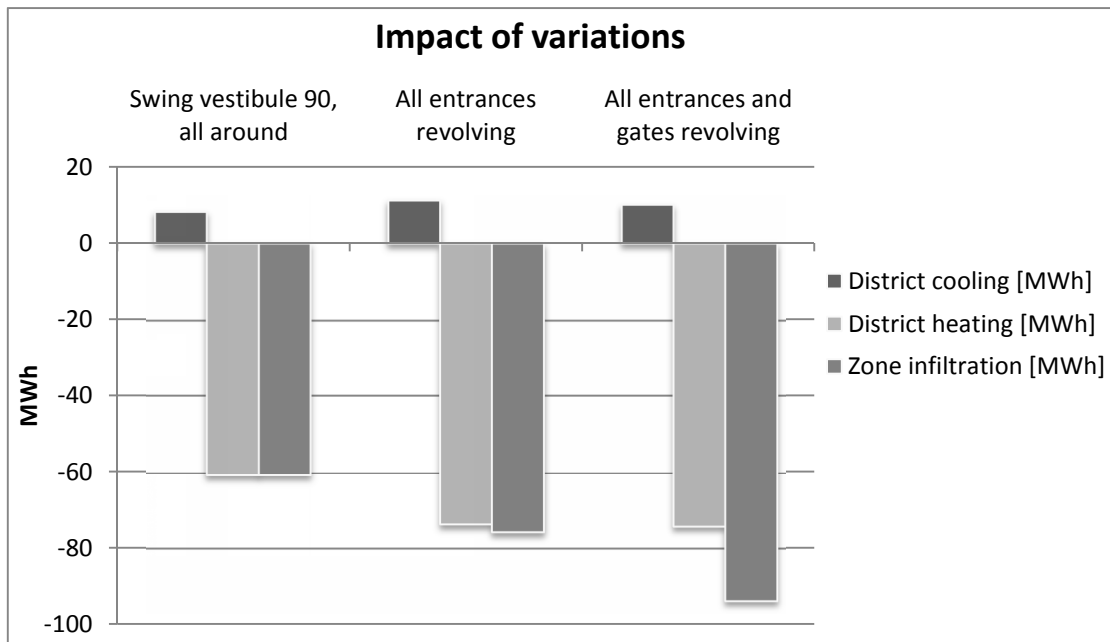


Figure 8.30. Impacts on infiltration, cooling and heating when changing the entrance types.

### 8.2.5 Revolving door study

It's of interest to see what impact revolving doors have at the different entrances of the building. In figure 8.31 the infiltration through the entrances for the reference case and with revolving doors is presented. Changing to revolving doors seem to have the most effect on the "Other entrances" and the least on the gates.

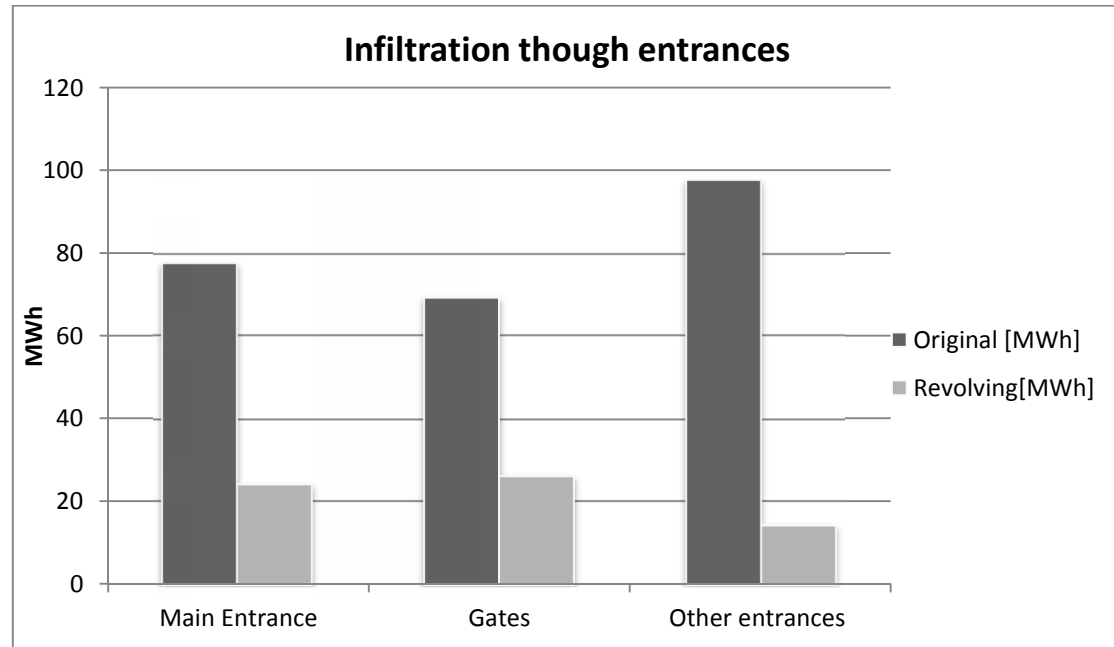


Figure 8.31. Comparison of the infiltration through the entrances with the original entrance solutions and with revolving doors.

## 8.2.6 Impact on the indoor climate

By changing the entrance to a type which decreases the infiltration will affect the indoor quality. In figure 8.32 the CO<sub>2</sub> levels are presented for the reference model and the optimizing cases. It is clear that both the extreme values and the mean CO<sub>2</sub> level is increased by changing to entrance solutions which lower the infiltration. In figure 8.33 the indoor temperature is presented. It is clear that changing to entrance solutions which lower the infiltration will increase the mean indoor temperature and also increase the lowest temperature, while the maximum indoor temperatures are kept the same.

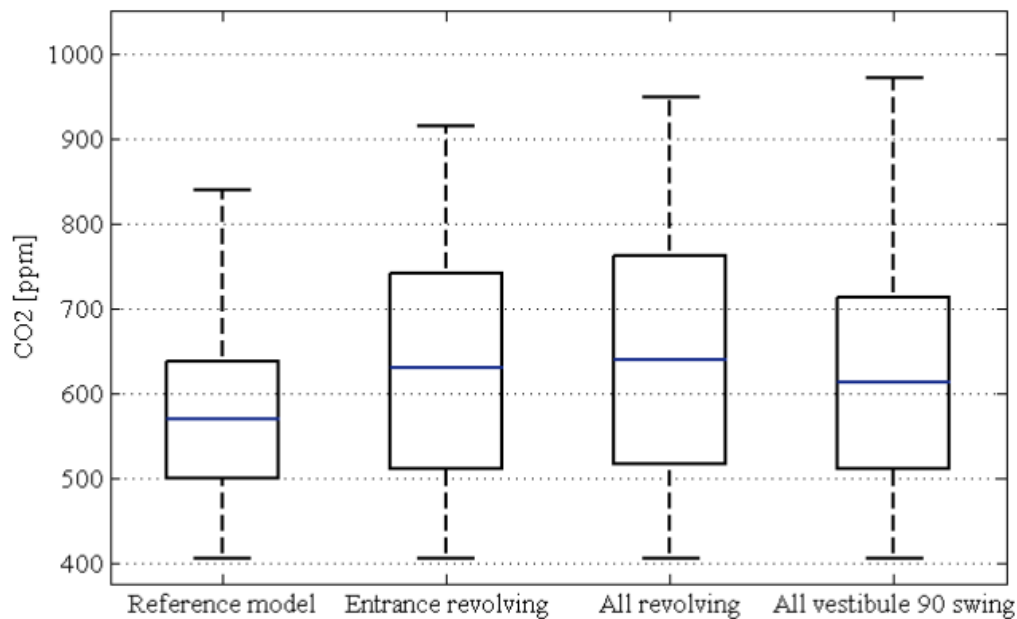


Figure 8.32. CO<sub>2</sub> level with different entrance solutions.

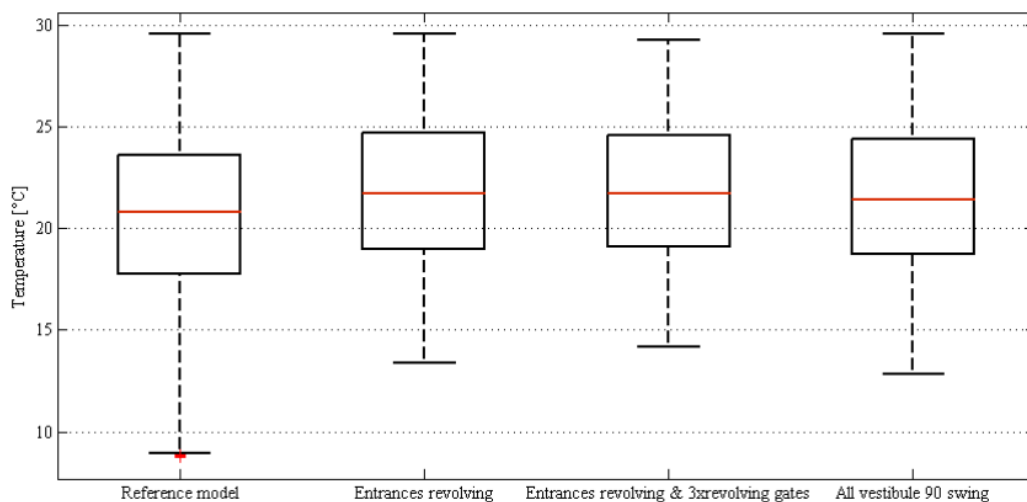


Figure 8.33. Temperature distribution with different entrance solutions.

## 9 Discussion and conclusions

In this chapter the thesis will be discussed and general conclusions will be made. Additionally the results from the case studies will be discussed and conclusions will be drawn.

### 9.1 General

The purpose of this thesis was to find calculation models for different entrance types and implement these in a building simulation software to study the energy performance of different entrances. I consider the purpose to be fulfilled and that I learned a lot during the process. Different parts of the process proved to be very time demanding. If more time was given more simulations would have been conducted on various scenarios. In the beginning of the thesis work I had the hope to be able to code an infiltration model for revolving doors with different input parameters such as door dimensions and door speed. But I can just conclude that for both open-type doors and revolving doors there are a lack of published measurements and studies to be able to create such a model.

### 9.2 Revolving doors

The revolving door proved to be more energy efficient than all other entrance solutions. The highest infiltration reduction from changing to a revolving door was seen at cases with a designed negative pressure difference and low flows of people. The smallest reduction is found where there is a low flow of people and a designed positive pressure difference.

The revolving door is the most sensitive to changes in the flow of people. As an explanation the usage model of the revolving doors is strongly simplified while the models for open-type doors are based on statistical data. The leakage through the door seals remains constant while the air exchange due to the revolving motion of the door is directly connected to the door usage schedule.

Overall by using the door models described in this thesis. The revolving door has shown a great potential in reducing infiltration through entrances. In most cases at least 5 times less air is infiltrated through a revolving door compared to the best open type door solutions. This is even more than what the manufacturers advertises.

An interesting result was that having all entrances and gates as revolving doors in NET was not more effective than having only the entrances revolving and keeping the gates as single sliding doors. The explanation to this deviation is that when replacing the gates to three revolving doors an external roof was added to allow people to wait outside. This roof however had a great impact on the solar heat gain with increased heat consumption as a result. The increased heating consumption was of the same magnitude as the reduction in infiltration resulting in equal heating results for the two cases.

Finally there is still a great need of measurements to be conducted on revolving doors and more importantly published ones. A design engineer shouldn't have to use data from 1962 in order to have a scientific base for his calculations.

### 9.3 Open-type doors

In this thesis the swing doors perform worse than sliding doors in all setups except when placed in a 90 ° vestibule. In the Yuill report it was concluded that the air flow through the entrance with swing doors was greatly affected by the direction the doors were opened and how they were located relative to each other. Even though the swing doors in a 90 ° vestibule is considered the best performing open-type entrance in the thesis it won't be any guarantee it will be the best one for any other case. In average slide doors in vestibules reduces the infiltration by 30% compared to a single door while sliding doors in a 90 ° degree vestibule reduces the infiltration by 52%.

The cases with a mechanically induced pressure difference proved to have great effects on the infiltration both for the total building infiltration and the infiltration through the entrance. This fact is important to consider when designing buildings with unbalanced ventilation and when evaluating the need of calibration and need for maintenance of existing systems. The reduction in infiltration losses due to a +5 Pa mechanically induced pressure difference looks very promising in terms of reducing energy losses but other facts have to be considered. As an example inducing this pressure difference with increased supply ventilation, more supply air need to be heated and with the lower return air flow the energy recovery will be lowered.

### 9.4 Comparison of results between simple office model and NET

An important difference between the results of the simple office model and the results of simulations conducted on NET is the impact of the infiltration change through the entrance on the total building infiltration. In the simple office model a change of 1 MWh through the entrance result in an equal change of the total building infiltration. In the simulations of NET a change in infiltration through one entrance does not impact the total infiltration amount in the same magnitude. As an example a revolving door provides 24 MWh of infiltration through the main entrance of NET while which is 53,9 MWh less than the reference case. Yet the reduction of the total building infiltration is only 12 MWh.

The mayor difference between the simple office model and NET is that the office model is a one zone model with fixed indoor temperature while NET is a multi zone model with a great indoor temperature range. If the infiltration through one entrance in NET is reduced it will affect all zones in the building and all the temperatures which will affect the heating system and other systems.

It can be concluded that the infiltration though entrances have different impacts on different buildings. There is a great potential in reducing the infiltration though entrances but to get the most out of it the different systems in the building must be properly designed.

## 9.5 Air curtains

In Sweden it is very common with the use of air curtains at building entrances. The manufacturers claim that an air curtain will reduce the infiltration through an entrance with 50-80% fan and heating energy included. Due to the lack of research and with a complete absence of published studies the air curtains were left out. Obtaining calculation methods for open-type doors and revolving doors were work enough. Implementing a model for air curtains on the calculation models described in this thesis will be simple when sufficient performance data for the air curtain is obtained.



## 10 Recommendation for further studies

The most crucial parameter in energy modeling of building entrances is the frequency of door usage. This frequency is commonly estimated from either real occupancy data, field measurements or estimated occupancy loads. There is a great need of probability models and tools which can be applied on different types of entrances. A model for open-type doors could be fed with sensor setup, entrance dimensions, operation speeds, user behavior and estimated people flow. Resulting in a probable door opening frequency and the amount of time where both doors in a vestibule are open. For revolving doors a model which predicts the hourly usage rate of the door is needed. It could be fed with data such as, door capacity, sensor setup, user behavior and estimated flow of people.

There is a lack of published measurements conducted on both open-type doors and revolving doors, especially on full scale doors. There are of course reasons to why these haven't been done. Doors are rather expensive and large which requires large laboratories to be able to make high quality measurements in a very controlled environment. There is a growing interest in the Swedish industry and at least one laboratory is under construction. As a result of more high quality data about air flow through different entrances, more accurate calculation models can be constructed.

Another very important component used in entrances is the air curtain. This component is widely used in Sweden to reduce heat and energy flows through entrances. It is known that it reduces the energy loss but there is a great lack of knowledge of how much, especially under unfavorable conditions. CFD models and measurements in combination to validate the performance of an air curtain would be very useful for energy engineers.

In this report the energy performance of different entrance types have been calculated by the models presented. These models have been implemented on a few building types and the economic factors have been totally left out. A study where these models are used to analyze more types of buildings in combination with economy tools such as LCC for different entrance types would be very useful, for example refurbishment projects.

## 11 References

- ASHRAE (2009): *2009 ASHRAE handbook – fundamentals*. SI edition, American Society of Heating, Refrigeration and Air-Conditioning Engineers, Atlanta, GA. ISBN 1615831703.
- Allgayer, D. (2007): *Air and heat movement by revolving doors*. Saarbrücken: LAP Lambert.
- Archiexpo. (2013): [www.archiexpo.com](http://www.archiexpo.com)
- BELOK. (2013): *Förstudie – Entrée: Projektnummer 2012:7*
- Bengtsson, A. (2013): Photo of the Nils Ericsson Terminal.  
<http://www.flickr.com/photos/barracuda666/7723525162/>
- BESAM. (2013): [per.kristoffersson@assaabloy.com](mailto:per.kristoffersson@assaabloy.com), 28/3-2013
- Boon Edam. (2013): *Tourniket product leaflet*.  
<http://www.boonedaminternational.com/doorsystems/tourniket.asp>
- Boon Edam Tool. (2013): *Calculation tool for infiltration through revolving doors*. Contact Boon Edam.
- Bring A, Sahlin P and Vuolle M. (1999): *Models for building indoor climate and energy simulation, a report of IEA SHC Task 22*, International Energy Agency.
- Cho, H et al. (2010): *Energy saving impact of ASHRAE 90.1 vestibule requirements*, U.S Department of Energy
- Du, Lin. (2009): *Air Infiltration through Revolving Doors*. [Online] Available: <http://spectrum.library.concordia.ca/976715/1/MR67309.pdf>
- Equa. (2013): *Information available at the homepage*. [www.equa.com](http://www.equa.com)
- Hagentoft, C-E. (2003): *Introduction to Building Physics*, Studentlitteratur, Lund.
- Kohri, K. (2001): *A simulation analysis of the opening area of entrance doors and winter airflow into the entrance hall of a high-rise office building*. IBPSA Conference.
- Lindström, C. (2013): *Energy Efficient Design of Bus Terminals*. Gothenburg: Chalmers University of Technology.
- NREL. (2012): *Retail Building Guide for Entrance Energy Efficient Measures* [Electronic] Available: < <http://www.nrel.gov/docs/fy12osti/52290.pdf> > [2013-02-10].
- Salvalai, G. (2012): *Implementation and validation of simplified heat pump model in IDA-ICE energy simulation environment*, Energy and Buildings, Volume 49
- Sandberg, P et al (2007): *(Consideration of airtightness in the construction process – Stage B. Technical consequences and profitability assessments)*. SP Sveriges Tekniska Forskningsinstitut, SP Rapport 2007:23, Borås.
- Schutrum, L F et al. (1962): *Air Infiltration through Revolving Doors*. ASHRAE Transactions vol 67, pp 488-506

WJE. (1997): *Air Leakage Testing WJE No. 972737*. [Electronic] Available: <<http://web.archive.org/web/20010303110316/http://www.cranedoor.com/wje.htm>> [2013-02-10]

Woloszyn et al. (1999): *Airflow through large vertical openings in multizone modeling*. Available: <[http://www.ibpsa.org/proceedings/BS1999/BS99\\_D-09.pdf](http://www.ibpsa.org/proceedings/BS1999/BS99_D-09.pdf)>

Wulfinghoff, D. (1999). *Energy Efficiency Manual*. Energy institute press.

Younes et al. (2012) *Air infiltration through building envelopes: A review* Journal of Building Physics January 2012 35: 267-302, first published on October

Yuill, GK et al. (1999): *Impact of high use automatic doors on infiltration. Final report*, ASHRAE 763-RP

Zmeureanu, R., Stathopoulos, T., Schopmeijer, M., Siret, F., and Payer, J. (2001): *Measurements of Air Leakage through Revolving Doors of Institutional Building*. J. Archit. Eng.

## APENDIX A: Pressure differences

### Stack effect

Stack pressure is a hydrostatic pressure which is caused by the mass of an air column located inside or outside of a building. The pressure depends on the density of the air and the height above the reference point ( $z=0$ ). The density of air depends on the local barometric pressure, temperature and humidity ratio (ASHRAE, 2009).

Temperature differences between indoor and outdoor air causes differences in stack pressure which will drive airflows across the building envelope, this effect is called the stack effect. The stack effect is also known as the buoyancy effect. The effect on air density caused by the moisture ratio is generally negligible, except for hot humid climates where air is warm and nearly saturated (ASHRAE, 2009).

For an enclosed volume with leakages just like a normal building the mass flow of air in and out of the volume must be equal. Since the driving force is pressure difference there will be a specific level or levels in the building where the pressure difference is equal to zero. That level is called the Neutral Pressure Plane (NPL). By having the NPL as the reference height the stack effect can be calculated (ASHRAE, 2009).

The following equations are used to calculate the stack effect

$$\Delta P_s = z * (\rho_e - \rho_i) * g \text{ [Pa]}$$

$z$  is the vertical distance, in the downward direction, from the neutral pressure plane [m]

$\rho_e$  is the external air density  $\left[\frac{\text{kg}}{\text{m}^3}\right]$

$\rho_i$  is the internal air density  $\left[\frac{\text{kg}}{\text{m}^3}\right]$

$g$  is the gravitational acceleration  $\left[\frac{\text{m}}{\text{s}^2}\right]$

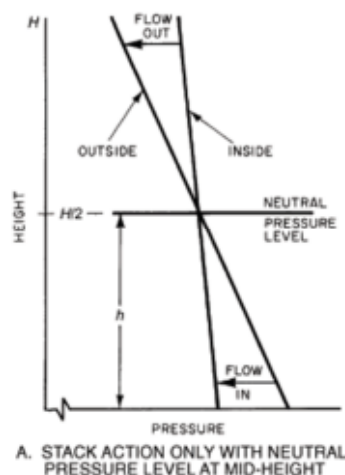


Figure 0.1 Illustration of the pressure profile caused by the stack effect with the neutral pressure plane at mid height (ASHRAE, 2009)

## Wind induced pressure

Wind is the motion or movement of air that occurs naturally in our outdoor climate due to barometric pressure differences. When the wind hits an object the kinetic energy is transformed into a force which over an area results into pressure. Wind induces a positive pressure on the part of the building which faces towards the wind, windward side (Hagentoft, 2003). Sharp edges of the building separates the wind flow inducing negative pressure along the side and the leeward face of the building (ASHRAE, 2009).

$$\Delta P_w = C_p * \frac{\rho_a v^2}{2} [Pa]$$

$C_p$ - Wind pressure coefficient

$\rho_a$ - Density of air  $\left[\frac{kg}{m^3}\right]$

$v$ - Wind velocity at a specified reference height  $\left[\frac{m}{s}\right]$

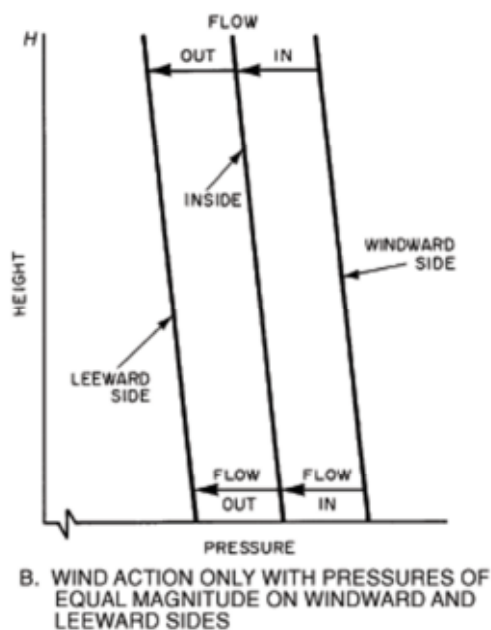


Figure 0.2. Illustration of the pressure profile caused by wind pressure (ASHRAE, 2009)

The wind pressure coefficient  $C_p$  is an empirically derived parameter mostly based on wind tunnel experiments. A negative value on  $C_p$  means that there is wind suction on the envelope, the wind want to suck air out of the building.

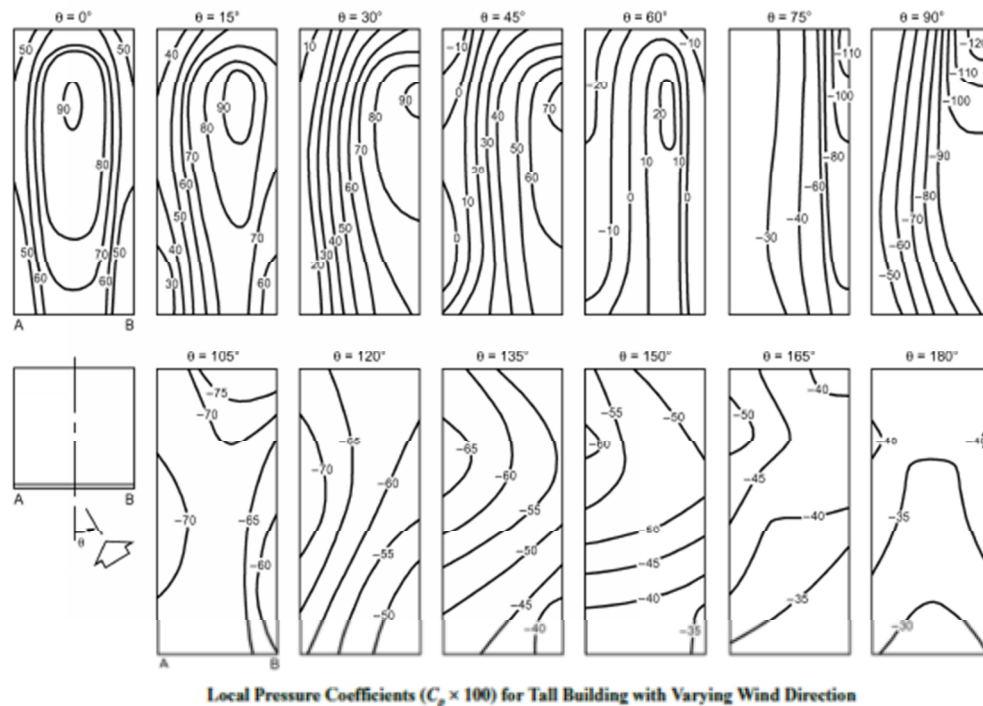


Figure 0.3 Local wind pressure coefficients on the different faces of a building (ASHRAE, 2009)

The strength of the wind depends on the surface roughness and the height above ground. A reference level for wind velocity must be specified; commonly the building height is used for wind pressure calculations.

$$U_z = U_m * k * z^a$$

$U_m$ - Wind speed measured at a weather station at 10 m height

$z$ - Height of the building

$k$  and  $a$  are constants and examples of these can be found in the table below. (Hagentoft, 2003)

Terrain coefficient	$k$	$a$
Open, flat country	0,68	0,17
Country with scattered wind breaks	0,52	0,20
Urban	0,35	0,25
City	0,21	0,33

Figure 0.4 Terrain coefficients (Hagentoft, 2003)

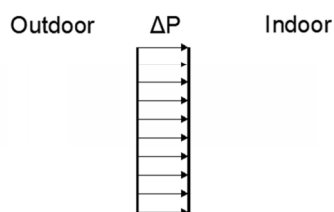
## Mechanically induced pressure

Depending on the ventilation for the building there will be either a positive, negative or neutral pressure difference induced by the ventilation system. A negative pressure difference results in air flow out of the building and a positive pressure difference results in a flow in to the building. (Hagentoft, 2003)

Examples of pressure differences induced by different types of ventilation systems:

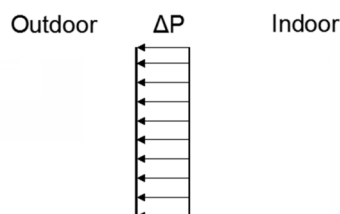
An extract ventilation system where fans remove air from the building and fresh air is provided through air inlets and openings will provide a positive pressure difference.

Extract Ventilation



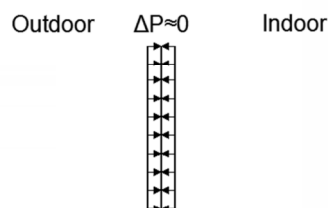
A supply ventilation system where fans supply air to the building and the exhaust air is pushed out through openings and outlets will provide a negative pressure difference.

Supply Ventilation



Balanced ventilation with both supply and exhaust fans aim to provide no pressure difference but some small imbalances will occur and small pressure differences will be induced.

Balanced Ventilation



Air exhausted from a building by a central exhaust system must be balanced by increasing airflow into the building through openings and the other way around for air supplied by a central system. Wrong design of the exhaust system can cause depressurization. Depressurization can increase the radon flow into the building, cause moist outdoor air to penetrate into the building envelope which might condensate and induce mold growth. Pressure differences induced by unbalanced ventilation at balanced ventilation systems have been measured to an average of 3 to 6 Pa (ASHRAE, 2009)



## APENDIX B: Entrance types

Illustrative explanation of the open-type doors mentioned in the thesis.



*Figure 0-1. Single sliding door.*



*Figure 0-2 Sliding doors with a vestibule.*



*Figure 0-3. Sliding doors with a 90 ° vestibule.*



*Figure 0-4. Single swing doors.*

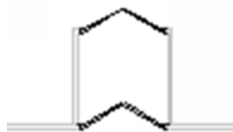


*Figure 0-5 Swing doors with a vestibule.*



*Figure 0-6. Swing doors with a 90° vestibule.*

## APENDIX C: Door usage data and usage schedule input of NET

		Passing people							
		Entrances				Gate			
		Main		Other					
		Weekdays	Weekends	Weekdays	Weekends	Weekdays	Weekends	Weekdays	Weekends
00:00-00:59	0%	21	10	4	2	2	1		
01:00-01:59	0%	0	0	0	0	0	0		
02:00-02:59	0%	0	0	0	0	0	0		
03:00-03:59	0%	0	0	0	0	0	0		
04:00-04:59	0%	13	7	2	1	1	0		
05:00-05:59	1%	132	66	18	9	8	4		
06:00-06:59	4%	412	206	55	28	25	12		
07:00-07:59	11%	1073	537	144	72	64	32		
08:00-08:59	8%	822	411	111	55	49	25		
09:00-09:59	5%	540	270	73	36	32	16		
10:00-10:59	4%	418	209	56	28	25	13		
11:00-11:59	5%	508	254	68	34	31	15		
12:00-12:59	6%	574	287	77	39	34	17		
13:00-13:59	6%	579	290	78	39	35	17		
14:00-14:59	8%	813	406	109	55	49	24		
15:00-15:59	10%	1003	502	135	68	60	30		
16:00-16:59	10%	1022	511	138	69	61	31		
17:00-17:59	7%	763	381	103	51	46	23		
18:00-18:59	5%	499	250	67	34	30	15		
19:00-19:59	3%	320	160	43	22	19	10		
20:00-20:59	2%	249	125	34	17	15	7		
21:00-21:59	2%	211	105	28	14	13	6		
22:00-22:59	1%	122	61	16	8	7	4		
23:00-23:59	1%	73	36	10	5	4	2		
People per day		10186	5093	1371	686	11000	5500		

Time	Study of south-west entrance											
	Sliding door 90° vestibule				Swinging door vestibule				Swinging door 90° vestibule			
	Weekdays		Weekends		Weekdays		Weekends		Weekdays		Weekends	
	CA	CA/CD	CA	CA/CD	CA	CA/CD	CA	CA/CD	CA	CA/CD	CA	CA/CD
00:00-00:59	0.01	0.02	0.01	0.01	0.02	0.02	0.01	0.01	0.01	0.01	0.03	0.04
01:00-01:59	0.00	0.00	0.00	0.00	0.00	0.00	0.00	0.00	0.00	0.00	0.00	0.00
02:00-02:59	0.00	0.00	0.00	0.00	0.00	0.00	0.00	0.00	0.00	0.00	0.00	0.00
03:00-03:59	0.00	0.00	0.00	0.00	0.00	0.00	0.00	0.00	0.00	0.00	0.00	0.00
04:00-04:59	0.01	0.01	0.00	0.00	0.01	0.01	0.00	0.00	0.00	0.02	0.01	0.01
05:00-05:59	0.08	0.13	0.04	0.07	0.11	0.17	0.05	0.08	0.06	0.09	0.15	0.24
06:00-06:59	0.22	0.34	0.13	0.19	0.28	0.44	0.16	0.25	0.15	0.24	0.38	0.59
07:00-07:59	0.35	0.54	0.27	0.42	0.62	0.95	0.33	0.50	0.35	0.54	0.62	0.95
08:00-08:59	0.34	0.52	0.24	0.34	0.53	0.81	0.28	0.43	0.11	0.48	0.60	0.92
09:00-09:59	0.27	0.42	0.16	0.24	0.33	0.50	0.20	0.31	0.11	0.32	0.47	0.72
10:00-10:59	0.22	0.34	0.13	0.19	0.29	0.44	0.16	0.25	0.15	0.24	0.38	0.59
11:00-11:59	0.26	0.40	0.15	0.23	0.31	0.48	0.19	0.30	0.30	0.30	0.45	0.70
12:00-12:59	0.28	0.43	0.17	0.26	0.35	0.53	0.21	0.33	0.12	0.33	0.49	0.75
13:00-13:59	0.28	0.43	0.17	0.26	0.35	0.54	0.22	0.33	0.12	0.33	0.49	0.76
14:00-14:59	0.33	0.51	0.22	0.33	0.52	0.80	0.28	0.43	0.11	0.47	0.59	0.91
15:00-15:59	0.35	0.54	0.26	0.40	0.62	0.95	0.31	0.47	0.35	0.54	0.62	0.95
16:00-16:59	0.35	0.54	0.26	0.40	0.62	0.95	0.31	0.48	0.35	0.54	0.62	0.95
17:00-17:59	0.32	0.50	0.21	0.32	0.48	0.74	0.27	0.41	0.38	0.44	0.57	0.88
18:00-18:59	0.26	0.40	0.15	0.23	0.31	0.47	0.19	0.29	0.19	0.30	0.45	0.69
19:00-19:59	0.18	0.28	0.10	0.15	0.23	0.36	0.13	0.20	0.13	0.20	0.32	0.50
20:00-20:59	0.15	0.23	0.08	0.12	0.19	0.29	0.10	0.16	0.10	0.16	0.27	0.41
21:00-21:59	0.13	0.20	0.07	0.10	0.16	0.25	0.09	0.13	0.09	0.14	0.23	0.36
22:00-22:59	0.08	0.12	0.04	0.06	0.10	0.15	0.05	0.08	0.05	0.08	0.14	0.22
23:00-23:59	0.05	0.07	0.04	0.04	0.06	0.09	0.03	0.05	0.03	0.05	0.09	0.14

Time	Study of Gateopening															
	Sliding door 90° vestibule				Swinging door vestibule				Swinging door 90° vestibule				Sliding door vestibule			
	Weekdays		Weekends		Weekdays		Weekends		Weekdays		Weekends		Weekdays		Weekends	
	CA	CA/CD	CA	CA/CD	CA	CA/CD	CA	CA/CD	CA	CA/CD	CA	CA/CD	CA	CA/CD	CA	CA/CD
00:00-00:59	-0.001	-0.001	-0.001	-0.001	0.001	-0.001	-0.002	-0.002	-0.001	-0.001	-0.001	-0.001	-0.001	-0.001	0.001	0.001
01:00-01:59	-0.002	-0.002	-0.002	-0.002	-0.003	-0.002	-0.003	-0.002	-0.001	-0.001	-0.001	-0.001	-0.002	-0.002	-0.003	-0.002
02:00-02:59	-0.002	-0.002	-0.002	-0.002	-0.002	-0.002	-0.003	-0.002	-0.001	-0.001	-0.002	-0.001	-0.002	-0.002	-0.003	-0.002
03:00-03:59	-0.002	-0.002	-0.002	-0.002	-0.002	-0.002	-0.003	-0.002	-0.001	-0.001	-0.002	-0.001	-0.002	-0.002	-0.003	-0.002
04:00-04:59	-0.002	-0.001	-0.002	-0.001	-0.002	-0.002	-0.002	-0.002	-0.001	-0.001	-0.002	-0.001	-0.002	-0.002	-0.003	-0.002
05:00-05:59	0.003	0.003	0.001	0.001	0.004	0.003	0.001	0.001	0.002	0.002	0.000	0.000	0.003	0.003	0.001	0.001
06:00-06:59	0.015	0.012	0.006	0.005	0.019	0.015	0.008	0.006	0.010	0.008	0.004	0.003	0.013	0.007	0.006	0.006
07:00-07:59	0.041	0.032	0.020	0.015	0.053	0.041	0.026	0.020	0.029	0.022	0.014	0.011	0.047	0.037	0.023	0.018
08:00-08:59	0.031	0.024	0.015	0.011	0.040	0.031	0.019	0.015	0.022	0.017	0.010	0.008	0.036	0.028	0.017	0.013
09:00-09:59	0.020	0.016	0.009	0.007	0.026	0.020	0.012	0.009	0.014	0.011	0.006	0.005	0.023	0.018	0.010	0.008
10:00-10:59	0.015	0.012	0.007	0.005	0.019	0.015	0.008	0.006	0.010	0.008	0.004	0.003	0.017	0.013	0.006	0.006
11:00-11:59	0.019	0.015	0.008	0.007	0.024	0.019	0.011	0.008	0.013	0.010	0.006	0.004	0.022	0.017	0.010	0.007
12:00-12:59	0.022	0.017	0.010	0.008	0.028	0.021	0.013	0.010	0.012	0.012	0.007	0.005	0.025	0.019	0.011	0.009
13:00-13:59	0.022	0.017	0.010	0.008	0.028	0.021	0.013	0.010	0.012	0.012	0.007	0.005	0.025	0.019	0.011	0.009
14:00-14:59	0.031	0.024	0.015	0.011	0.040	0.031	0.019	0.014	0.022	0.017	0.010	0.008	0.036	0.027	0.017	0.013
15:00-15:59	0.039	0.032	0.019	0.014	0.050	0.038	0.024	0.018	0.027	0.021	0.013	0.010	0.044	0.034	0.021	0.016
16:00-16:59	0.039	0.032	0.019	0.015	0.051	0.039	0.024	0.019	0.028	0.021	0.013	0.010	0.045	0.035	0.022	0.017
17:00-17:59	0.029	0.022	0.014	0.011	0.037	0.029	0.018	0.013	0.020	0.016	0.009	0.007	0.033	0.026	0.016	0.012
18:00-18:59	0.019	0.014	0.008	0.006	0.024	0.018	0.011	0.008	0.013	0.010	0.006	0.004	0.021	0.016	0.009	0.007
19:00-19:59	0.011	0.009	0.005	0.004	0.014	0.011	0.006	0.004	0.008	0.006	0.003	0.002	0.013	0.010	0.005	0.004
20:00-20:59	0.008	0.006	0.003	0.002	0.011	0.008	0.004	0.003	0.006	0.004	0.002	0.001	0.009	0.007	0.004	0.003
21:00-21:59	0.007	0.005	0.002	0.002	0.008	0.007	0.003	0.002	0.004	0.003	0.001	0.001	0.006	0.005	0.003	0.002
22:00-22:59	0.003	0.002	0.000	0.000	0.004	0.003	0.000	0.000	0.002	0.001	0.000	0.000	0.003	0.003	0.001	0.000
23:00-23:59	0.001	0.001	-0.001	0.000	0.001	0.001	-0.001	-0.001	0.000	0.000	-0.001	-0.001	0.001	0.001	-0.001	-0.001

	Revolving door study							
	Main		Other				Gate	
	Weekdays	Weekends	Weekdays	Weekends	Weekdays	Weekends	Weekdays	Weekends
	Usage	Usage	Usage	Usage	Usage	Usage	Usage	Usage
00:00-00:59	0,02	0,01	0,00	0,00	0,00	0,01	0,00	0,00
01:00-01:59	0,00	0,00	0,00	0,00	0,00	0,00	0,00	0,00
02:00-02:59	0,00	0,00	0,00	0,00	0,00	0,00	0,00	0,00
03:00-03:59	0,00	0,00	0,00	0,00	0,00	0,00	0,00	0,00
04:00-04:59	0,01	0,01	0,00	0,00	0,00	0,00	0,00	0,00
05:00-05:59	0,11	0,06	0,01	0,00	0,00	0,04	0,02	0,02
06:00-06:59	0,34	0,17	0,05	0,01	0,12	0,12	0,06	0,06
07:00-07:59	0,89	0,45	0,12	0,03	0,32	0,32	0,16	0,16
08:00-08:59	0,68	0,34	0,09	0,02	0,25	0,25	0,12	0,12
09:00-09:59	0,45	0,22	0,06	0,01	0,16	0,16	0,08	0,08
10:00-10:59	0,35	0,17	0,05	0,01	0,13	0,13	0,06	0,06
11:00-11:59	0,42	0,21	0,06	0,01	0,15	0,15	0,08	0,08
12:00-12:59	0,48	0,24	0,06	0,01	0,17	0,17	0,09	0,09
13:00-13:59	0,48	0,24	0,06	0,01	0,17	0,17	0,09	0,09
14:00-14:59	0,68	0,34	0,09	0,02	0,24	0,24	0,12	0,12
15:00-15:59	0,84	0,42	0,11	0,03	0,30	0,30	0,15	0,15
16:00-16:59	0,85	0,43	0,11	0,03	0,31	0,31	0,15	0,15
17:00-17:59	0,64	0,32	0,09	0,02	0,23	0,23	0,11	0,11
18:00-18:59	0,42	0,21	0,06	0,01	0,15	0,15	0,07	0,07
19:00-19:59	0,27	0,13	0,04	0,01	0,10	0,10	0,05	0,05
20:00-20:59	0,21	0,10	0,03	0,01	0,07	0,07	0,04	0,04
21:00-21:59	0,18	0,09	0,02	0,01	0,06	0,06	0,03	0,03
22:00-22:59	0,10	0,05	0,01	0,00	0,04	0,04	0,02	0,02
23:00-23:59	0,06	0,03	0,01	0,00	0,02	0,02	0,01	0,01